The Prostaglandin E2 Receptor 1 (EP1) Antagonizes AngII in the Collecting Duct

By: David Eckert

This thesis is submitted as a partial fulfillment of the M.Sc. program in Cellular and Molecular Medicine.

Department of Cellular and Molecular Medicine

Faculty of Medicine

University of Ottawa

Abstract

Prostaglandin E_2 (PGE_2), a metabolite of arachidonic acid, plays a role in water and sodium reabsorption in the collecting duct of the kidney. The collecting duct is responsible for the fine tuning of water and electrolytes. Only a small fraction of the filtered water and sodium is reabsorbed in the collecting duct, a fraction crucial to the regulation of water and electrolyte balance. This current study addresses the role of EP1, one of four PGE_2 receptors, in the collecting duct. It is well documented that PGE_2 inhibits sodium and water reabsorption in the collecting duct, however the exact mechanism is still debated. To determine whether the EP1 receptor mitigates AngII renal effects, an *in vivo* study was performed with EP1-/- mice. Global EP1-/- knockout mice were crossed with a renin overexpressing mouse line (herein denoted as "Ren") and subjected to a high salt (HS) and low salt (LS) diet. Ren mice displayed an 11mmHg increase in systolic blood pressure (BP) on a HS diet and a decrease in BP of 14mmHg on a LS diet compared to the normal salt (NS) diet. Ren EP1-/- mice did not display a significant increase or decrease in BP on a HS or LS diet. On a LS diet, Ren EP1-/- displayed a drop in urine osmolarity (1641 mOsm/ kgH_2O) vs. wild type (WT) mice (2107 mOsm/ kgH_2O), consistent with increased sodium reabsorption. Narrowing in on the collecting duct, Ren EP1-/- mice had enhanced αENaC levels compared to Ren mice. In *ex vivo* microperfusion experiments, EP1-/- tubules show no response to PGE_2 in the presence of AVP, whereas PGE_2 inhibits AVP induced water reabsorption in WT mice. An increase in αENaC membrane accumulation due to EP1 gene ablation results in increased sodium reabsorption subsequently leading to a rise in BP. This contributes to the lack of salt sensitivity in EP1-/- mice. Overall, the EP1 receptor in the collecting duct represents a potential therapeutic target for the treatment of hypertension.

Table of Contents

List of Figures

LIST OF TABLES

Abbreviations

ACR	Albumin to creatinine ratio
AngII	Angiotensin II
AQP	Aquaporin
ATP	Adenosine triphosphate
AVP	Arginine-vasopressin
BP	Blood Pressure
BSA	Bovine serum albumin
cAMP	Cyclic adenosine monophosphate
CCD	Cortical collecting duct
COX	Cyclooxygenase
Cr.	Creatinine
DAG	Diacylglycerol
DNA	Deoxyribonucleic acid
dpm	Disintegration per minute
ELISA	Enzyme-linked immunosorbent assay
ENaC	Epithelial Na^+ channel
gB.W	Gram body weight
GFR	Glomerular filtration rate
EP	E-prostanoid receptor
HS	High Salt
IF	Immunofluorescence
IMCD	Inner Medulla Collecting Duct

IP3	Inositol-1,4,5-trisphosphate
J_{Na+}	Sodium Flux
Jv	Water Flux
LS	Low Salt
NS	Normal Salt
NSAID	Non steroidal anti-inflammatory drug
OMCD	Outer medullary collecting duct
PBS	Phosphate buffered saline
PCR	Polymerase chain reaction
PG	Prostaglandin
PGE_2	Prostaglandin E_2
PI3K	Phosphatidylinositol 3 kinase
PIP_2	Phosphatidylinositol-4,5-bisphosphate
PKC	Protein Kinase C
RIPA	Radioimmunoprecipitation assay
SIADH	Syndrome of Inappropriate Antidiuretic Hormone Secretion
SLP	Sulprostone (EP1 + EP3 Agonist)
SFO	Subfornical Organ
TBS-T	Tris buffered saline-Tween 20
UaV	Urinary Volume
Vte	Transepithelial Voltage
WT	Wild Type

Acknowledgments

I first would like to thank my colleagues and friends who have helped me throughout my way. I would like to thank my supervisor, Dr. Richard L. Hébert, for sticking with me and giving this great opportunity. I appreciate the guidance and support provided by my thesis advisory committee members, Dr. Chris Kennedy and Dr. Mario Tiberi. I would like to thank Joe Zimpelmann for all his work in performing challenging tubular dissections. Big thanks to Kim Yates and Eileen Franklin for their help in performing the mice studies. Last but not least, I thank my Mom and Dad for their support during the ups and downs of my masters.

The dissection and running of microperfusion experiments on isolated tubules were performed by Joe Zimpelmann. The immunofluorescent experiments were a collaboration between Dr. Alex Gustol, Dr. Baptiste Lacoste and I.

1 Introduction

1.1 Kidney

The kidney is responsible for a key number of functions in vertebrates and is located in the posterior of the abdomen[1]. This includes but is not limited to: the conservation of water and key electrolytes (e.g Na^+,K^+, Cl^-); maintenance of blood pH through H^+ reabsorption; secretion of waste products from metabolic processes (e.g urea, creatinine, urobilinogen). The kidney plays a major role in blood pressure regulation through the secretion of renin, the rate limiting enzyme involved in the production of the potent vasoconstrictor Ang II.

The healthy human kidney is made up of approximately one million nephrons[2], the basic structural and functional unit of the kidney. There are five main components of the nephron from the beginning to end:

- **Glomerulus.** A network of capillary beds that is surrounded by the Bowman's capsule of the kidney. It is responsible for filtering blood in the afferent arteriole.
- **Proximal Tubule.** Reabsorption of the majority of electrolytes (approx. 65-80% of filtrate). All the glucose reabsorption happens in this section of the kidney.
- **Loop of Henle.** Responsible for creating the concentration gradient in the medulla by using a countercurrent exchange mechanism. The concentration gradient is used to concentrate urine for excretion.

- **Distal Tubule.** Site of hormonal based regulation for certain ions. The early part of this segment is part of the macula densa, the auto regulatory response element of the kidney.
- **Collecting Duct.** Responsible for the fine tuning of the body's fluid balance through the hormonal regulation of water, sodium and urea reabsorption.

1.2 Collecting Duct

The collecting duct of the kidney is sub divided into three categories. In proximal to distal order they are: cortical collecting duct (CCD); outer medullary collecting duct (OMCD); and the inner medulla collecting duct (IMCD). The CCD is located in the cortex of the kidney, the OMCD is located at the border between the medulla and the cortex, and the IMCD is situated deep in the medulla. Principal cells, cells responsible for the reabsorption of sodium and water, compose 60% of the collecting duct cells[3]. Intercalated cells regulate pH balance through H^+ and HCO_3^- excretion, representing the remaining 40% of the cells [3]. Sodium reabsorption is the strongest in the CCD, whereas water transport occurs all throughout the collecting duct. Urea transport, a process involved in maintaining medulla osmolarity, takes place in the IMCD.

1.2.1 IMCD Water Transport

In the IMCD, water reabsorption is regulated by the antidiuretic hormone arginine vasopressin (AVP). In response to increased plasma osmolarity or decreased blood volume, AVP production is boosted in the hypothalamus and released by the posterior pituitary into the blood

stream[4,5]. AVP binds to the V2R receptor on the principal cells of the IMCD and stimulates the reabsorption of water through osmosis. The V2R receptor is a classical G-coupled protein receptor type G_s[6]. When activated by the binding of AVP, the activated G-protein dissociates into its two subunits $G_{\beta\gamma}$ and $G_{\alpha s}$. $G_{\alpha s}$ is an activator of activate adenylyl cyclase (AC), an enzyme that converts ATP into cAMP.

AQP2 is the water channel responsible for the reabsorption of water on the lumenal membrane[5]. Increased cAMP stimulates water transport via AQP2 in the collecting duct in three main ways. cAMP phosphorylates protein kinase A (PKA), a protein that phosphorylates downstream targets. Immediate actions of PKA include the de-polymerization of F-actin (filamentous) into G-actin (glomerular), allowing for an easier transport of AQP2 to the luminal membrane[7]. PKA also directly phosphorylates AQP2, enhancing the exocytosis of AQP2[8]. For long term regulation, AQP2 protein production is upregulated in a PKA-independent method[9].

1.2.2 CCD Sodium Transport

Sodium is reabsorbed along the entire length of the nephron from the glomerular filtrate. ~65% of filtered sodium is normally reabsorbed by the proximal tubule, largely through the actions of the SGLT co-transporters and the Na^+/H^+ antiporter[10]. Only ~3% of the filtered sodium load is reabsorbed in the IMCD by principal cells in a hormonal dependent manner[10]. Despite the relatively small magnitude of sodium reabsorption by the collecting duct, the fine-tuning of sodium reabsorption that occurs in the collecting duct has been proven to be instrumental in the regulation of Na^+ levels and blood pressure in numerous studies [11,12,13].

The ion transport of sodium from the urine back into the blood is driven by the ENaC transporter via facilitated diffusion on the apical membrane[1]. Once inside the principal cell, the Na^+/K^+ATPase pump on the basolateral membrane transfers the sodium out of the cell and back into the blood stream. ENaC transport of sodium from the luminal side into the cell is widely accepted as the rate limiting step in sodium reabsorption along the collecting duct[14].

1.2.2.1 ENaC

The ENaC tetramer transporter is composed of three homologous subunits: α,β,γ[14]. ENaC controls the reabsorption of Na^+ and Li^+ in many parts of the body including the lung, colon, kidneys and sweat glands. ENaC is only functionally active when inserted into the apical membrane of the principal cells of the collecting duct. Amiloride, a well-known blocker of the ENaC channel, is clinically used as a diuretic[15]. A gain-of-function mutation in ENaC induces severe hypertension (Liddle's syndrome) whereas a loss-of-function mutation leads to natriuresis (pseudohypoaldosteronism)[1].

Just like AQP2, ENaC is a highly regulated protein and the end target of many Renin-angiotensin-aldosterone-system (RAAS) cellular pathways. AVP induces activation of ENaC, though not at the same potency as AQP2[16]. One of the main aldosterone responses is the upregulation of αENaC[17]. Aldosterone binds to the mineralocorticoid receptor (MR), a nuclear hormone receptor in the principal IMCD cells, initiating the transcription of the αENaC mRNA transcript[18]. AngII can also directly bind to the lumenal AT1a receptors enhancing sodium reabsorption through the stimulation of αENaC[12]. Although links between PGE_2 and ENaC signaling have been discussed[19], no direct link has been found.

Of the three ENaC subunits, the production of the fully functional α unit is the rate limiting step in the assembly of the fully functional ENaC subunit[14]. The cleavage of the alpha subunit from 85kDa to 40kDa by serine proteases at the furin consensus cleavage sites has been associated with enhanced sodium transport[20,21]. The ß subunit contains a ubiquitination site that is responsible for ENaC's degradation and recycling[22]. Mutations in the ubiquitin ligase domain of the ß subunit results in increased or decreased ENaC channel trafficking[22]. Elevated cleavage of the γ subunit from 85kDa to 70kDa has been observed in low-Na^+ rats[23], suggesting the γ cleavage results in enhanced activation of the ENaC channel.

1.3 Renal Prostaglandins

Renal prostaglandins (PG) play a paramount role in maintaining homeostatic renal blood flow as well as salt excretion[24]. Prostaglandin E2 (PGE_2) is a major PG produced in the medulla and macula densa via cyclooxygenase (COX) enzymatic activity (figure 1). COX-1 has been shown to be constitutively expressed in the kidney while COX-2 is inducibly expressed[25].

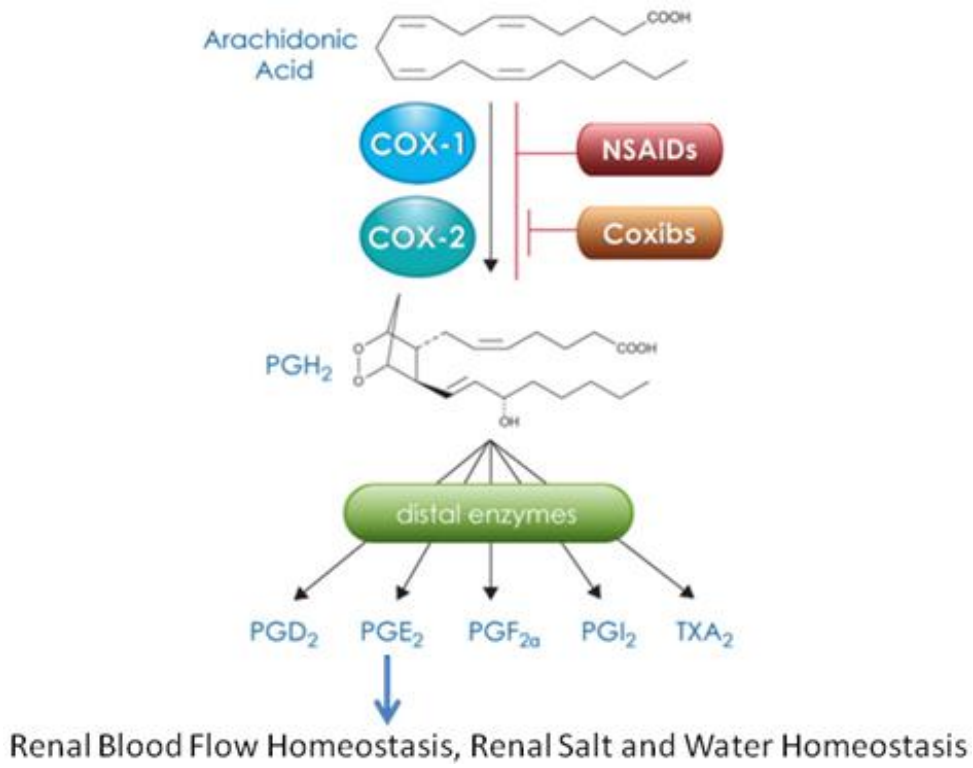

Figure 1. Schematic representation of the prostaglandin synthesis pathway. Arachidonic acid is liberated by PLA_2 from membrane phospholipids and transformed into PGH_2 by cyclooxygenases (COX-1 or COX-2). COX-1 and COX-2 activity is inhibited by NSAIDs, COX-2 is exclusively inhibited by Coxibs. PGE_2 is produced by PGE synthase (PGES).

PGE_2 exerts its actions through four different GPCRs, EP1 through EP4, as seen in figure 2[26]. EP2 is mainly found in interstitial cells[27] and the vasculature smooth muscle of the afferent arteriole[26]. EP4 is found in the juxtaglomerular cells of the afferent arteriole and promotes renin release[28]. EP1 and EP3 have been detected and implicated in sodium and water transport along the collecting duct[27], however the exact signaling pathway remains elusive.

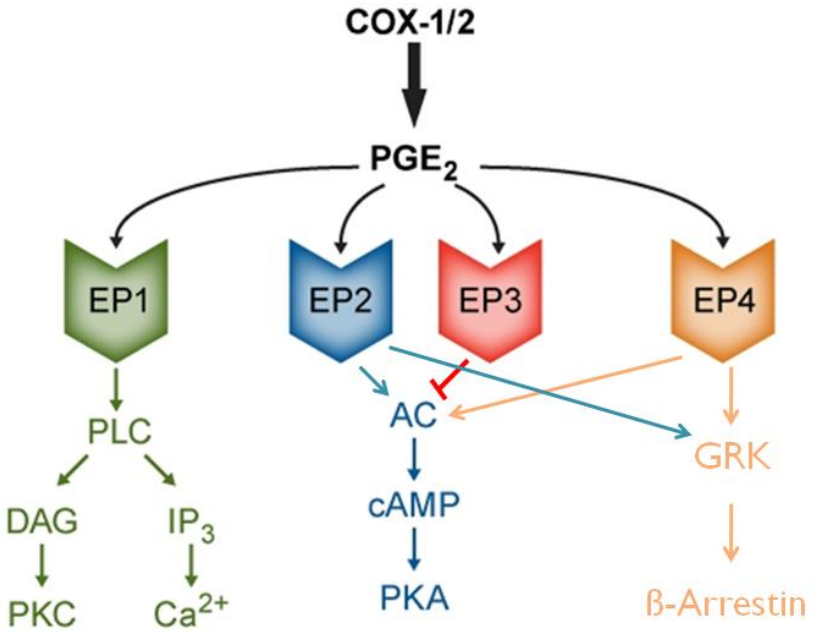

Figure 2. PGE_2 signaling pathways through receptors EP1 through EP4. Activation of EP_1 (coupled to G_q) activates PKC and increases intracellular Ca^{2+} through PLC[29]. Activation of EP_3 (coupled to G_i) inhibits cAMP production via adenylate cyclase (AC) blockade[30]. Activation of EP_2 or EP_4 (both coupled to G_s) stimulates cAMP production via AC[27] and activates ß-Arrestin through GRK[31].

PGE_2 is a well known diuretic and natriuretic compound in the collecting duct. In isolated rabbit CCD tubules, PGE_2 at 10^{-7}M decreases AVP induced water flux (J_v)[32]. PGE_2 has also been found to inhibit sodium reabsoprtion on isolated rabbit CCD tubules, an effect nullified upon the addition of an EP1 antagonist (AH6809)[33]. Studies using various PGE_2 antagonists and agonists have shown that water and sodium transport inhibition occurs through a Ca^{2+} and Gi coupled mechanism inhibiting cAMP production[32,33,34].

During the early stages of dehydration, plasma Na^+ builds up as a result of fluid loss. As a compensating mechanism, urinary Na^+ excretion is increased to relive the build up of plasma Na^+, a process termed dehydration natriuresis[35]. Water deprivation[36],[37] and elevated tonicity[38],[39]

have been found to increase PGE_2 synthesis in the renal collecting duct. For instance, 24h dehydrated microsomal prostaglandin E synthase-1 knockout mice were unable to maintain normal plasma osmolarity compared to their WT counterparts[36]. These findings prove that PGE_2 acts as a buffer towards AVP and AngII through its renal salt and water handling.

1.4 EP1 vs. EP3

There have been conflicting reports in the literature as to whether or not the Gi linked EP3 receptor and/or the Gq linked EP1 receptor is responsible for inhibiting sodium and water reabsorption in the collecting duct[27]. In 1993, Hébert *et al.* found that the sulprostone (SLP), an EP1 and EP3 agonists (EP1 K_i = 21nM, EP3 K_i = 0.6nM) , reverses AVP induced water transport in the collecting duct[32]. This effect is eliminated with pretreatment of pertussis toxin[32], indicating a clear involvement of the Gi linked EP3 receptor. Tamma *et al.* showed in 2003 SLP inhibited AVP induced AQP2 membrane translocation in rat IMCD primary cell culture, an effect still observed in the presence of an EP1 antagonist (SC-19220)[40]. This suggests that EP3 is the inhibitory receptor in the IMCD, not EP1. Gonzalez at al. showed in 2009 that SLP inhibited aldosterone upregulated αENaC expression in rat IMCD primary cell culture, a phenomenon blunted upon the addition of SC19220[41]. This suggests that EP1 is the main PGE_2 receptor in the IMCD. Figure 3 shows the current thinking with regards to the diuretic effects of PGE_2 has in the collecting duct.

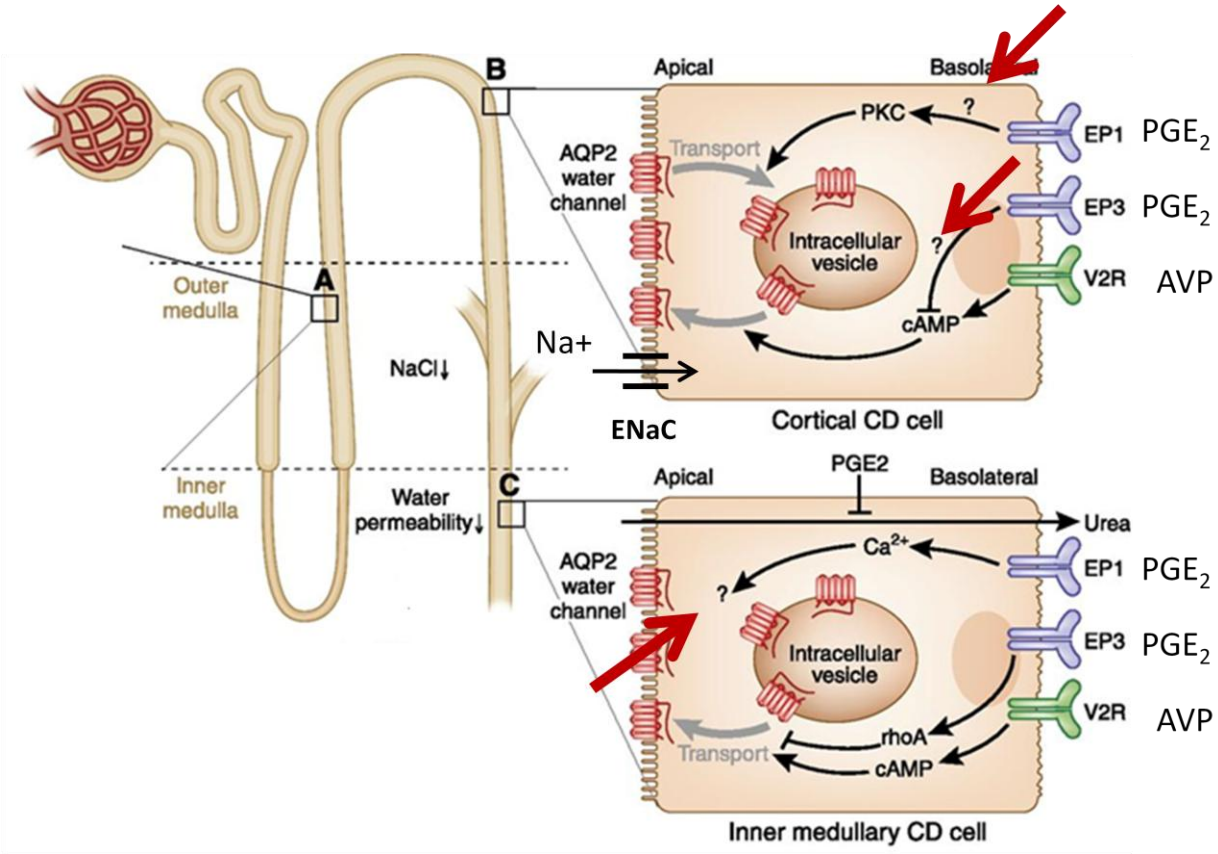

Figure 3. Hypothesized diuretic effects of the kidney along the collecting duct. Arrows indicate the question marks showing the ambiguity as to the exact signaling mechanism. Adapted from Olesen *et al.*[27].

1.5 EP1 in the Hypothalamus

EP1-/- mice were generated in 2007 by Guan *et al.* at the University of Vanderbilt to examine the renal effects the EP1 receptor has on the contribution to hypertension[42]. A major finding from this study was EP1's function as a vasoconstricting agent in the mesenteric arteries[42]. Unexpectedly, the urinary concentrating defect of EP1-/- mice was found not to be due to EP1's actions in the collecting duct, but rather EP1's role in the production of AVP within

the hypothalamus[43]. To prove a direct role of EP1 on the brain AngII response, adenoviral-mediated reconstitution of EP1 receptor in the subfornical organ (SFO) was performed in EP1-/- mice[44]. Briefly, the SFO is active in osmotic, cardiovascular and energy regulation in the brain. Successful EP1 receptor adenovirus insertion into EP1-/- mice rescued the Ang II pressor response that was blunted in EP1 mice[44]. Taken together, these two studies prove an indirect role of the EP1 receptor on hypothalamus AVP release (figure 4).

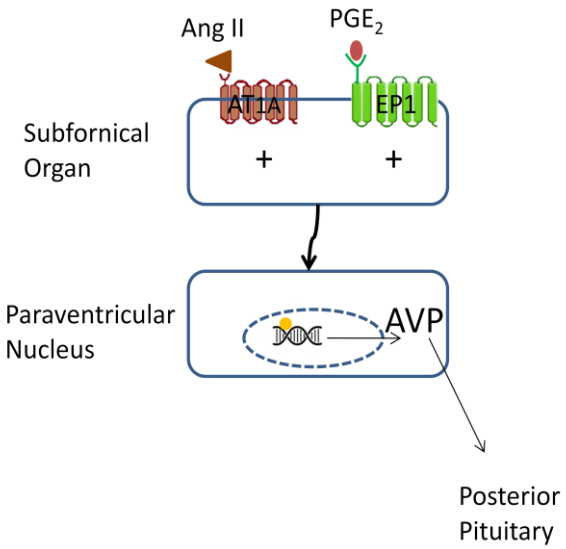

Figure 4. Simplified schematic representation of the EP1 and AT1a receptor's role in the neural networks controlling AVP release. Projections from one nucleus to another are represented with arrows. Positive signs indicate a stimulation of an excitatory projection.

1.6 NSAIDs and the Kidney

Non-steroidal anti-inflammatory drugs (NSAIDs) are available as over the counter medication in Canada. Current clinical guidelines discourage the use of NSAIDs for those with high blood pressure as NSAIDs can result in an unsafe rise in blood pressure[45]. NSAIDs can

induce different types of kidney damage including[46]: electrolyte and acid-base disorders; acute interstitial nephritis, nephrotic syndrome and papillary necrosis. Taking NSAIDS while on a diuretic and an ACEI inhibitor results in what is known as a "triple whammy" effect whereby significant renal impairment occurs[47]. A practical application of this study is to find the link between NSAIDs, the EP1 receptor and renal dysfunction.

1.7 Salt Sensitivity

On average, adult Canadians consume about 3,400 mg of sodium per day[48]. This is significantly above the level recommended as the upper tolerable limit for health, which is 2,300 mg per day[48]. Salt sensitivity is a measure of how much the blood pressure changes in response to dietary salt changes. Certain populations are more susceptible to blood pressure increases as a result of augmented sodium intake (e.g African Americans and Southern Asians)[49]. The popular belief among many is that either the kidneys[50,51,52], the vasculature[53,54,55] or a combination of the two are responsible for salt sensitivity. Another practical application of this study is to examine the kidney's role in salt sensitivity.

1.8 RAAS System

The RAAS system is the body's natural mechanism of maintaining normal fluid balance and blood pressure. In cases of blood loss or a drop in pressure, the macula densa senses a lower renal perfusion pressure and a reduced NaCl concentration. This activates the juxtaglomerular

cells in the kidney to release renin. Renin catalyzes the rate limiting step of the RAAS system, the conversion of angiotensinogen to angiotensin I. Angiotensin I is converted to Angiotensin II (AngII) via the ACE enzyme found on the surface of pulmonary and renal endothelium. AngII is the main RAAS system effector with numerous effects on the body including: driving a thirst response, increasing aldosterone secretion in the adrenal cortex, activating the sympathetic system, blood vessel constriction and AVP secretion from the posterior pituitary lobe.

The renal collecting duct is one of the main loci for RAAS system effects. AngII can directly bind AT1a receptors in collecting duct principal cells to promote enhanced sodium reabsorption[11]. Aldosterone promotes sodium transport by increasing in the abundance of the αENaC subunit[17]. AVP promotes water transport by increasing AQP2 levels in the apical membrane[5]. The end result of these changes is an increase in the effective circulating volume, which causes a negative feedback on the juxtaglomerular cells release of renin.

2 Hypothesis

The natriuretic and diuretic effects of EP1 receptor activation by PGE_2 in the collecting duct are beneficial defense mechanisms against excessive RAAS activation.

2.1 Objectives

1. Evaluate the natriuretic and diuretic effects of mice lacking the EP1 receptor in a hypertensive setting.
2. To determine the renal physiological roles of the EP1 receptor and AngII on mice feed high and low salt diets.

3 Methods

3.1 Animals

All procedures were approved by the Animal Care and Veterinary Service (ACVS) at the University of Ottawa. Global EP1-/- and global EP3-/- mice on a C57BL/6 background were generously donated by Dr. Richard M. Breyer (Vanderbilt University, Nashville, TN). EP1-/- were generated using a hit and run strategy whereby a stop codon and an EcoRI restriction site was introduced into exon 2[42]. The EP1-/- mice were backcrossed for ~10 generations from a C57BL/6 background onto a FVB/NJ background.

Hypertensive TTRhRen (Ren) mice were generously donated by Dr. Timothy L. Reudelhuber (Université de Montréal, Montréal, QC). Expression of a modified human pro-renin cDNA transgene was achieved under control of a 3-kb region of the mouse transthyretin promoter[56]. The synthesis of active human renin was optimized by introducing a furin cleavage site flanked between the pro and active segments of the renin transgene. Cleavage of the pro segment from the renin transgene occurs by the ubiquitously expressed serine proteases in cells expressing this construct. EP1-/- mice and Ren mice were crossed together to generate the Ren EP1-/- genetic line along with the corresponding WT, Ren and EP1-/- littermates.

All mouse chows were provided by Harlan Tekland. The sodium deficient diet (TD.90228) contained <0.02%wt. NaCl; the normal salt diet (TD.2018) contained 0.4%wt. NaCl; the high salt diet (TD.92012) contained 8%wt. NaCl. The male mice were given a four day transition period between each diet change to acclimatize to the new diet. Male mice were

rotated through the salt diets in the following manner (figure 5). Subsets of mice were sacrificed at the 8-10 week mark on the NS diet for pathology and IHC experiments.

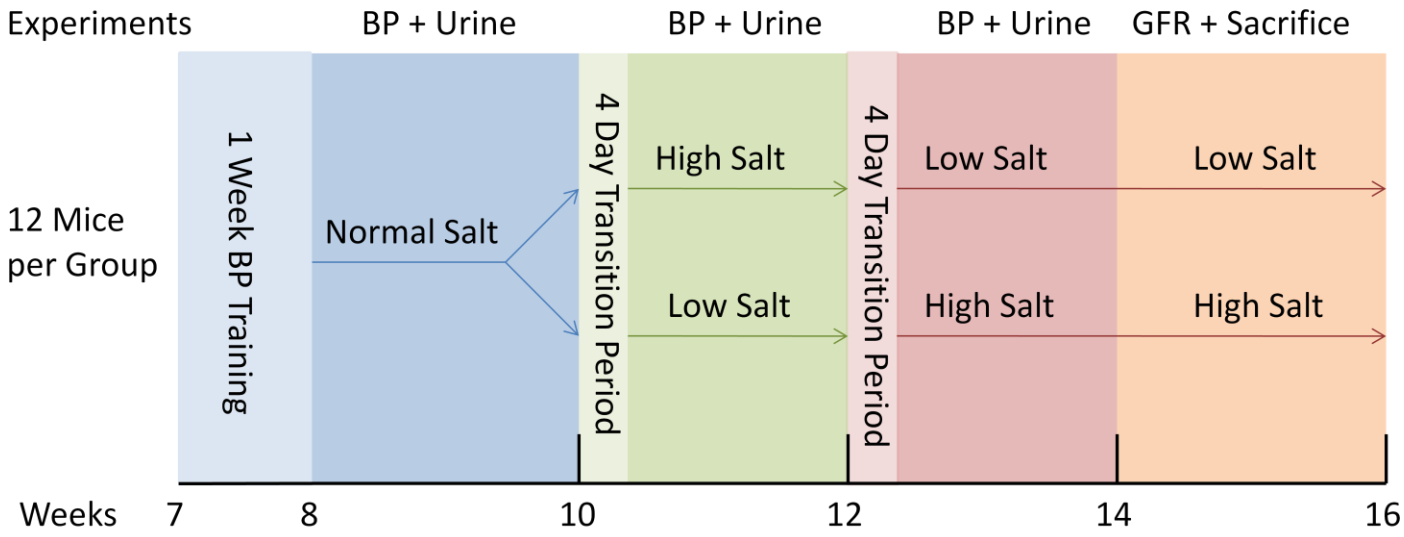

Figure 5. Flow chart illustration of the *in vivo* study design and the rotation of the mice on the different salt diets.

3.2 PCR Genotyping

REDExtract-N-Amp Polymerase Chain Reaction (PCR) ReadyMix Kit (Sigma-Aldrich MO, USA) was used to extract DNA from freshly snipped ear tissue as per manufacturer's protocol. The EP1 gene was amplified using the forward 5′-ACC AGC GCT GCC TAT CTT CTC CAT -3′ and reverse 5′- GTC AAC AAG CTG GGA AGG AA AAG GCT ATG AA-3′ primers. The Ren transgene was amplified using the forward 5′- CAT GGG CTT CAT TGA ACA G-3′ and reverse 5′-AAA GAA CAA TCA AGG GTC -3′ primers. The EP1 construct was subjected to an EcoRI restriction digestion (Fisher Scientific) as per manufacturer's protocol. Both the EP1 and Ren amplified DNA was run on a 1% gel and bands were visualized using ethidium bromide.

3.3 Blood Pressure Measurement

Blood pressure was measured via tail-cuff plethysmography (BP 2000, Visitech systems, Apex, NC). Mice were trained for five days to acclimatize to the system. Following the training period, daily systolic blood pressure was measured at the same time each day for five days. During the measurement period, 5 preliminary readings were performed followed by 10 actual readings. Systolic blood pressure readings for each day were retained if there was a minimum of 4 out of 10 successful readings and the standard deviations for all the readings were less than 20 mmHg.

3.4 Metabolic Cage Measurement

Daily urine output as well as daily food and water intake were monitored using specially designed metabolic cages (Techniplast, West Chester, PA). Water intake, urine output and food intake was recorded for mice on a 24 h basis for three days straight. Results shown are the average water consumed in 24 h during the three day observation period. Body weights were taken immediately before and after the experiment. Data was retained from the metabolic cages if the mice lost no more than 10% of their starting body weight. Food, water and urine output were normalized to the average body weight of the mice before and after the metabolic cages.

3.5 Urine Analysis

All urine analysis was performed on spot urine that was kept frozen at -80^{o}C. Urine albumin was quantified using a Mouse Albumin ELISA set (Albuwell M, Exocell), as per manufacturer's guidelines. Urine creatinine was quantified using a picric acid assay (Creatinine Companion, Exocell) as per manufacturer's guidelines. AVP concentrations were determined using an ELISA kit (Cayman Chemicals, Ann Arbor, MI) as per manufacturer's guidelines. Urine osmolarity was measured using a freezing point depression system (Advance Instruments Inc., Norwood, MA).

3.6 Glomerular Filtration Rate and Hematocrit Measurement

Glomerular filtration rate was estimated by fluorescein isothiocyanate (FITC)-inulin (Sigma-Aldrich, MO, USA) plasma clearance. 5% FITC-inulin was prepared in 0.9% NaCl. To remove residual FITC not bound to inulin, the solution was filled into a 1000 Daltons cut-off dialysis membrane (Spectra/Pro 6, Spectrum Laboratories Inc., Rancho Dominguez, CA). The dialysis membrane filled with FITC-inulin was stirred suspended in 0.9% NaCl for 24 hrs at room temperature. Prior to use, the dialyzed solution was sterilized by filtration through a 0.22 µm filter (Sigma-Aldrich, MO, USA). The conscious mouse was restrained in a 50 ml Falcon tube and 5% FITC-inulin (3.74 µl/ g body weight) was injected in the tail vein. Approximately 20 µl blood was collected in a heparinized capillary tube (Thermo Fisher Scientific) by puncture of the saphenous vein using a sterile 23-gauge syringe needle. On average, this yields 10 µl of plasma following centrifugation (1,500 G, 10 min). Blood was sampled via the saphenous vein at

3, 7, 10, 15, 35, 55, and 75 minutes post injection of FITC-inulin. Hematocrit percentage was measured from the 3 minute mark collection. A two-compartment clearance model was employed for the calculation of GFR. At any given time (x), the plasma concentration of the tracer (Y) equals $Ae^{-\alpha tx} + Be^{-\beta tx}$ + Plateau. The parameters of the above equation were calculated using a non-linear regression curve fitting program (GraphPad Prism, GraphPad Software, Inc., San Diego, CA). GFR was calculated using the equation: GFR = I/ (A/α + B/β), where I is the amount of FITC-inulin delivered by the i.v. injection, A (Span 1) and B (Span 2) are the y-intercept values of the two decay rates, and α and β are the decay constants for the distribution and elimination phases, respectively.

3.7 Sacrifice Procedure

Mice were anaesthetized using isoflurane (3.5%) in 100% O_2. The abdominal cavity was cut open and the diaphragm removed to reveal the heart. Blood collection was performed through a cardiac puncture into the left ventricle using a heparinized 27 guage needle. The blood was spun down at 2,000g for 10 minutes and the plasma was stored at -80^{o}C. The left kidney was excised, weighed, and transversely split into two. Half of the kidney was used for electrophysiological experiments; the other half was placed in 4%PFA for 24h fixation. The right kidney was excised, weighed, and microdissected into the medulla and cortex. The medulla and cortex components were flash frozen in liquid nitrogen and stored at -80^{o}C. Both tibias were excised from the mice and lengths measured using an electronic caliper.

3.8 Immunoblotting

Kidney tissue was pulverized with a COE Capmixer and suspended in RIPA lysis buffer (150 mM NaCl, 1% Triton X-100, 0.5% sodium deoxycholate, 0.1% SDS and 50 mM Tris pH 8.0), supplemented with protease and phosphatase inhibitors (Thermo Scientific). The supernatant was then centrifuged at 16,000g for 20min and the pellet was discarded. Protein concentration was determined using a Lowry based assay (Biorad). Supernatants were treated with 6x Laemmli loading buffer and 50 μg of proteins resolved on SDS-polyacrylamide (8%) gels and transferred to nitrocellulose. Membranes were then blocked for 1 h with 70µm filtered 3% nonfat dry milk (NFM) in Tris-buffered saline (TBS) (pH 7.4) containing 0.05% (w/v) Tween 20 (TBST). The membranes were incubated overnight with the following primary antibodies in 1% NFM TBST: 1:500 anti-COX-1 (N^{o}160109,Cayman Chemical), 1:500 anti-COX-2 (N^{o}160106, Cayman Chemical). Detection was performed with either mouse or rabbit 1:5000 anti-IgG-HRP (Promega, Madison, WI). The blots were visualized with enhanced chemiluminescence (SuperSignal West Pico Chemiluminescent Substrate, Thermo Scientific, Rockford, IL, USA) and detected using film. Digital images were taken using a Chemidoc MP system (Bio-Rad, Hercules, CA, USA) and normalized to β-actin (Sigma-Aldrich, MO, USA).

3.9 Histology and Immunofluorescence

Following 24h PFA fixation, kidney slices were washed three times in PBS and sent off to the University of Ottawa Pathology department for paraffin embedding. Slides were permeabilized in xylene and rehydrated through a graded series of alcohol. PAS staining was

performed as per protocol (Sigma Aldrich) and imaged under x40 and x63 magnification (Axioskop 2 Imager A1, Zeiss, Germany). A pathogolist blinded towards the identities of the groups examined the sections looking for signs of kidney damage and abnormalities.

For immunofluorescence, slides were blocked with 10% donkey serum in 1%BSA PBS for 1 hour followed by overnight primary antibody incubation with 1:200 mouse anti-AQP2 (sc-515770,Santa Cruz) and 1:200 rabbit anti-αENaC (SPC-403, Stressmarq).1:100 Cy3 and Alexfouro488 conjugated secondary antibodies were incubated for one hour and the nuclei were counterstained with Hoechst 33342. The slides were mounted and images analyzed using a Zeiss AxioImager.M2/ApoTome.2 Microscope (Zeiss, Jena, Germany).

3.10 IMCD Water Flux Microperfusion

IMCD water perfusion experiments were performed as previously described[57]. Male mice at ~6 weeks old were sacrificed using a 5%CO_2/95%O_2 mixture. The kidneys were quickly removed, and 1 to 2 mm coronal slices were placed in chilled dissection dishes for freehand dissection of IMCD tubules, distinguished from other segments based on various properties: diameter difference, cell heterogeneity, translucency. The microdissected IMCD was then transferred to a chamber for in vitro perfusions and measurement of net fluid reabsorption (J_v).

Microdissected IMCD tubules were transferred to a thermostatically controlled chamber of 1 cm^3 volume and cannulated using concentric micropipettes. Bath solution was continuously exchanged at 0.5 ml/min by an infusion pump and was maintained at 37^oC. The dissecting solution consisted of (mM): NaCl, 137; $MgCl_2$, 1; MgSO4, 0.8; KCL, 5; $CaCl_2$, 0.25; Tris HCl,

10; Na_2HPO_4, 0.33; glutamine, 2; KH_2PO_4, 0.44; and L-lactate, 2. The perfusate composition was (in mM): NaCl, 115; $NaHCO_3$, 25; KCl, 5; $CaCl_2$, 1.5; $MgCl_2$, 1.2; glucose, 8; HEPES, 5; Urea, 10; NH_4Cl, 5 (pH 7.4, 310 mOsmol). The composition of bath medium was (in mM): NaCl, 190; $NaHCO_3$, 25; KCl, 5; $CaCl_2$, 1.5; $MgCl_2$, 1.2; glucose, 8; HEPES, 5; Urea, 10; NH_4Cl, 5, and BSA, 0.1% (pH 7.4, 450 mOsmol). The perfusate, which contained ^{3}H-inulin (75 µCi/ml) as a volume marker was collected into a constriction pipette of known volume (between 90 and 130 nl) and counted for ^{3}H-inulin (New England Nuclear, Boston, MA). The perfusion rate was maintained between 12-20 nl/min by adjusting the hydrostatic pressure. In control studies, 30 min of equilibration were allowed and then, three collections were made for calculation of basal Jv in $nl \cdot mm^{-1} \cdot min^{-1}$. Then 10^{-12} M AVP (Sigma) was added to the bath and five timed collections were made to determine net volume reabsorption (Jv). Following the five collections, 10^{-7} M SLP or 10^{-7}M PGE_2 was added into the basolateral bath and an additional five collections were made to determine Jv. Jv was calculated as the difference between the perfusion rate V_o and the collection rate V_L, both in nl/min, normalized to tubule length (L, in mm): $Jv = (V_o - V_L)/L$, where $V_o = V_L (C_L/C_o)$, where C_o and C_L are perfusate and collected fluid concentrations in cpm/nl, respectively.

3.11 CCD Transepithial Voltage Measurements

A CCD tubule was cannulated using concentric micropipettes as performed in the water transport studies. Transepithelial voltage (Vte) was measured across the CCD tubule using two probes, one inserted into the lumen of the tubule with the other inserted in the basolateral bath. The composition of the bath, dissection, and perfusate medium was (in mM): NaCl, 101; $NaHCO_3$, 22; KCL, 5; $CaCl_2$, 1; $MgSO_4$, 1.2; glucose, 10.5; glutamine, 2; L-lactate, 2;

phosphoric acid, 1.2, and Hepes, 32.5 (pH 7.4, osmolality 300 mOsmol). BSA (1%, Sigma, St. Louis, MO) was added into the bath and dissection solutions prior to the experiments. The perfusion rate was maintained between 12-20 nl/min by adjusting the hydrostatic pressure. The Vte is measured at the perfusion end via a perfusion pipette that is connected to an electrometer (WPI, KS-700). The perfusion pipette is fitted with a fluid exchange pipette, permitting multiple reloading with different solutions during one experiment. Fluid changes in the lumen are accomplished by switching a hydrostatic pressure head from one channel to another. When indicated, PGE_2 was added at a concentration of 10^{-7}M into the basolateral bath while AngII was added at a concentration of 10^{-6}M into the lumen of the CCD tubule.

3.12 Statistics

Data was analyzed using GraphPad Prism 6 software. Values are expressed as means ± standard error of the mean (SEM). For sacrifice parameters and metabolic cage parameters, statistical analyses were performed using a one-way ANOVA. Two-way ANOVA analysis was performed on all other tests. Post hoc testing was performed using a Tukey post-test. Fluorescent images were analyzed using the FIJI variant of the image-analysis program ImageJ.

4 Results

4.1 Confirming the Ren and EP1 Genotype

Mice were genotyped before the start of the study to confirm identity. Figure 6 shows a representative electrophoresis gel of DNA following the amplification and digestion of the EP1 gene. One band (1065bp) indicates an EP1+/+ genotype, two bands (616, 449) bp indicates an EP1-/- genotype, and three bands (1065,616, 449bp) indicates an EP1+/- genotype. Three control mice were run on the far right of the gel to confirm the banding pattern. Mouse 123 is homozygous for the knockout EP1 gene. Mouse 159,119 and 158 are heterozyogous for the knockout EP1 gene. Mouse 117 is homozygous for the WT EP1 gene.

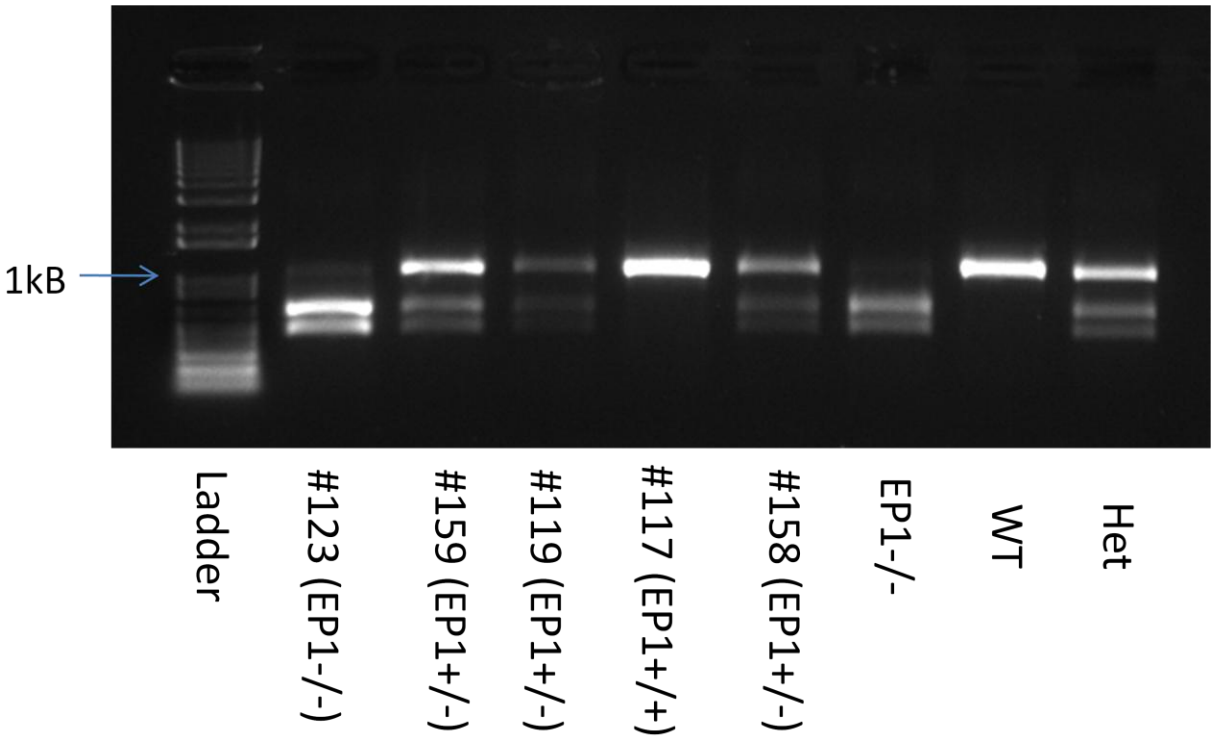

Figure 6. Electrophoresis gel confirming the EP1 genotype of mice used in the study. The presence of one band at 1065bp indicates a mouse positive for the EP1 gene, the presence of two bands at 616, 449bp indicates a mouse negative for the EP1 gene, the presence of three bands at 1065, 616 and 449bp indicates a mouse heterozygous for the EP1 gene. A 1 kbp DNA ladder was loaded into the first lane.

Figure 7 shows the representative electrophoresis gel of DNA following the amplification of the Ren gene if present. A band at ~650bp indicates the presence of the Ren gene, no band indicates the absence of the Ren gene. Mouse 187 and 198 test positive for the Ren gene while mouse 185 and 181 test negative for the Ren gene.

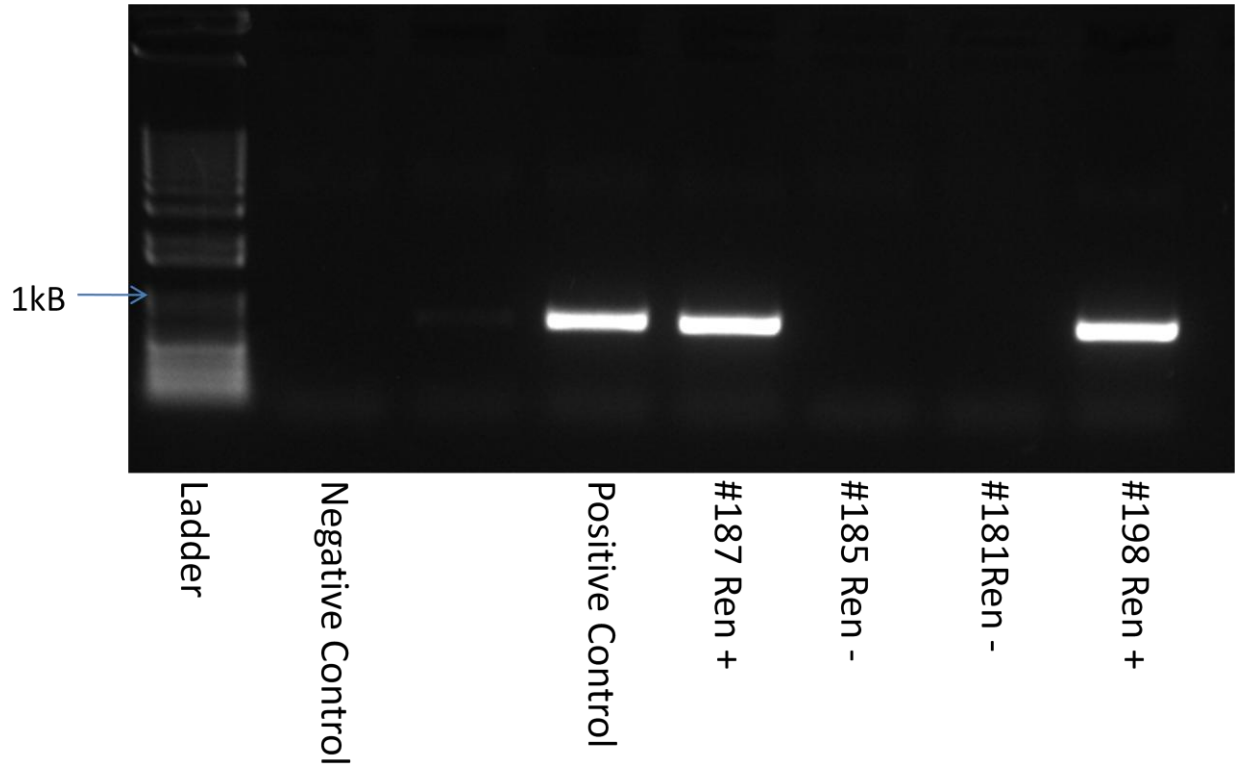

Figure 7. Horizontal electrophoresis gel confirming the presence or absence of the overexpressing renin gene in mice. A band at ~650bp indicates the presence of the overexpressing renin gene, no band indicates the absence of the overexpressing renin gene. A 1 kbp DNA ladder was loaded into the first lane.

4.2 Physiological Parameters at Sacrifice

The tibia length was recorded for an accurate measurement of growth. The kidney weight was taken and normalized to body weight to screen for renal hypertrophy. Body weight was normalized to kidney weight to screen for adiposity. EP1-/- and Ren EP1-/- mice both have shorter tibia lengths compared to WT mice, indicating slightly stunted growth. This is consistent with previous findings[58]. Kidney weights were unchanged, indicating no renal hypertrophy. Body weights were unchanged, indicating no differences in adiposity.

	WT	EP1-/-	Ren	Ren EP1-/-
Mouse Weight (g)	29.7± 0.6	27.8± 0.6	31.1± 0.5	28.6± 1.0
Kidney Weight (g)	0.198± 0.006	0.203± 0.004	0.214± 0.006	0.192± 0.008
Tibia Length (mm)	17.55± 0.11	16.88± 0.13***	17.73± 0.04	16.99± 0.14**
KW(mg)/Tibia(mm)	11.2± 0.3	12.0± 0.2	12.1± 0.3	11.3± 0.4
BW(g)/Tibia(mm)	1.69± 0.03	1.65± 0.03	1.75± 0.02	1.68± 0.05
*p <0.05,**p<0.01, ***p<0.001 vs. WT				
n=12				

Table 1. Physiological parameters at sacrifice of 16 weeks old mice. KW = kidney weight, BW = body weight. Tibia length is slightly shorter for EP1-/- and Ren EP1-/- mice compared to WT mice. N=12.

4.3 Systolic Blood Pressure

Blood pressure (BP) was measured in the four mice groups on the three diets (figure 8). WT mice have a standard systolic blood pressure of 127mmHg on a NS diet, a BP reading that does not change on a HS or LS diet. EP1-/- mice have an identical NS BP reading as the WT mice (127mmHg) and their BP does not vary based on the salt diet.

The NS systolic BP of Ren mice is 150mmHg, a value that jumps to 161mmHg on a HS diet but drops to 136mmHg on a LS diet. The Ren EP1-/- mice do not experience a significant BP drop while on a LS diet (150mmHg), nor do they experience a statistical increase in BP on a HS diet (156mmHg) when compared to their BP on a NS diet (152mmHg).

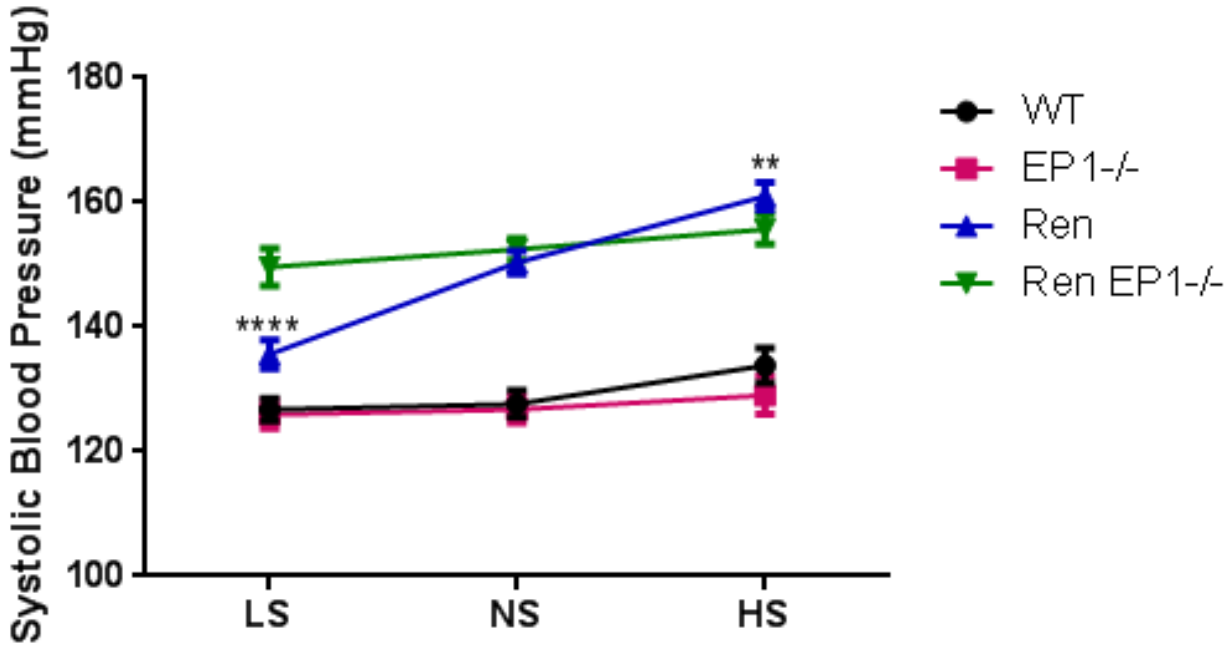

Figure 8. Average systolic blood pressure measured by tail cuff from five days of measurements on each salt diet. Statistical comparison was performed comparing the BP of mice on a LS and HS diet to the NS diet. The systolic blood pressure drops for Ren mice on a LS diet, while increasing for Ren mice on a HS diet. ** = $p<0.01$, **** = $p<0.0001$. N =11-12.

4.4 Urinary Concentrating Ability

Ren mice are clearly salt sensitive, increasing their BP on a HS diet and decreasing their BP on a LS diet. This response is blunted in Ren EP1-/- mice, setting up the basis for the study.

To try to understand whether the kidney's actions could account for the changes in salt sensitivity, the urinary output and water intake was analyzed.

Urine output (figure 9), water intake (figure 10) and food intake (figure 11) were collected from mice individually housed in metabolic cages. A ~10 fold increase in the UaV was observed on the WT HS mice compared to the WT NS diet (figure 9). No statistical change in UaV was observed between the WT LS mice compared to the WT NS diet, consistent with published results[59,60].

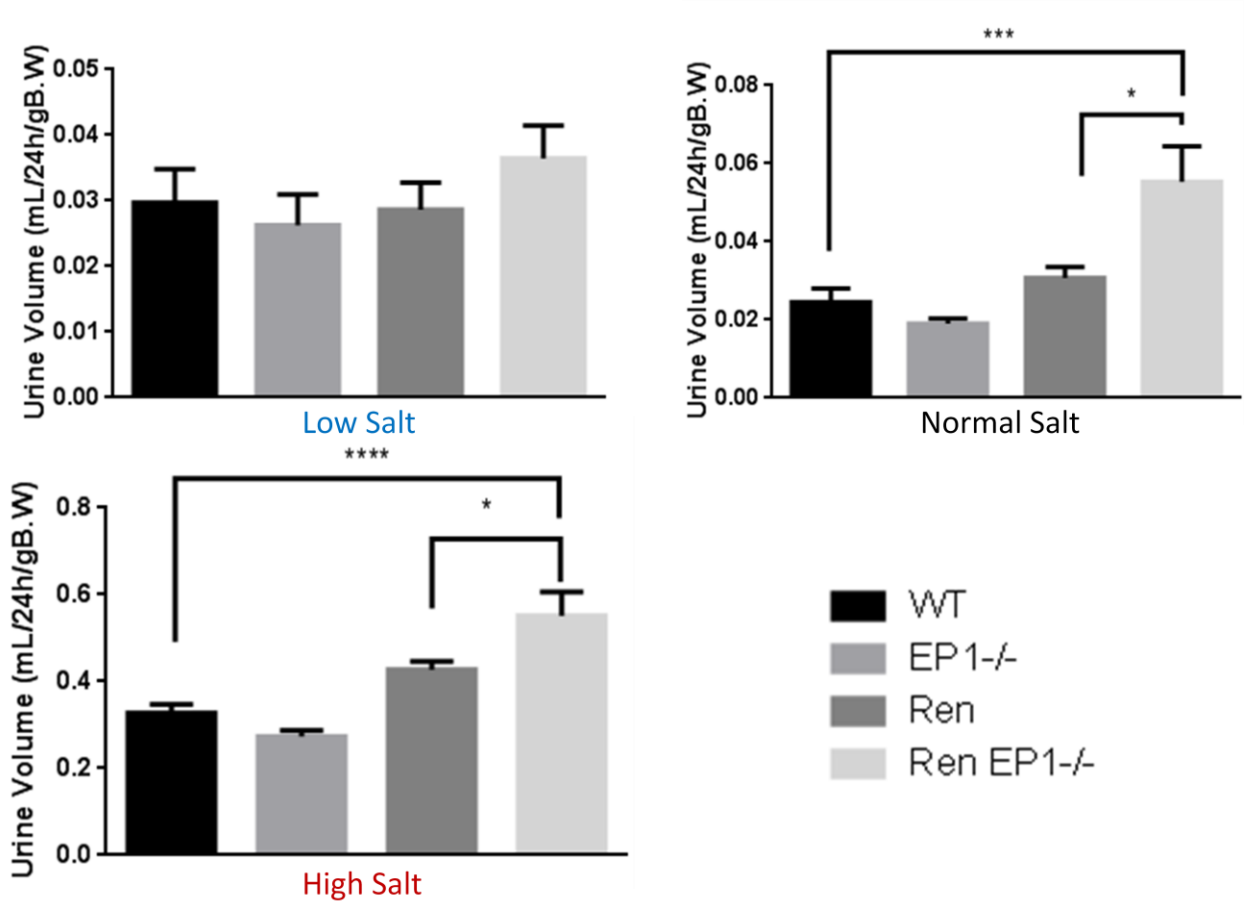

Figure 9. Urine volume (mL) per 24 hours corrected per gram body weight on low, normal and high salt diets. No statistical change was observed on a LS diet. Ren EP1-/- are

polyuric compared to Ren mice on a NS and HS diet. * = $p<0.05$, *** = $p<0.001$, **** = $p<0.0001$. N = 10-12.

On the NS diet, EP1-/- and Ren mice display the same urinary output and water intake as the WT mice (0.024 mL UaV/24h/gB.W, 0.14mL H_2O/24h/gB.W). The EP1-/- results are consistent with literature findings[43]. Ren EP1-/- mice are unexpectedly polyuric (0.055 mL UaV/24h/gB.W) and polydipsic (0.19mL H_2O/24h/gB.W) compared to WT mice. On a LS diet, the Ren EP1-/- mice display similar urine output and water intake (0.036 mL UaV/24h/gB.W, 0.17mL H_2O/24h/gB.W) compared to WT mice. On a HS diet, Ren mice have a statistically increased water intake (0.71mL H_2O/24h/gB.W) compared to WT (0.56mL H_2O/24h/gB.W) mice. Ren EP1-/- maintain their polyuria (0.55 mL UaV/24h/gB.W) compared to Ren mice (0.43 mL UaV/24h/gB.W) and their polydipsia (0.77mL H_2O/24h/gB.W) compared to WT mice on a HS diet.

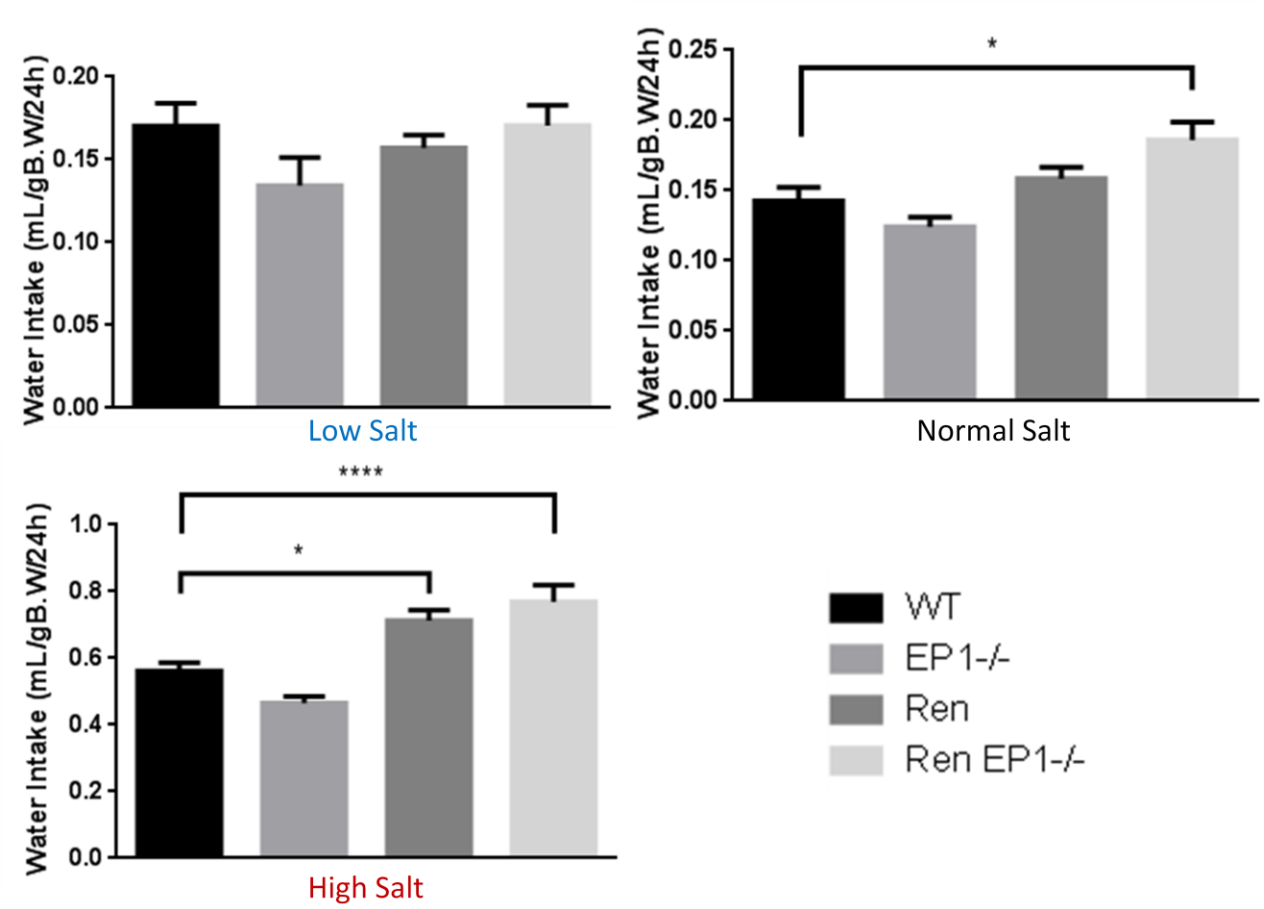

Figure 10. Water intake (mL) per 24 hours corrected per gram body weight on low, normal and high salt diets. No statistical change was observed on a LS diet. Ren EP1-/- are polydipsic compared to WT mice on a NS and HS diet. Ren mice have elevated water intake compared to WT mice only on a HS diet. *$p<0.05$, ****$p<0.0001$. N = 10-12.

All values were corrected for body weight to account for differences in size. No change was found in the food intake between all the groups indicating that the mice had been properly acclimatized to the new food within four days.

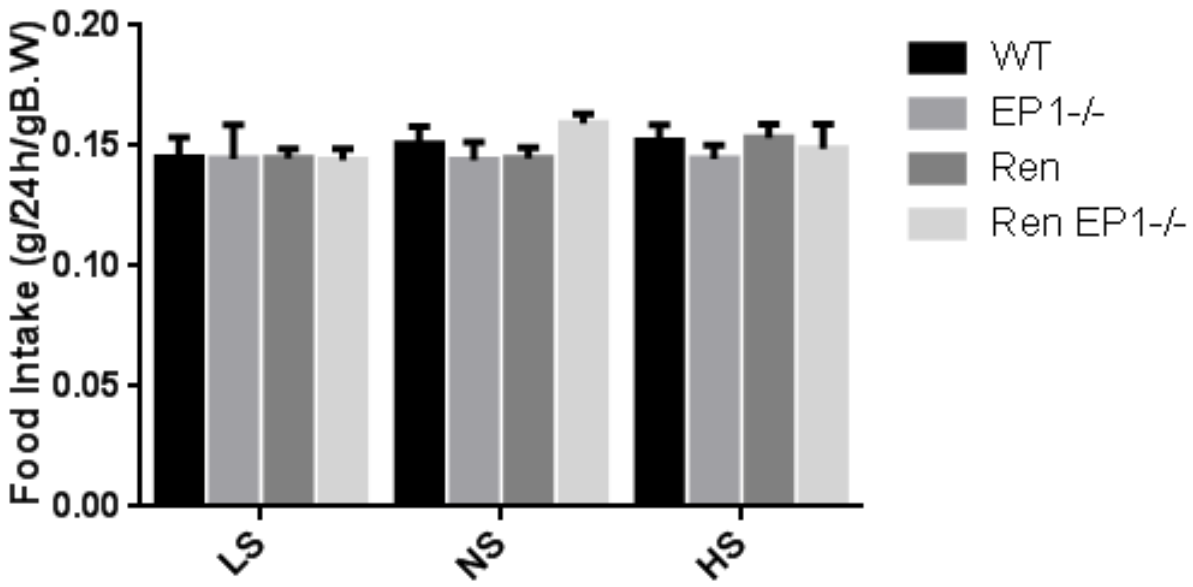

Figure 11. Food intake (g) per 24 hours corrected per gram body weight on low, normal and high salt diets. No statistical change was observed between any groups. N = 10-12

4.5 Urinary Osmolarity

According to the metabolic cage data, the urinary concentrating defect displayed by Ren EP1-/- is inextricably linked to NaCl intake. To understand the link between the urinary concentrating defect and NaCl, urinary electrolyte values were analyzed. In general, there are five major components that contribute to urinary osmolarity: Na^+,Cl^-,K^+,urea and glucose (if diabetic). Measuring the urine osmolarity gives an indirect measurement on the NaCl content in the urine (figure 12).

Despite Ren mice having the same urinary output and water intake as WT mice, their osmolarity is depressed (1900mOsm/kgH_2O) compared to WT mice (2414mOsm/kgH_2O) on a NS diet. Ren EP1-/- have a lower osmolarity (1412mOsm/ kgH_2O) compared to Ren mice

(1900mOsm/kgH_2O). There is no difference in osmolarity between WT (2414mOsm/kgH_2O) and EP1-/- mice (2693 mOsm/ kgH_2O). On a LS diet, the osmolarity drops in Ren EP1-/- mice (1641 mOsm/ kgH_2O) vs. WT mice (2107 mOsm/ kgH_2O). The spot urine osmolarity difference is ablated between Ren (1032 mOsm/ kgH_2O) and Ren EP1-/- (772 mOsm/ kgH_2O) mice on a HS diet.

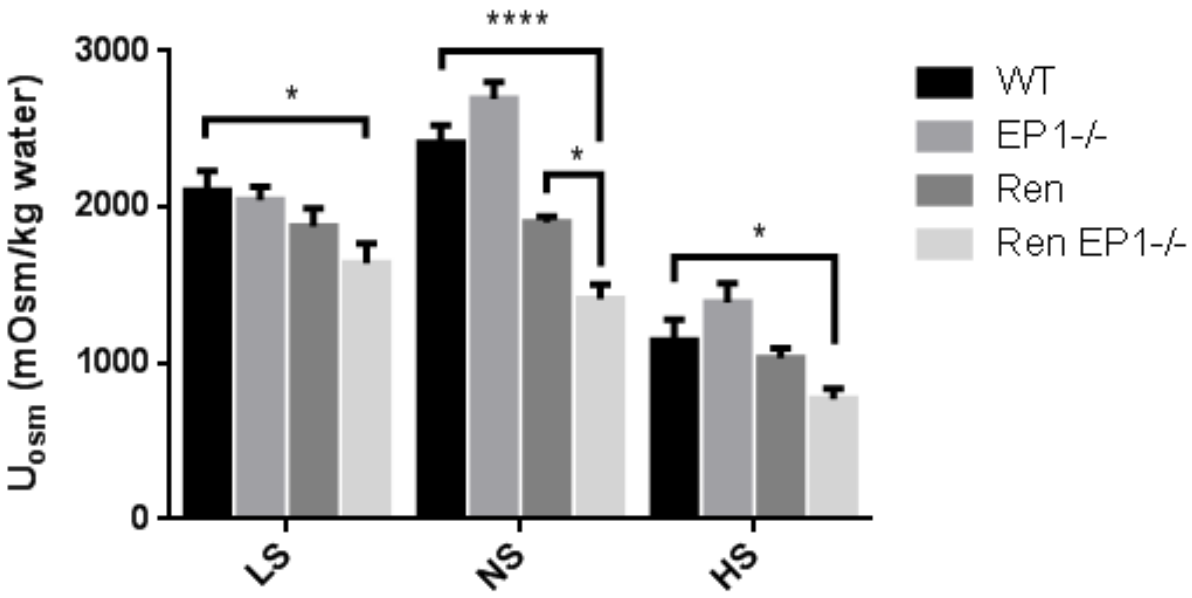

Figure 12. Spot urine osmolarity measurements using freezing point depression. On a LS diet, the osmolarity is depressed in Ren EP1-/- mice compared to WT mice. On a NS diet, the osmolarity of Ren EP1-/- mice is lower compared to Ren and WT mice. On a HS diet, the osmolarity is decreased in Ren EP1-/- mice compared to WT mice. * = $p<0.05$, **** = $p<0.0001$. N = 6-12.

4.6 AVP Levels

The changes seen in the urine osmolarity can be due to either a change in water content or an actually change in solute content. To try and tease out the difference between the two,

urinary AVP levels were measured as an indicator of water transport. Urinary AVP levels were measured with an increased focus on the interesting groups to date, the Ren and the Ren EP1-/- mice (figure 13). On a NS diet, AVP levels in EP1-/- (2447pg/mg Cr.) and Ren (2135pg/mg Cr.) mice trend lower but are not statistically changed from WT mice (3021 pg/mg Cr.). The EP1-/- results are consistent with previously published results[43]. Urinary AVP levels were statistically diminished in Ren EP1-/- mice (1260pg/mg) compared to Ren mice. On a LS diet, there were no changes in AVP levels between any groups (1367-1647 pg/mg Cr.). AVP levels dramatically spiked for WT mice on a HS diet (5063pg/mg Cr.) compared to the NS diet but remained the same in EP1-/- (2250pg/mg Cr.), Ren (2081pg/mg Cr.), and Ren EP1-/- (1147pg/mg Cr.) mice.

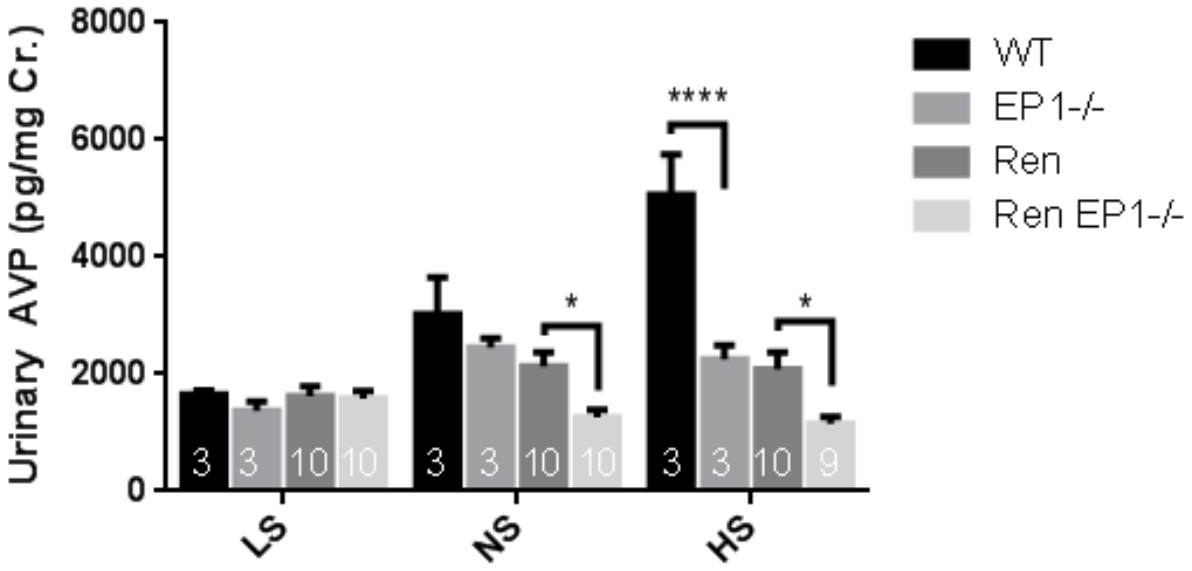

Figure 13. Spot urine AVP levels measured using an ELISA corrected per mg of creatinine measured using a picric acid assay. No significant changes in AVP levels on a LS diet. Ren EP1-/- have reduced AVP levels on a NS diet compared to Ren mice. On a HS diet, EP1-/- mice have less circulating AVP compared to WT mice. * = $p<0.05$, **** = $p<0.0001$. The number of samples used per group is indicated in the bar graph.

Ren and EP1-/- mice have impaired AVP release, an effect exacerbated on a HS diet. The LS diet mitigates the differences in AVP release, providing for a valuable tool in understanding EP1's role in the collecting duct. The results up to this point beg the question, is the blood plasma composition altered in any groups? The easiest indicator is to take the blood hematocrit percentage.

4.7 Hematocrit

The hematocrit percent measures the number of red blood cells in the composition of blood. An elevated hematocrit could be due to dehydration[61] whereas a lower percent suggests anemia[62]. The hematocrit percentage ranged from a low of 43% to a high of 48%, with no statistical differences observed in any salt group (figure 14).

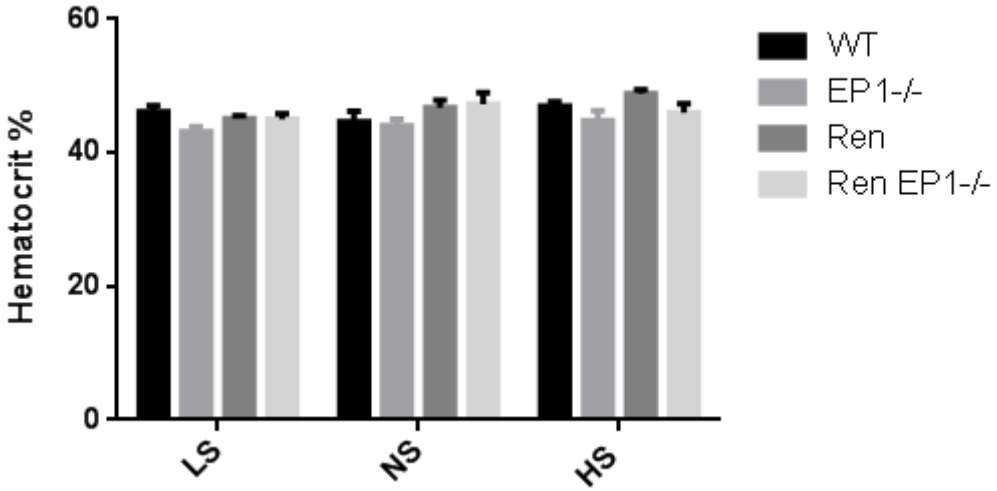

Figure 14. Hematocrit percent measured on samples taken from the saphenous vein. No change was observed between groups. N = 5-7.

4.8 GFR

There are two ways the kidney can eliminate solutes from the body. One of way is through inhibiting solute reabsorption. The other is through the simple of action of increasing the glomerular filtration rate (GFR). The GFR is between 6.08 and 7.32 µL/min/gB.W amongst the four mouse groups on the normal and low salt diet (figure 15). The only statistically change observed was between the Ren EP1-/- (10 µL/min/gB.W) mice and the WT (7.45 µL/min/gB.W) mice on the HS diet.

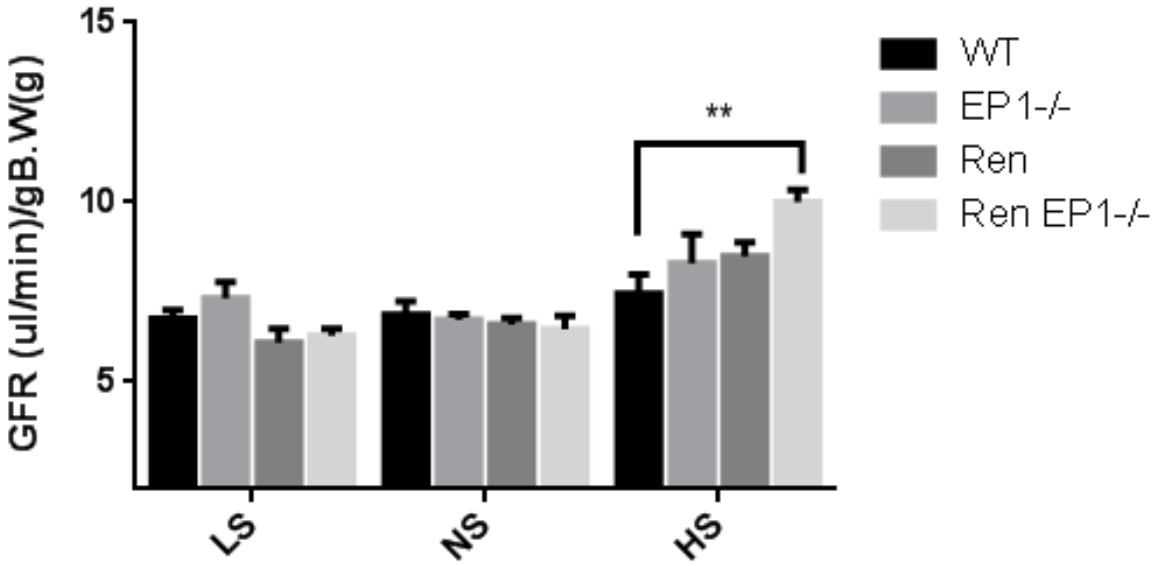

Figure 15. GFR measured by FITC inulin clearance in conscious mice. No statistical change was observed between the mouse groups on a LS and NS diet. The GFR is elevated on a HS diet for Ren EP1-/- mice compared to WT mice. N= 5-7.

The GFR data indicates that the Ren EP1-/- mice on a HS diet are hyperfiltrating. In order to confirm this theory and to assess glomerular function, quantification of albumin in the urine was performed.

4.9 ACR

Albumin to creatinine ratio (ACR) is a standardized test in evaluating kidney damage. The presence of albumin in urine is abnormal as albmumin is not normally filtered through the glomerulus[1]. The presence of albumin in urine indicates a porous filtration membrane[1]. On a NS diet (figure 16), the ACR is slightly elevated in Ren (89 ug/mg) and Ren EP1-/- mice (50ug/mg) compared to WT mice (22µg/mg). While this might be statistically relevant, it is physiologically meaningless. The diabetic mice consortium, a leading group dedicated to defining standards for kidney disease, states elevated ACR values are meaningful only if they show a minimum of a ten fold increase[63]. On a HS diet, both the Ren (260ug/mg) and Ren EP1-/- (335ug/mg) mice show a moderate increase in ACR levels compared to WT mice (50ug/mg). There is no statistical difference between the Ren and Ren EP1-/- ACR values.

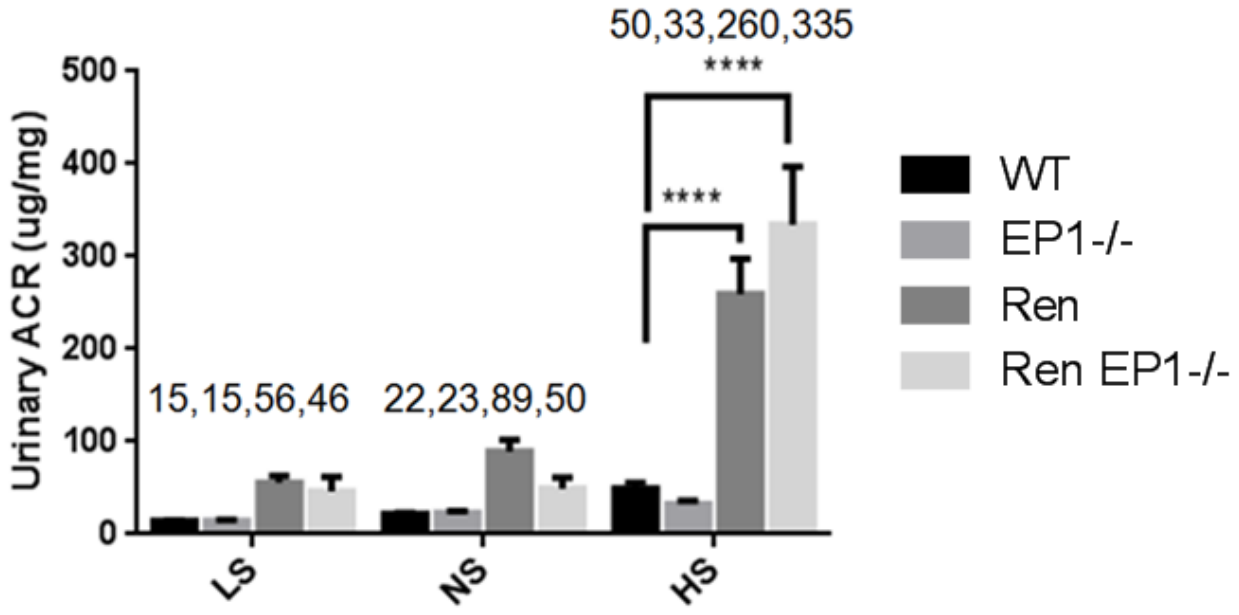

Figure 16. Urinary ACR values. Albumin was measured using an ELISA kit, creatinine was measured using a picric acid based assay. Ren and Ren EP1-/- display significantly increased ACR on a HS diet when compared to WT mice. Average ACR values are displayed above the bar graphs. **** = $p<0.0001$. N=4-6.

The ACR data raises the possibility that there might be kidney damage in certain mouse groups. One might argue that the observable changes the EP1 receptor or the Ren gene are having on fluid homeostasis is not due to their respective actions on solute transport, but rather their actions in preventing or exacerbating kidney damage. PAS staining histology was performed to look for signs of kidney damage.

4.10 PAS Staining Histology

PAS staining pathology was performed to conclusively examine whether or not there is kidney damage. Periodic Acid-Schiff (PAS) staining is routinely done on kidney biopsies to highlight the basement membrane when looking for glomerulus diseases. For the tubular component of the nephron, no necrosis was observed (figure 17). Cortical collecting duct dilation was observed, consistent with polyuria in the HS mouse groups. For the glomerulus, the PAS staining showed no overt signs of mesangial expansion, scaring or lesions (figure 18).

Normal Salt **Low Salt**

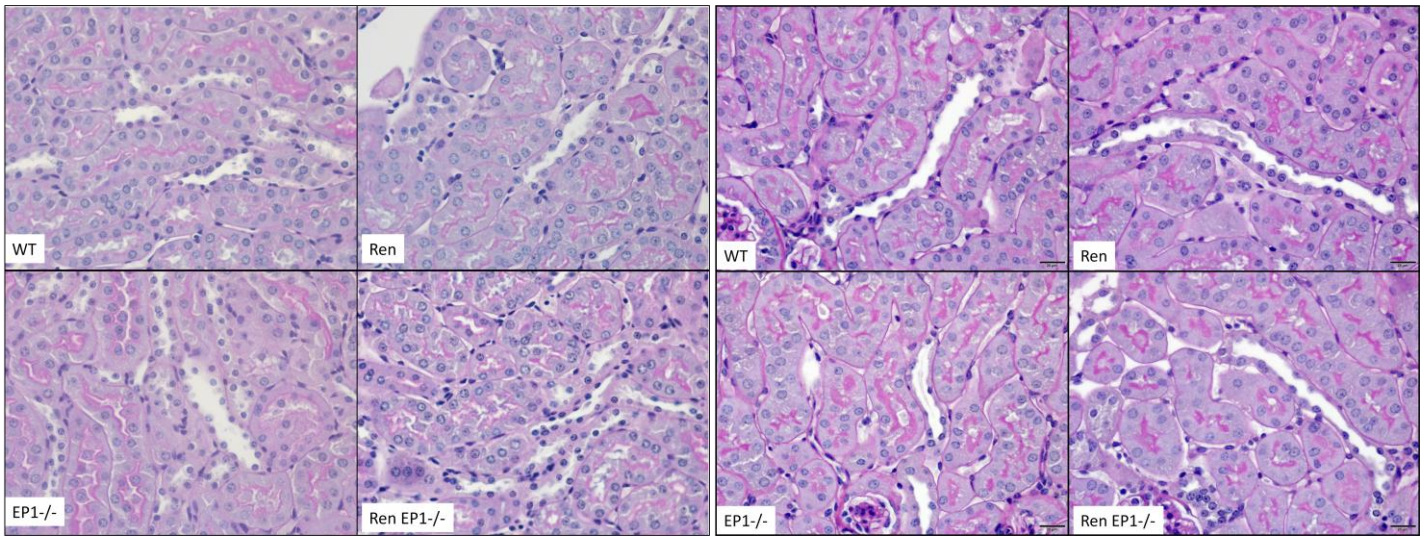

High Salt

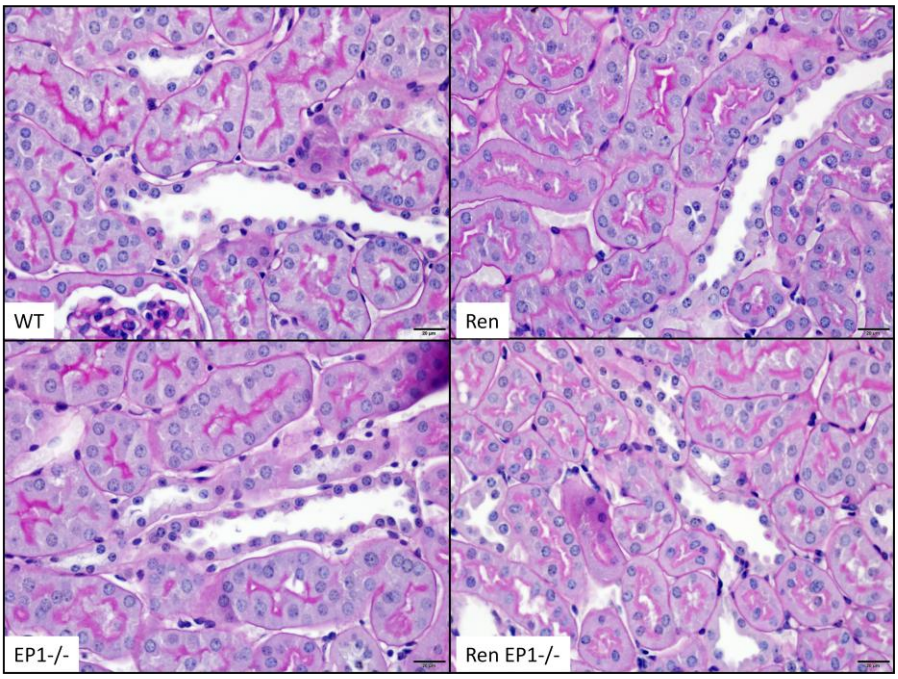

Figure 17. Representative PAS staining of CCD tubules in the kidneys of normal (top left), low (top right) and high (bottom) salt mice taken at 40x magnification. No tubular lesions were observed for any mouse group. Scale bars represent 20µm.

Normal Salt **Low Salt**

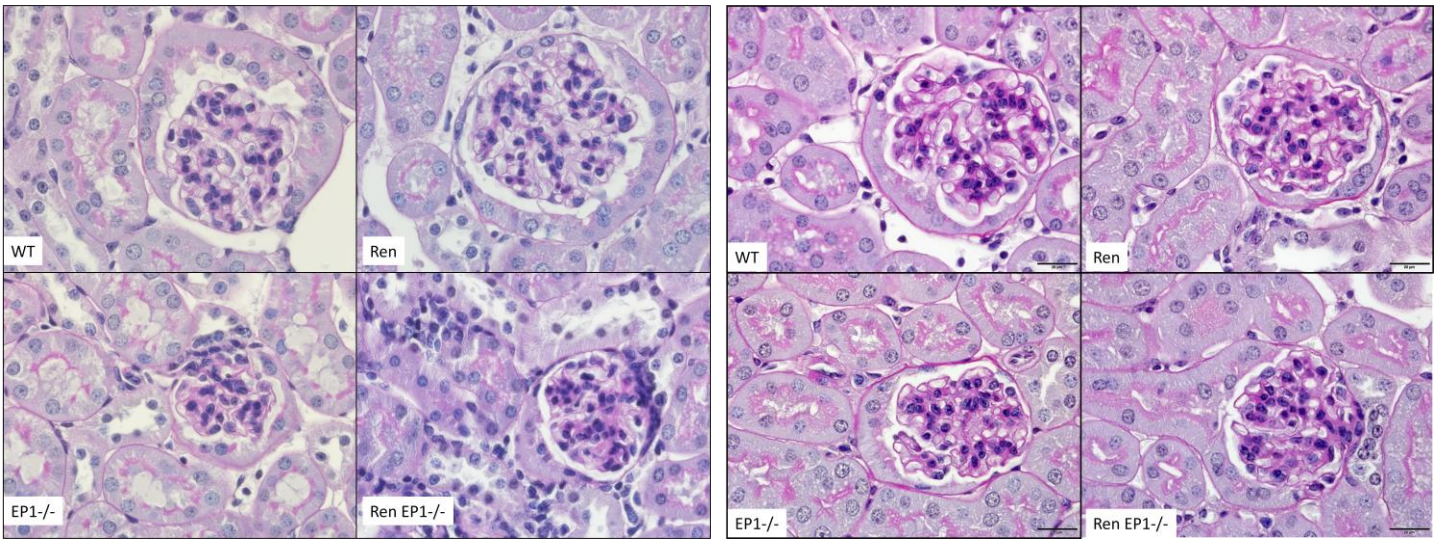

High Salt

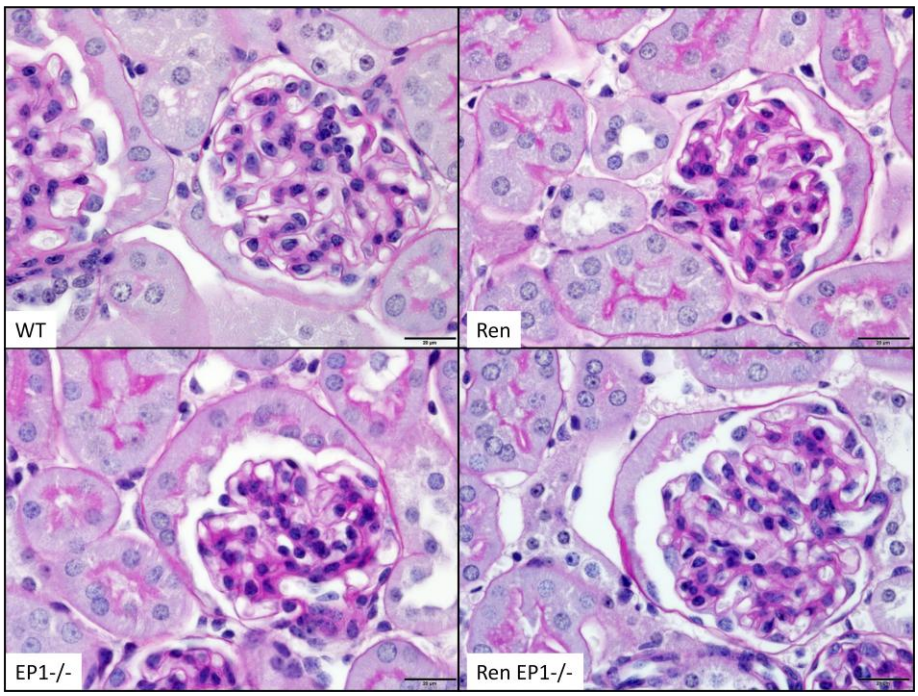

Figure 18. Representative PAS staining of the glomerulus in the kidneys on a normal (top left), low (top right) and high (bottom) salt kidneys taken at 63x magnification. No mesangial expansion, scaring or lesions were observed in any scenario. Scale bars represent 20µm.

4.11 COX-1 and COX-2 Levels

A key question is in what scenarios the EP1 receptor is more or less activated in the collecting duct? Medullar COX-1 and COX-2 levels were examined as a surrogate for PGE_2 levels. Renal medullary COX-1 levels were examined on the NS group to look for any changes (figure 19). Consistent with literature results, there were no changes in COX-1 levels in the EP1-/- (0.95 fold control), Ren (1.11 fold control), or Ren EP1-/- group (1.15 fold control).

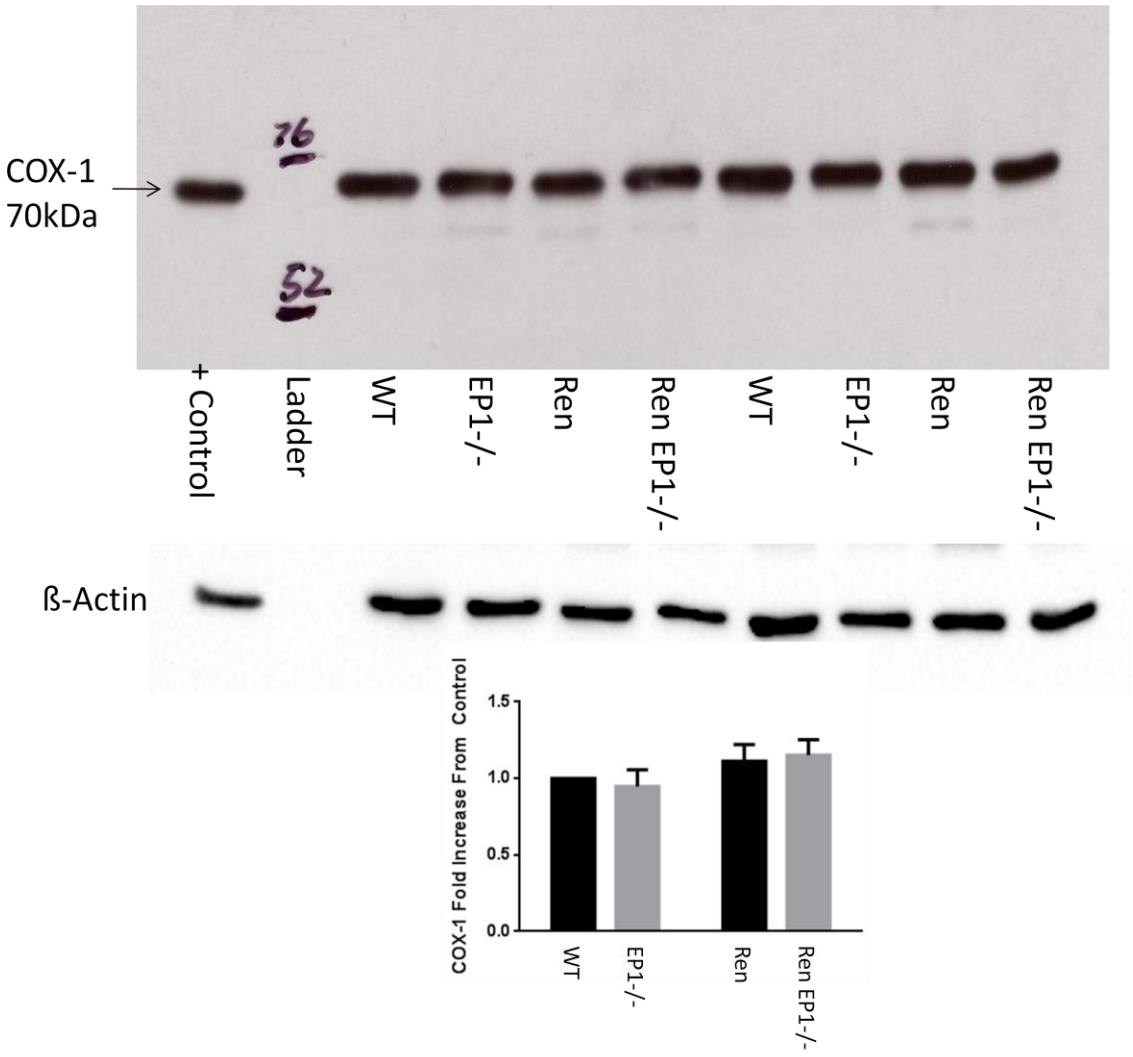

Figure 19. Semi quantitative values of COX-1 protein levels measured from the medulla of the normal salt mouse group. ß-actin was used as a loading control. Image quantification was

performed using ImageJ. Fold control represents the change in the COX-1/ß-actin ratio between the experimental groups and the WT mouse group. No statistical change observed between any group. N=8.

COX-2 (72kDa) levels were visually assessed for the four groups on the three salt diets (figure 20). COX-2 is found in the following samples: the positive control (papilla tip), all HS mouse groups, EP1-/- mice on a LS diet. There is no COX-2 signal on the other groups.

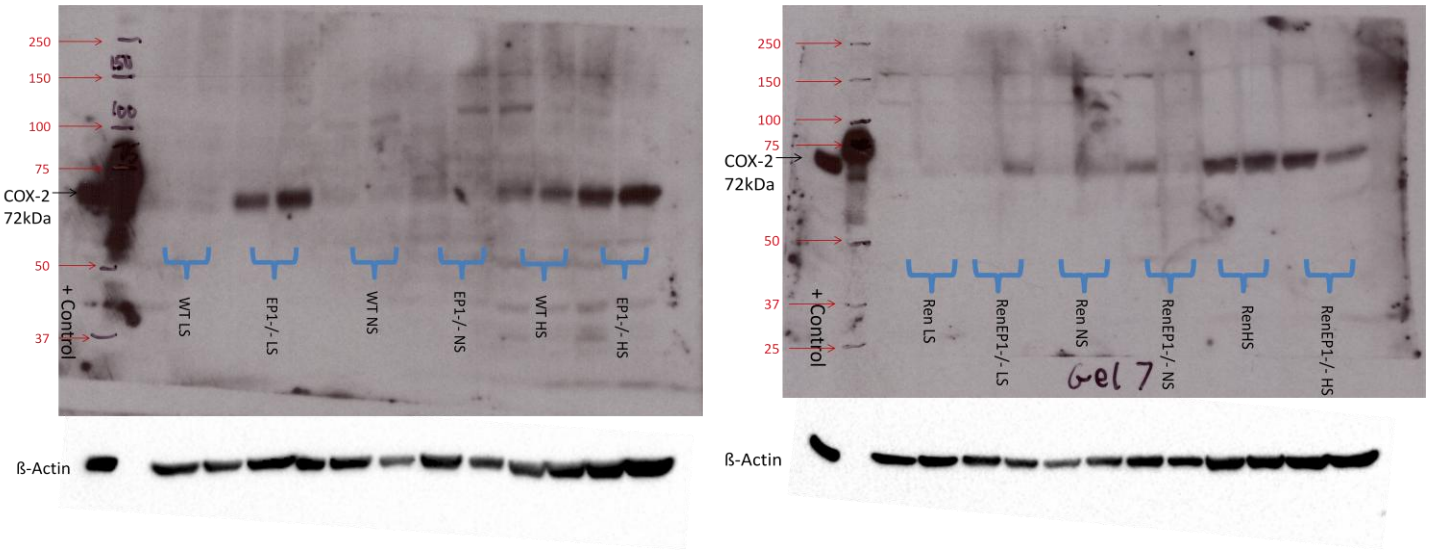

Figure 20. Representative blot of the semi quantification of COX-2 protein levels measured from the medulla of the WT and EP1-/- mice on the three salt diets (left blot) and Ren and Ren EP1-/- mice (right blot). ß-actin is used as a loading control. The strongest COX-2 signal is observed in the positive control (papilla tip). Moderate COX-2 signals are found in all HS mouse groups and EP1-/- mice on a LS diet. N=4-6.

4.12 Ex Vivo IMCD Water Perfusion

Ex vivo microperfusion experiments were performed on isolated IMCD tubules to look at the EP1's role on water transport (Jv). The IMCD was chosen as it contains the highest

percentage of water transporters in the collecting duct[16]. Baseline Jv values are around 0.5-1.0 nl/mm/min for both WT and EP1-/- tubules (figure 21). Upon the addition of AVP, the Jv increases to 4.7 nl/mm/min in the EP1-/- tubules and 3.6 nl/mm/min in WT tubules. With the addition of PGE_2, Jv stays constant at 4.9 nl/mm/min in EP1-/- tubules whereas WT Jv goes down to 1.4 nl/mm/min.

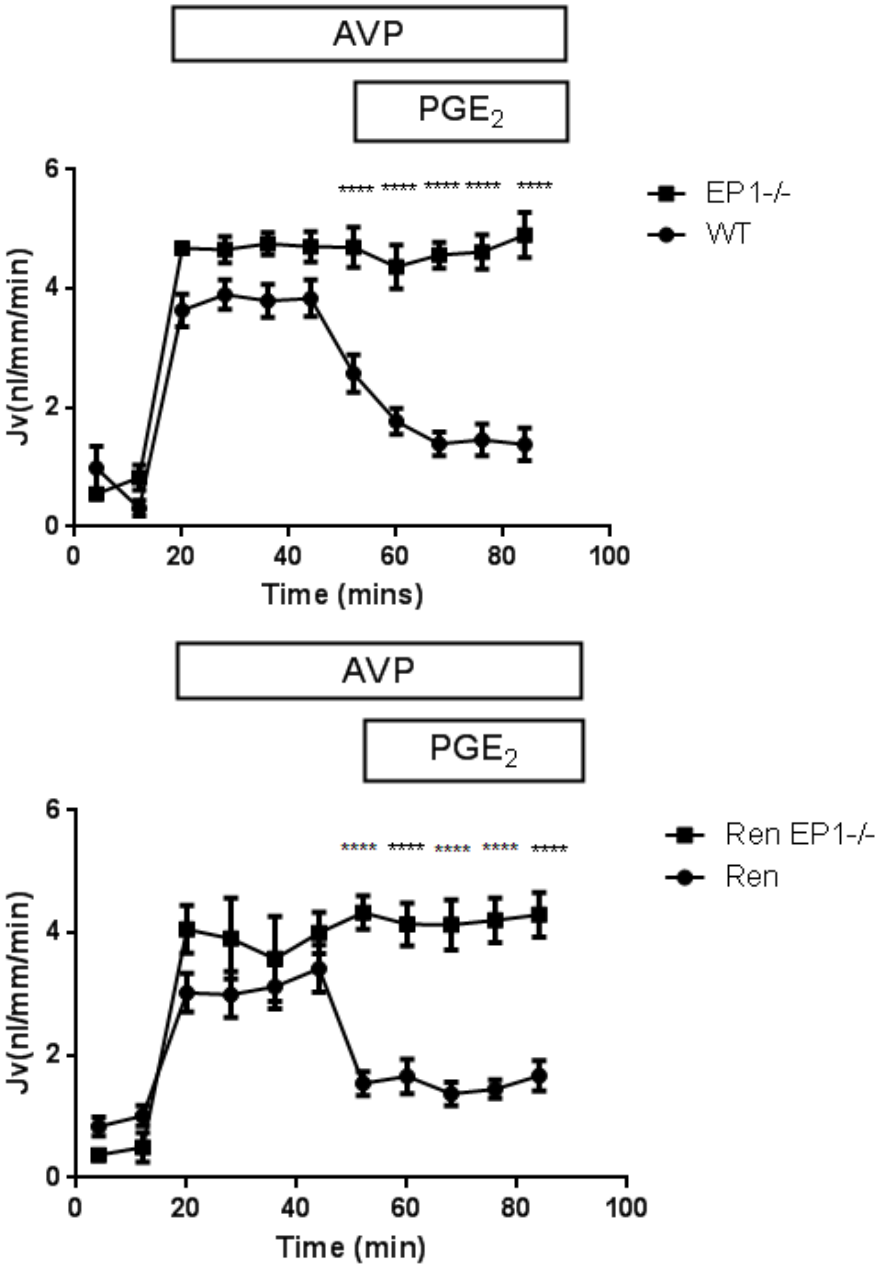

Figure 21. The water flux (J_v) in an isolated WT and EP1-/- IMCD tubule (top) and isolated Ren and Ren EP1-/- IMCD tubules (bottom). AVP was added at a concentration of 10^{-12}M into the bath solution following two baseline J_v collections. PGE_2 was added at a concentration of 10^{-7}M into the bath solution following four AVP J_v collections. The addition of AVP results in an increase in J_v for all mouse tubules. The addition of PGE_2 results in a decrease in J_v for WT and Ren tubules, but not EP1-/- and Ren EP1-/- tubules. N=5.

The same trend was observed between the Ren and Ren EP1-/- mice (figure 21). Baseline Jv values are around 0.5-1.0 nl/mm/min for both Ren and Ren EP1-/- tubules. Upon the addition of AVP, the Jv increases to 4.0 nl/mm/min in the EP1-/- tubules and 3.0 nl/mm/min in WT tubules. With the addition of PGE_2, Jv stays constant at 4.3 nl/mm/min in EP1-/- tubules whereas WT Jv goes down to 1.7 nl/mm/min.

These results were completely unexpected. There should be at least a partial reaction to PGE_2 in EP1-/- due to the actions of the other PGE_2 receptors, especially EP3. Further tests were performed as to understand why the EP1 mice showed no response to PGE_2.

To specifically target the EP1 and EP3 receptors sulprostone (SLP; an EP1 and EP3 agonist) was added in lieu of PGE_2. The WT and EP1-/- tubules showed similar responses to SLP as they did to PGE_2 (figure 22). Again, baseline Jv values were around 0.5-1.0 nl/mm/min. AVP increased Jv to 4.2 nl/mm/min for both groups. SLP decreased the Jv of the WT tubules back down to 2.0 nl/mm/min. When the EP1 antagonist SC19220 was added at a concentration of 10^{-6}M to WT tubules, the SLP induced drop went down to 2.6 nl/mm/min (n=1 results not shown). When the EP1 antagonist SC19220 was added at a concentration of 10^{-5}M, the SLP induced drop went down to only 3.7 nl/mm/min. SLP had no effect on the Jv of the EP1-/- tubules, the Jv remained around 5.4nl/mm/min.

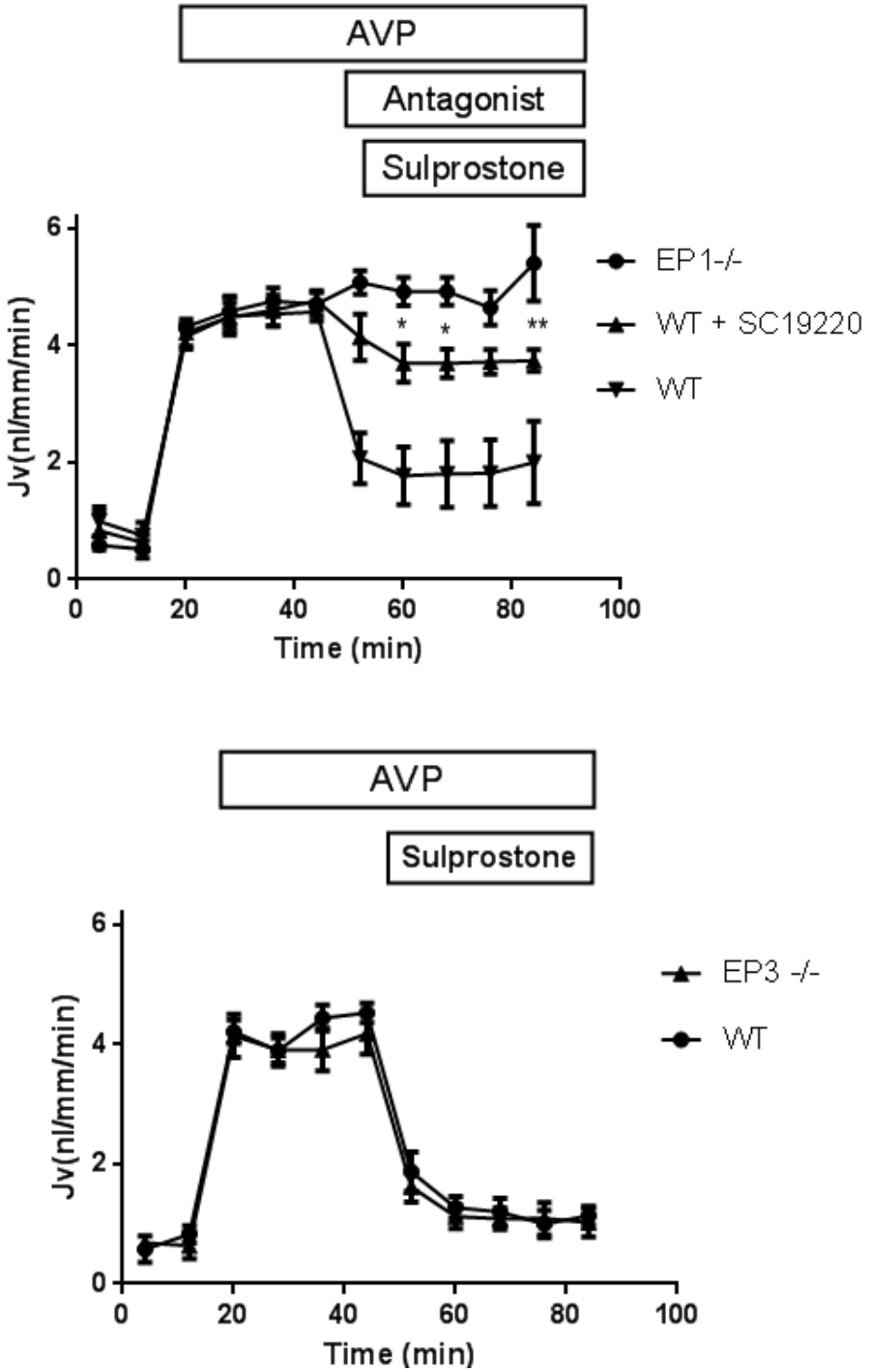

Figure 22. The water flux (J_v) in isolated IMCD tubule from FVB WT and EP1-/- mice (top), C57BL/6J WT and EP3-/- mice (bottom). AVP was added at a concentration of 10^{-12}M

into the bath solution following two baseline J_v collections. SLP was added at a concentration of 10^{-7}M into the bath solution following four AVP J_v collections. An EP1 antagonist (SC19220, Ki= 6.7mM) was added 10 minutes prior to the sulprostone addition at a concentration of 10^{-5}M for one trial. The PGE_2 induced decrease in Jv was blunted upon the addition of SC19220 and absent in EP1-/- tubules (top). There is no difference in the AVP or PGE_2 response between C57BL/6J WT and EP3-/- mice. N = 5-6.

To conclusively prove that EP3 has no involvement in IMCD water transport, the experiment was performed on EP3-/- mice (figure 22). As usual, baseline Jv is 0.5-1.0 nl/mm/min and AVP increases the flux to 4.2 nl/mm/min. SLP brings the water transport back down to 1.0 nl/mm/min. These results conclusively prove that PGE_2 acts through EP1 to inhibit water reabsoprtion, not EP3.

4.13 Ex Vivo Electrophysiology Experiments

Ex vivo electrophysiology microperfusion experiments were performed on isolated CCD tubules to look at the EP1's role on Na^+ transport. The CCD was chosen as it contains the highest percentage of sodium transporters in the collecting duct. An increase in the Vte (less negative) indicates a depolarization event, resulting in the loss of the electrochemical gradient used to transport Na^+ across the principal cell[64]. In essence, the Vte is inversely proportional to the Na^+ flux[64]. The first couple of minutes after the addition of PGE_2 contains noise due to the change of the fluid bath. The bar graph below shows the summary of the change in the Vte upon the addition of PGE_2 after five minutes of acclimatization to the addition of PGE_2.

On the LS diet, PGE_2 depolarizes the Vte by 4.3mV and 3.7mV in the WT and Ren CCD tubules, respectively (figure 23). The Vte depolarization is negligible at 0.7mV for the EP1-/- tubules and very minor in the Ren EP1-/- tubules at 1.8mV. On the NS diet, PGE_2 depolarizes the Vte by 10.7mV and 9.0mV in the WT and Ren CCD tubules, respectively (figure 24). The Vte depolarization is 1.1mV for the EP1-/- tubules and 1.2mV for Ren EP1-/- tubules. On the HS diet, PGE_2 depolarizes the Vte by 6.0mV and 3.9mV in the WT and Ren CCD tubules, respectively (figure 25). The Vte depolarization is 2.8mV for the EP1-/- tubules and minor in the Ren EP1-/- tubules at 1.6mV.

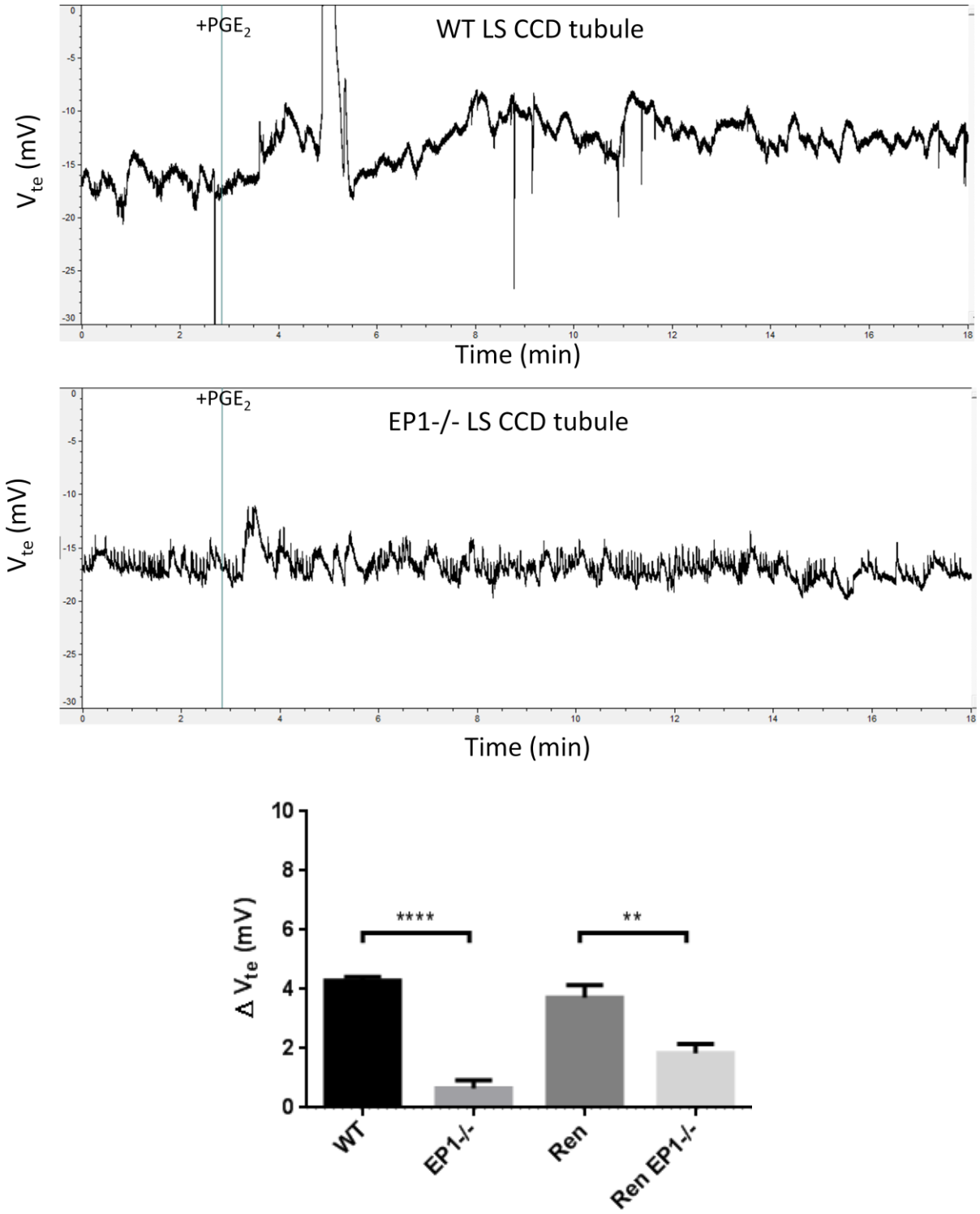

Figure 23. Representative tracing of the Vte over time of a WT (top) and EP1-/- (middle) CCD tubule on a LS diet. The vertical blue line indicates the addition of PGE_2. Summary graph of the change in Vte upon the addition of PGE_2 is shown on the bottom. N=5-6

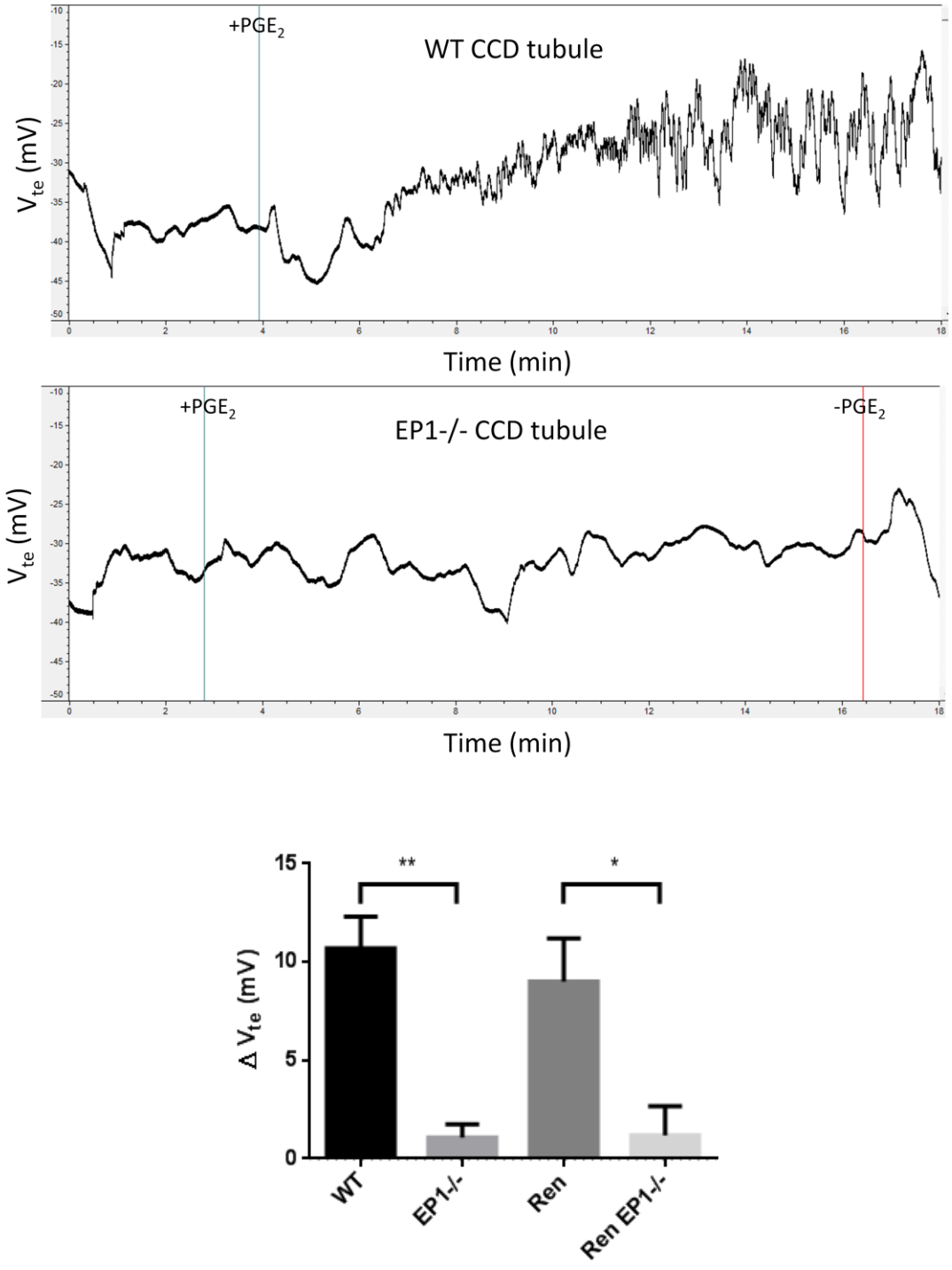

Figure 24. Representative tracing of the Vte over time of a WT (top) and EP1-/- (middle) CCD tubule on a normal salt diet. The vertical blue line indicates the addition of PGE_2, the vertical red line indicates the withdrawal of PGE_2. Summary graph of the change in Vte upon the addition of PGE_2 is shown on the bottom. N=5

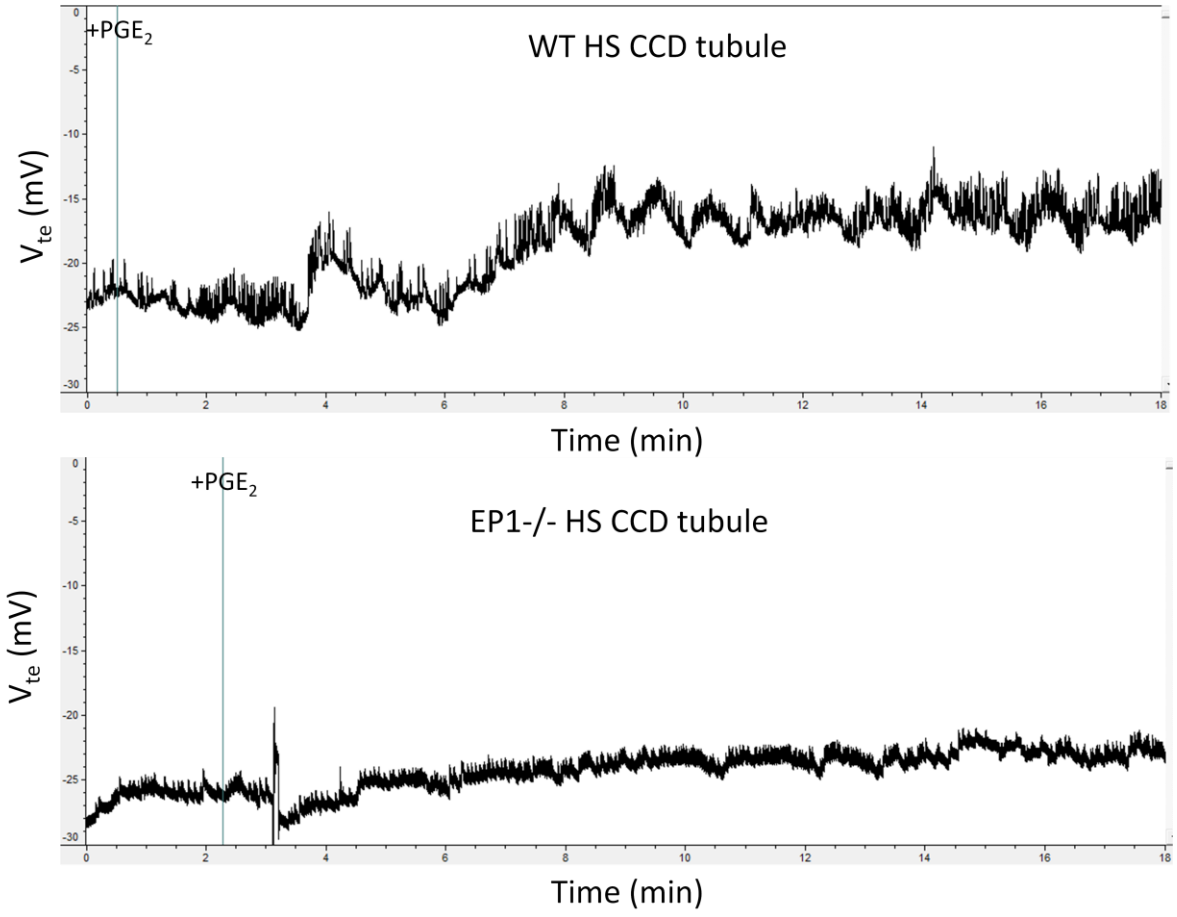

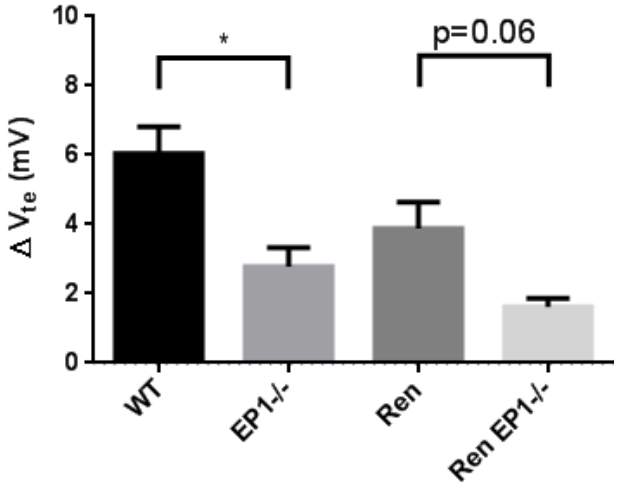

Figure 25. Representative tracing of the Vte over time of a WT (top) and EP1-/- (middle) CCD tubule on a high salt diet. The vertical blue line indicates the addition of PGE_2. Summary graph of the change in Vte upon the addition of PGE_2 is shown on the bottom. N=5-6

4.14 AngII Electrophysiology Experiments

Experiments were performed looking at the effect AngII has on PGE_2 inhibition of Na^+ transport to try to elucidate whether PGE_2 has a synergistic or antagonistic effect with AngII. AngII was added into the lumen of a WT NS tubule while PGE_2 was added in the basolateral bath consistent with the AT1a and EP1 receptors location. AngII induced a minor Vte depolarization of 2.1mV (figure 26). Following the addition of AngII, the PGE_2 Vte depolarization was minor at 2.0 mV.

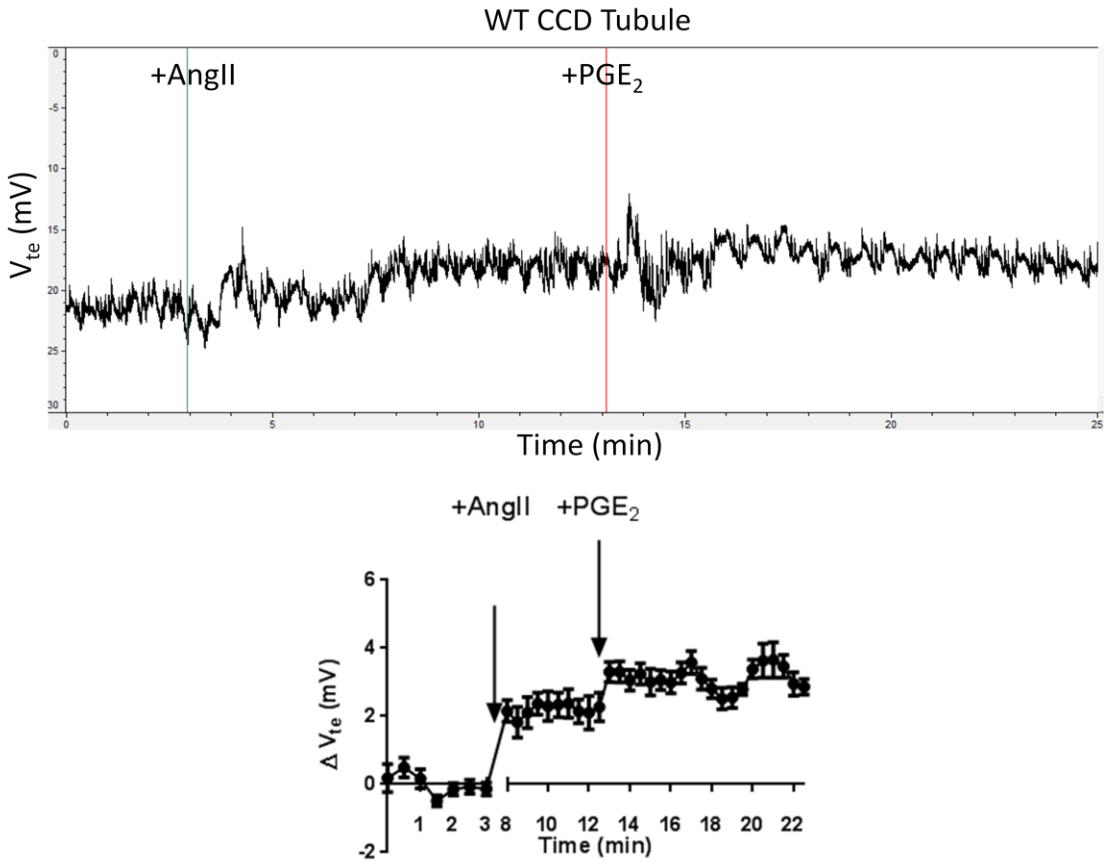

Figure 26. Representative tracing of the Vte over time of a WT CCD tubule upon the addition of AngII (vertical blue line) into the lumen followed by the addition of PGE_2 (vertical red line) into the basolateral bath. Summary time course chart of the change in Vte.

4.15 AQP2 and αENaC High Salt Immunofluorescence

Immunofluorescence of AQP2 and αENaC were performed on kidney sections looking for relative quantity and membrane localization. On a HS diet in all four groups, strong membrane localization of AQP2 was viewed in the IMCD (figure 27 and 28). No αENaC was observed in the AQP2 positive principal cells (figure 27 and 28). Note that αENaC does have a weak non-specific binding to intercalated cells and nuclei.

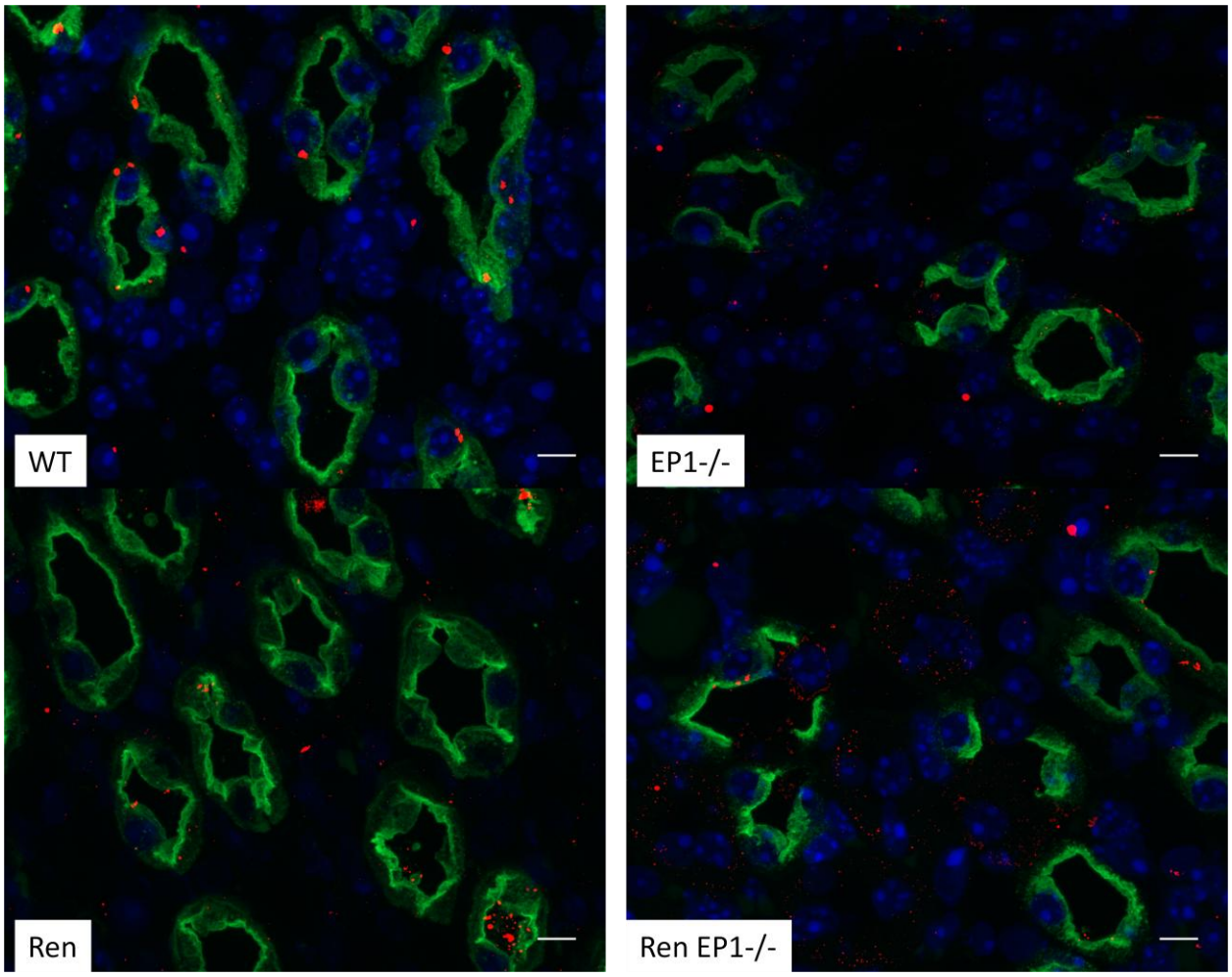

Figure 27. Representative images of the medulla stained for AQP2 and αENaC from the four mouse groups on a HS diet. Each panel is labeled with their corresponding mouse group in the bottom left corner. Green represents AQP2; red represents αENaC; blue represents the nuclei. Images taken under 100x magnification. Scale bars (white lines) represents 8μm.

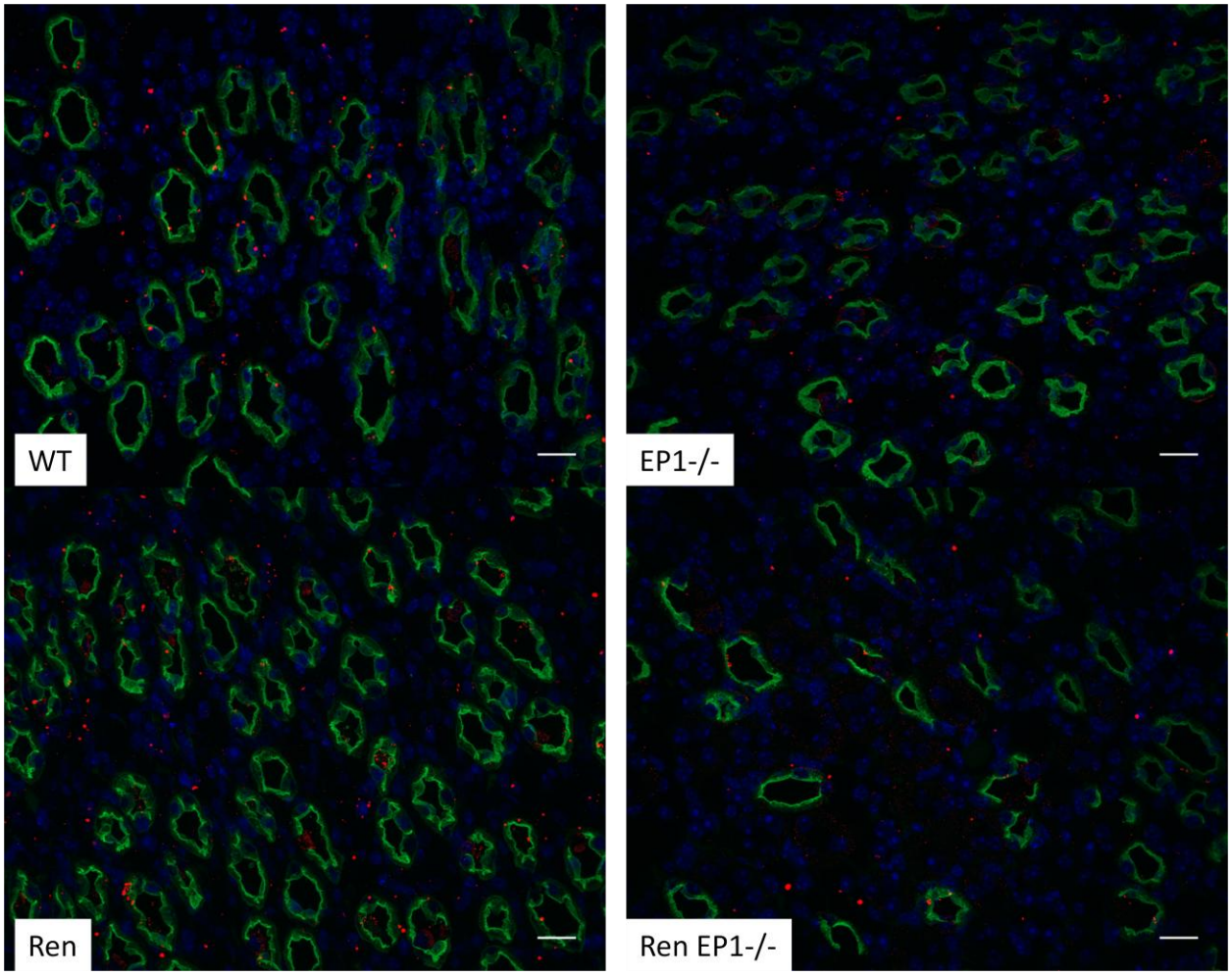

Figure 28. Representative images of the medulla stained for AQP2 and αENaC from the four mouse groups on a HS diet. Each panel is labeled with their corresponding mouse group in the bottom left corner. Green represents AQP2; red represents αENaC; blue represents the nuclei. Images taken under 40x magnification. Scale bars (white lines) represents 20μm.

The following observations were made of the CCD tubules on mice on the HS group (figure 29 and 30):

- There is no detectable expression level for αENaC in the WT nor the EP1-/- group
- There is detectable expression level of αENaC in Ren and Ren EP1-/- mice
- In the Ren and Ren EP1-/- group, αENaC is mostly located in the cytoplasm while AQP2 is by and large located on the membrane.

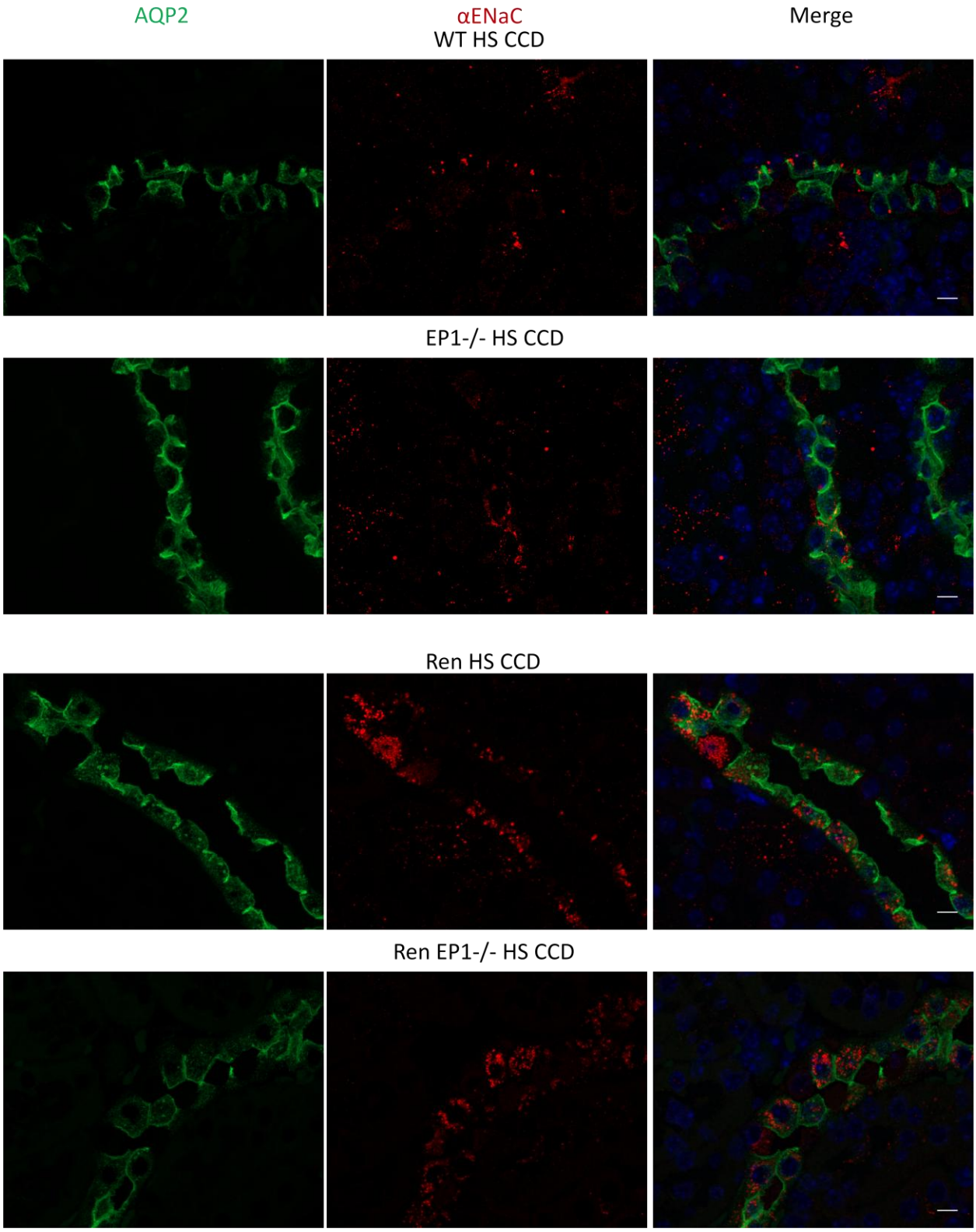
AQP2
αENaC
Merge
WT HS CCD
EP1-/- HS CCD
Ren HS CCD
Ren EP1-/- HS CCD

Figure 29. Representative images of CCD(s) stained for AQP2 and αENaC from the four mouse groups on a HS diet. Each row is labeled with their corresponding mouse group on top. Green represents AQP2 (left); red represents αENaC (middle); blue represents the nuclei. Images taken under 100x magnification. Scale bars (white lines) represents 8µm.

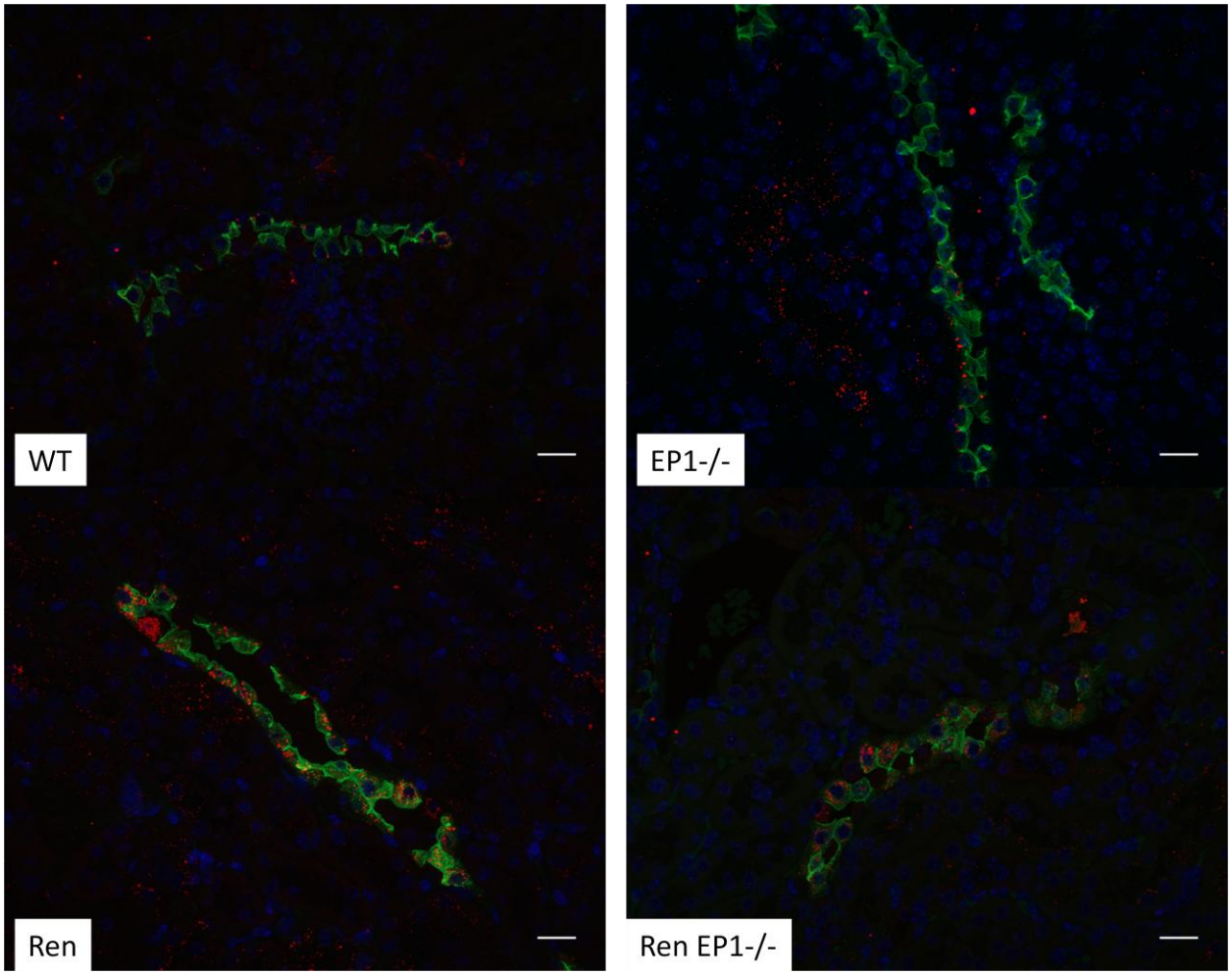

Figure 30. Representative images of CCD(s) stained for AQP2 and αENaC from the four mouse groups on a HS diet. Each panel is labeled with their corresponding mouse group in the bottom left corner. Green represents AQP2; red represents αENaC; blue represents the nuclei. Images taken under 40x magnification. Scale bars (white lines) represents 20µm.

4.16 AQP2 and αENaC Normal Salt Immunofluorescence

In all four groups, AQP2 is primarily located in the cytoplasm (figure 31 and 32) in the medulla of NS group mice. No αENaC was observed in the AQP2 positive principal cells.

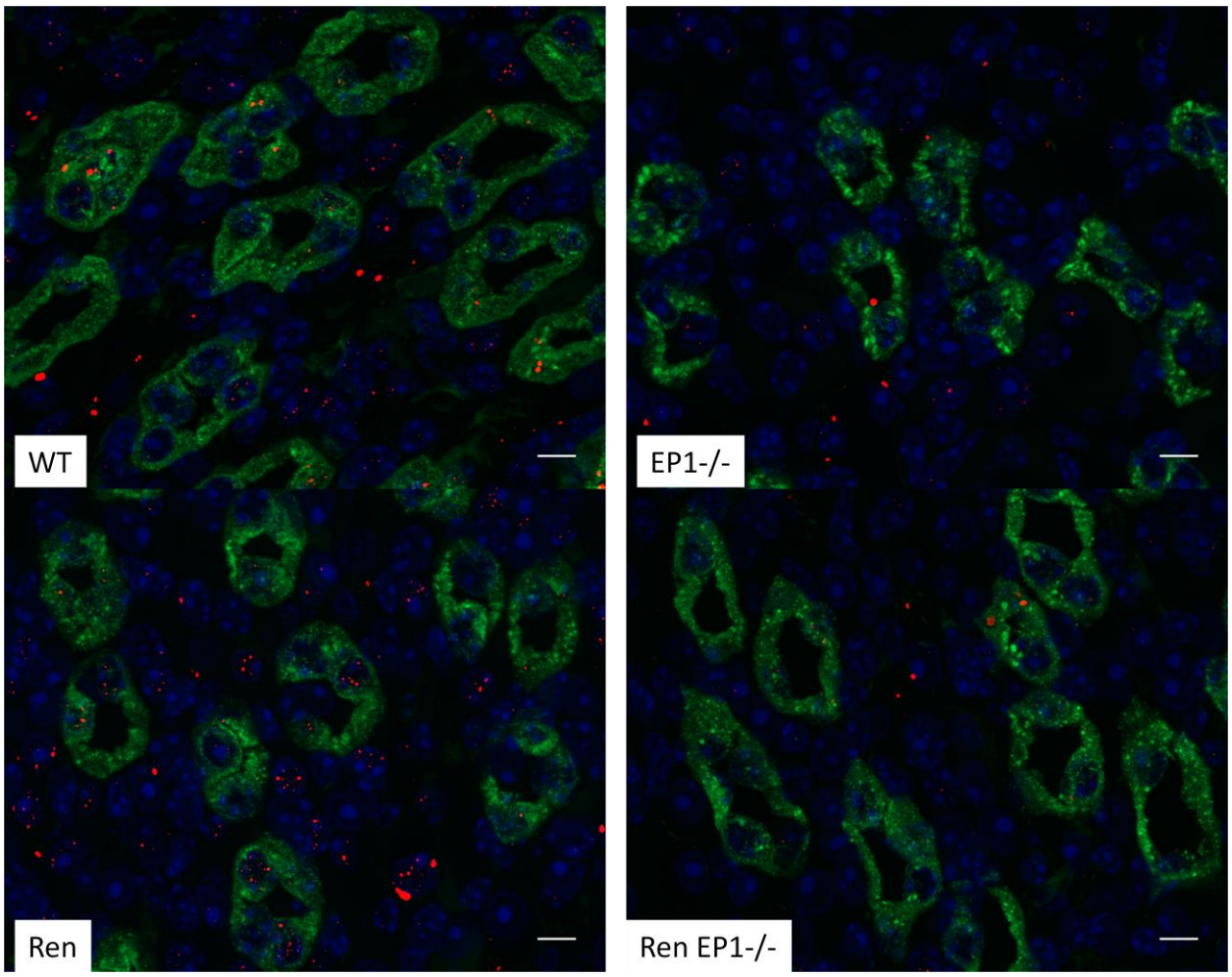

Figure 31. Representative images of the medulla stained for AQP2 and αENaC from the four mouse groups on a NS diet. Each panel is labeled with their corresponding mouse group in the bottom left corner. Green represents AQP2; red represents αENaC; blue represents the nuclei. Images taken under 100x magnification. Scale bars (white lines) represents 8µm.

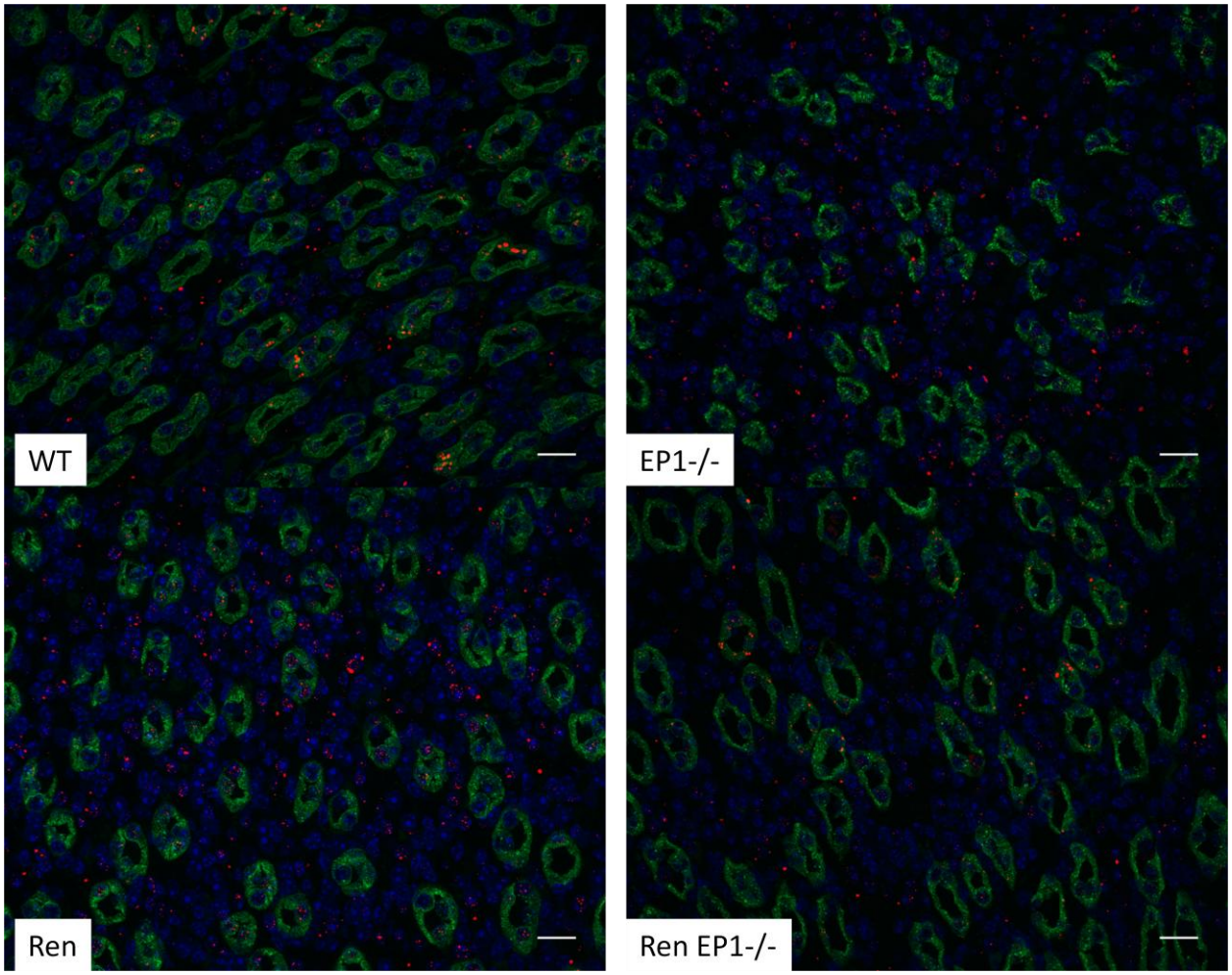

Figure 32. Representative images of the medulla stained for AQP2 and αENaC from the four mouse groups on a NS diet. Each panel is labeled with their corresponding mouse group in the bottom left corner. Green represents AQP2; red represents αENaC; blue represents the nuclei. Images taken under 40x magnification. Scale bars (white lines) represents 20μm.

The following observations were made of the CCD tubules of mice on the NS group (figure 33 and 34):

- There is moderate staining of αENaC in WT and EP1-/- group CCD tubules
- The αENaC staining Ren EP1-/- mice is slightly stronger and more abundant compared to the other mice.
- In all groups, both αENaC and AQP2 are diffusely located in the cytoplasm and membrane.

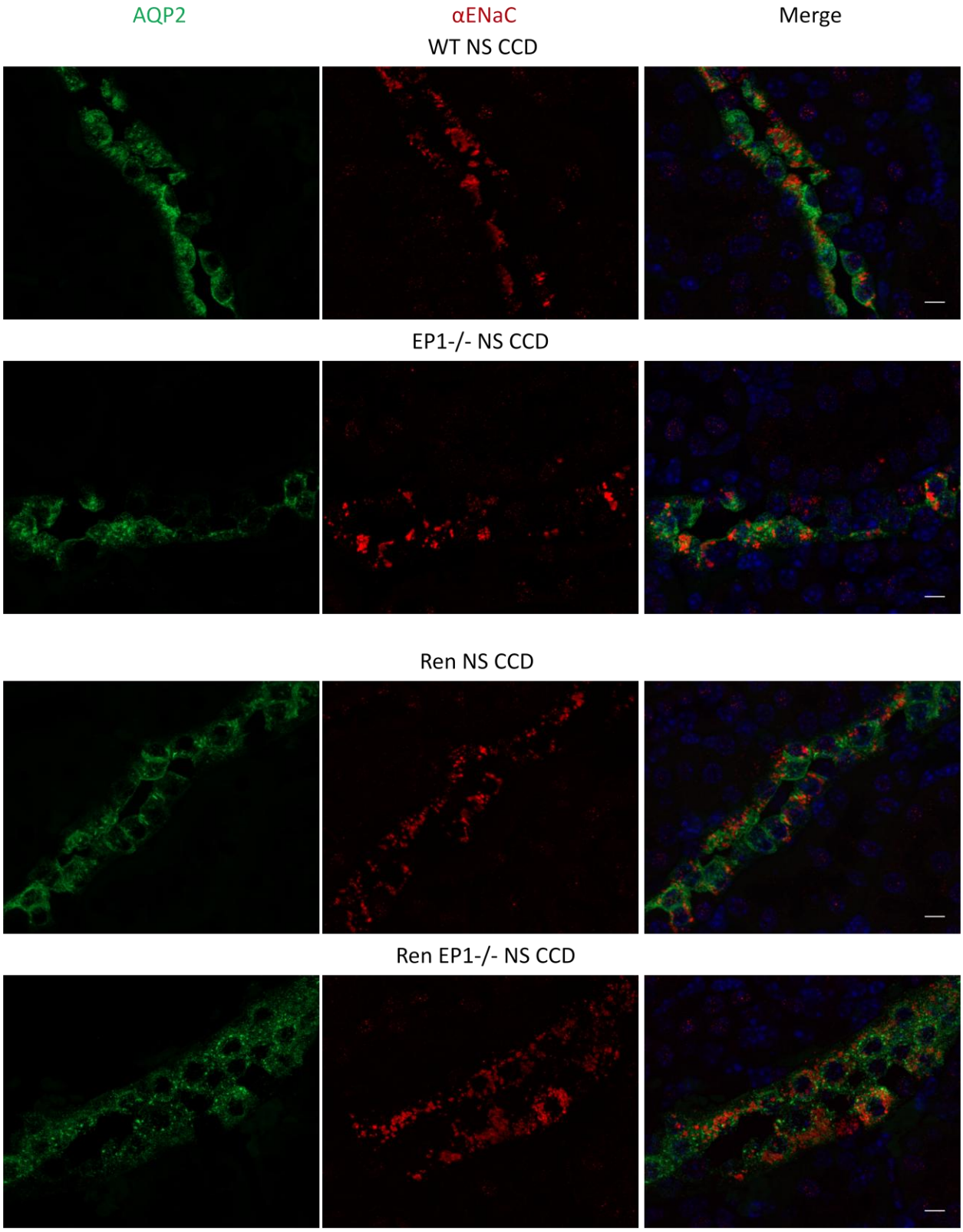
AQP2
αENaC
Merge
WT NS CCD
EP1-/- NS CCD
Ren NS CCD
Ren EP1-/- NS CCD

Figure 33. Representative images of CCD(s) stained for AQP2 and αENaC from the four mouse groups on a NS diet. Each panel is labeled with their corresponding mouse group in the bottom left corner. Green represents AQP2 (left); red represents αENaC (middle); blue represents the nuclei. Images taken under 100x magnification. Scale bars (white lines) represents 8µm.

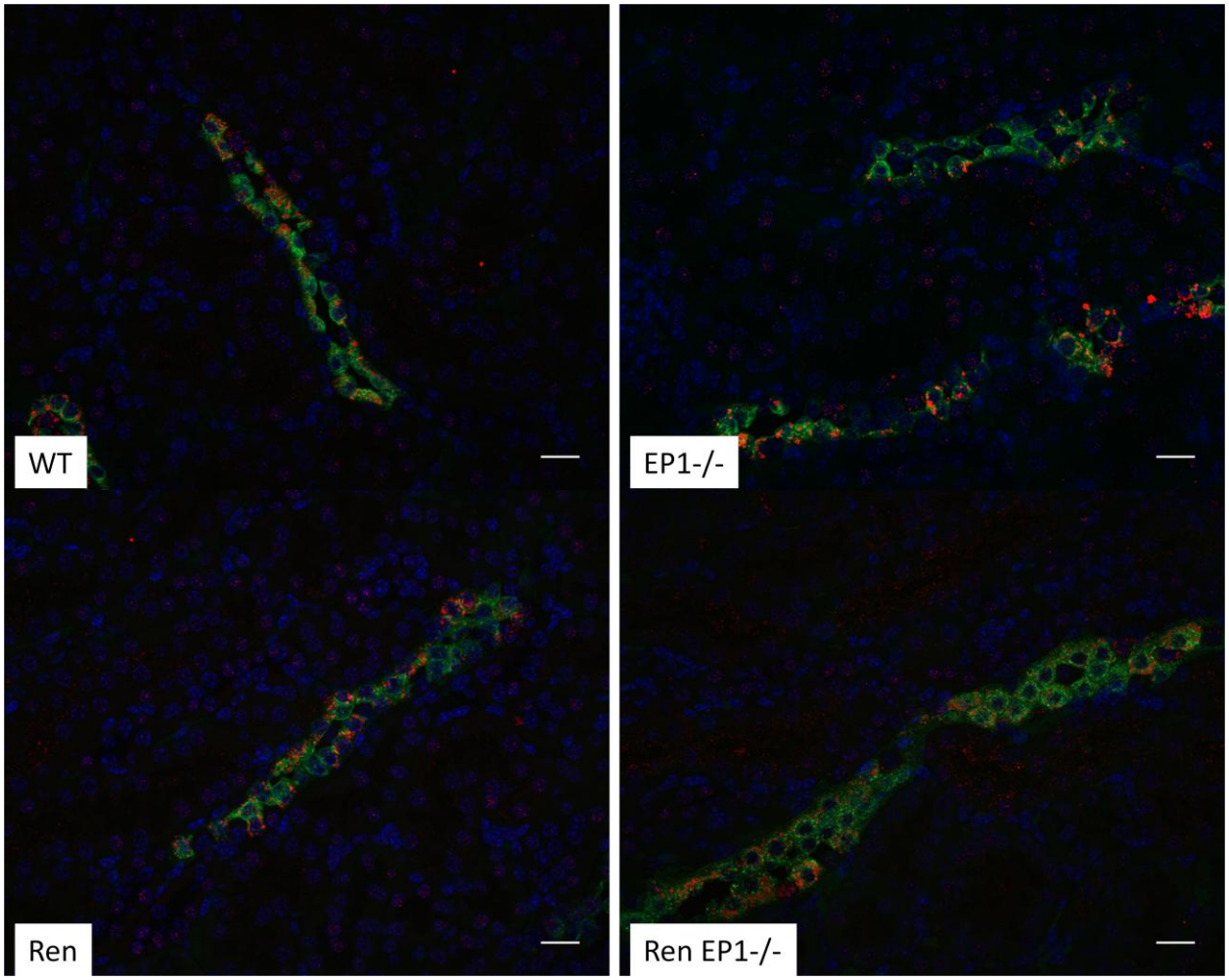

Figure 34. Representative images of CCD(s) stained for AQP2 and αENaC from the four mouse groups on a NS diet. Each panel is labeled with their corresponding mouse group in the bottom left corner. Green represents AQP2; red represents αENaC; blue represents the nuclei. Images taken under 40x magnification. Scale bars (white lines) represents 20µm.

4.17 AQP2 and αENaC Low Salt Immunofluorescence

In the medulla of all four LS groups, AQP2 was more membrane localized than the NS group but less membrane localized compared to the HS group (figure 35 and 36). αENaC was observed in some Ren EP1-/- AQP2 positive principal cells, but not present in the medulla of WT, EP1-/- or Ren mice.

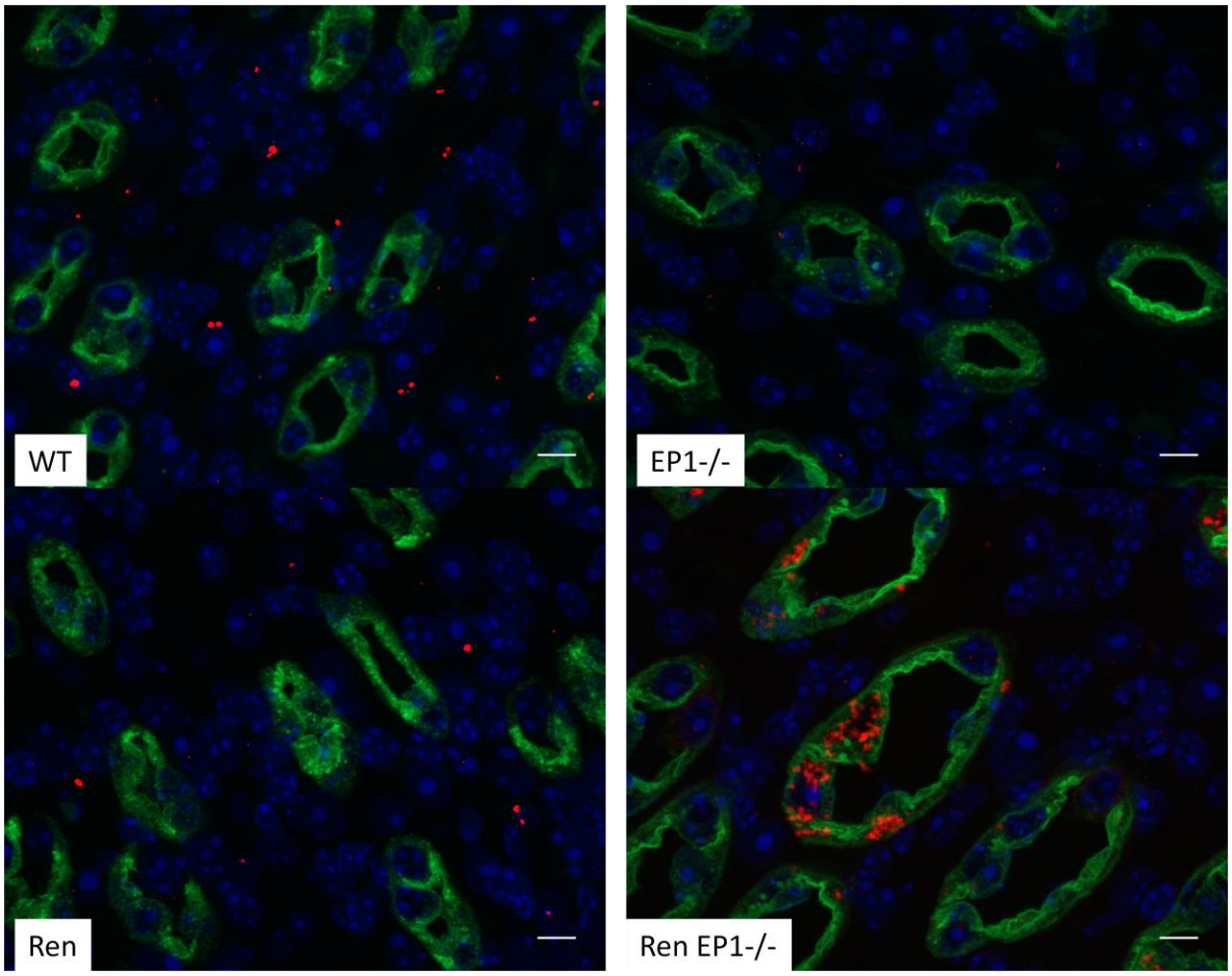

Figure 35. Representative images of the medulla stained for AQP2 and αENaC from the four mouse groups on a LS diet. Each panel is labeled with their corresponding mouse group in the bottom left corner. Green represents AQP2; red represents αENaC; blue represents the nuclei. Images taken under 100x magnification. Scale bars (white lines) represents 8µm.

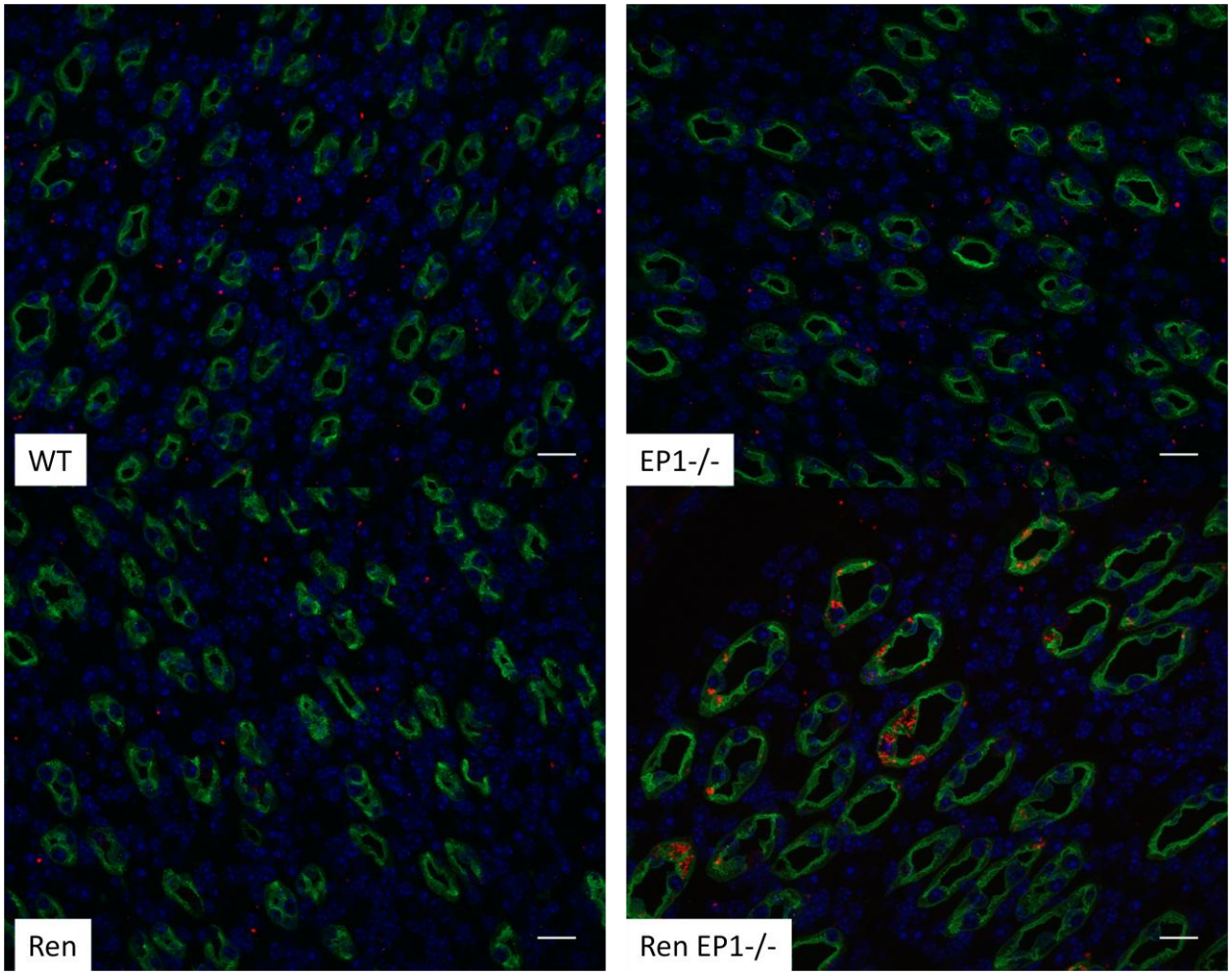

Figure 36. Representative images of the medulla stained for AQP2 and αENaC from the four mouse groups on a LS diet. Each panel is labeled with their corresponding mouse group in the bottom left corner. Green represents AQP2; red represents αENaC; blue represents the nuclei. Images taken under 40x magnification. Scale bars (white lines) represents 20µm.

The following observations were made of the CCD tubules of mice on the LS group (figure 37 and 38):

- The αENaC staining in EP1-/- tubules is more intense compared to the WT tubules.
- The αENaC staining in Ren EP1-/- tubules is more intense compared to the Ren tubules.
- αENaC expression levels are slightly stronger in the membrane of the RenEP1-/- mice compared to all other groups.

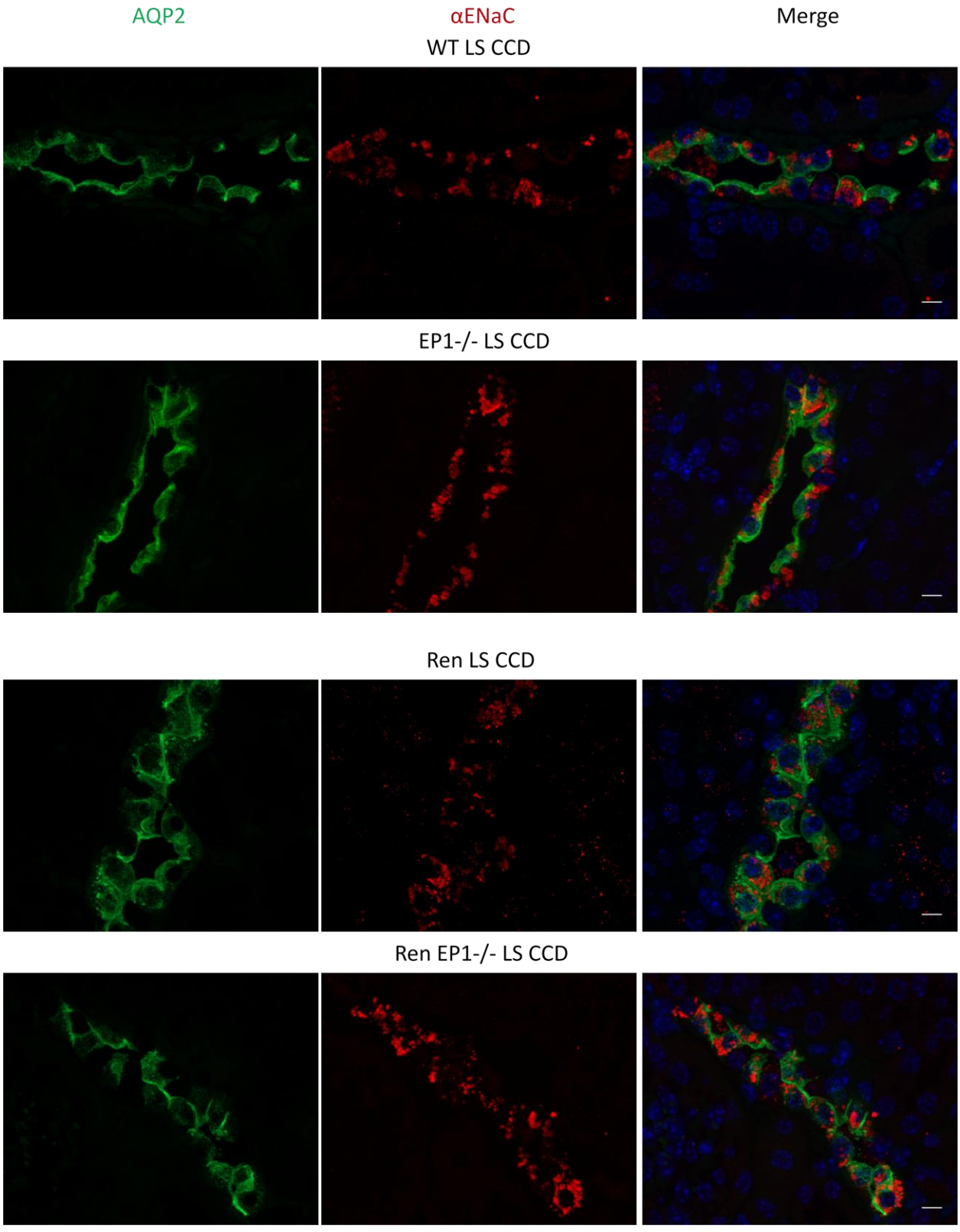
AQP2
αENaC
Merge
WT LS CCD
EP1-/- LS CCD
Ren LS CCD
Ren EP1-/- LS CCD

Figure 37. Representative images of CCD(s) stained for AQP2 and αENaC from the four mouse groups on a LS diet. Each panel is labeled with their corresponding mouse group in the bottom left corner. Green represents AQP2; red represents αENaC; blue represents the nuclei. Images taken under 100x magnification. Scale bars (white lines) represents 8µm.

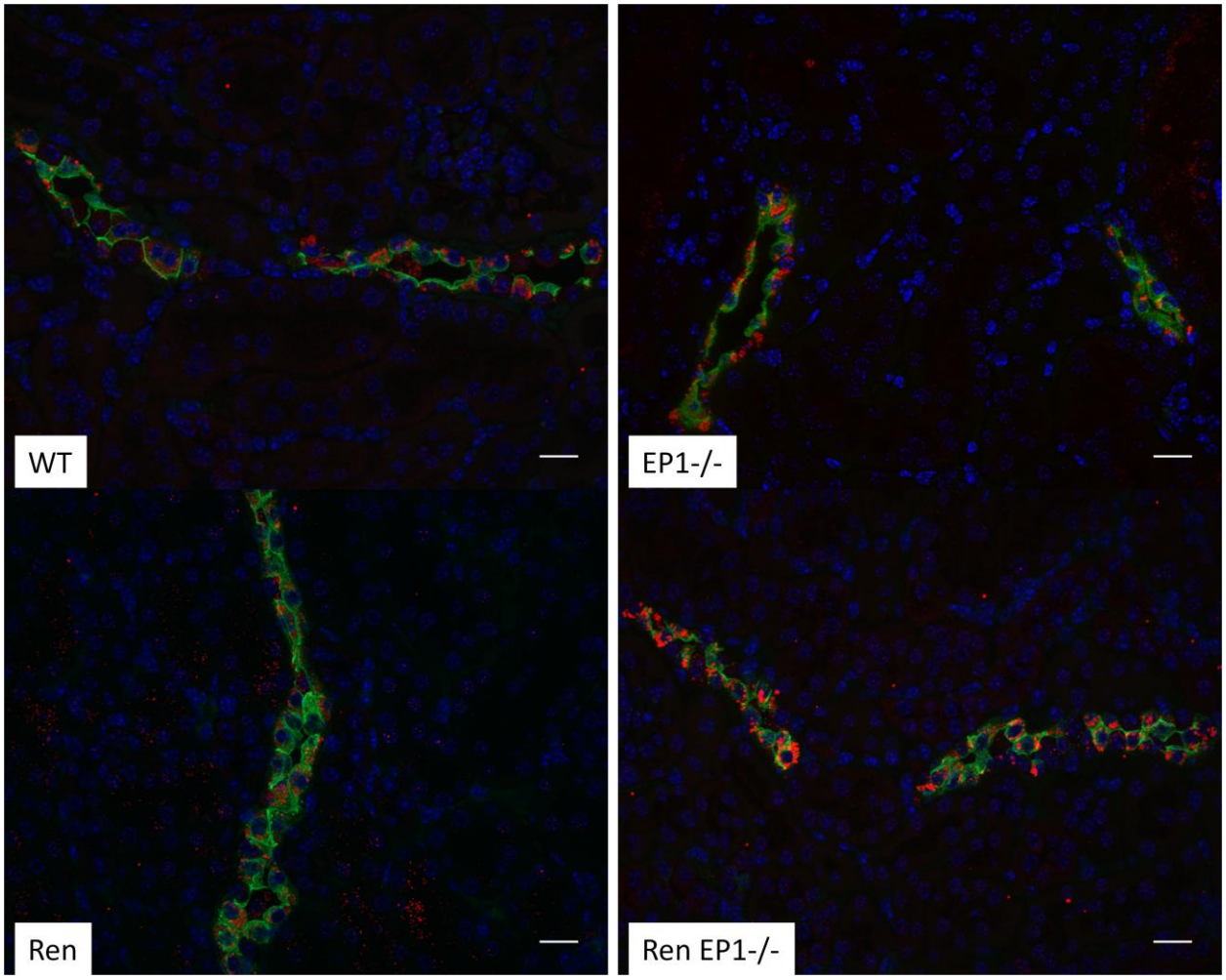

Figure 38. Representative images of CCD(s) stained for AQP2 and αENaC from the four mouse groups on a LS diet. Each panel is labeled with their corresponding mouse group in the bottom left corner. Green represents AQP2; red represents αENaC; blue represents the nuclei. Images taken under 40x magnification. Scale bars (white lines) represents 20µm.

5 Discussion

PGE_2's natriuretic and diuretic actions are established phenomenons. The underlying mechanisms, especially in the renal collecting duct, are poorly understood. The following questions inspired the study: 1) what is the goal of EP1 receptor activation on sodium and water transport; 2) does the collecting duct play a major role in determining salt sensitivity; 3) will knocking out the EP1 receptor enhance or diminish salt sensitivity? These answers are not obvious because blocking ENaC can have two opposing effects. Inhibiting ENaC can paradoxically aggravate hypernatremia through the inability to maintain the renal medullary osmotic gradient required for water transport[65].

AVP induced water reabsorption can have a positive and negative influence on BP. AVP induced water reabsorption serves to increase blood pressure by increasing effective circulating volume[66]. However, excessive AVP production in the case of SIADH leads to a reduction in blood pressure through the dilution of plasma[67].

The Vte was measured across a microdissected CCD experiment as a stand-in for sodium flux (J_{Na+}) in figure 24 and 25. Unfortunately, the electrophysiological results are inconsistent with current research, questioning the validity of the data. Research dictates there should be enhanced sodium transport in WT LS mice and very limited Na^+ transport in HS mice[68,69,70,71,72]. The electrophysiological data presented in this thesis indicates the opposite, the baseline Vte is

more depolarized in the WT LS group compared to the WT HS group. PGE_2 should have a minimal effect in HS WT mice because ENaC is absent, whereas it should have a larger influence on LS WT mice. The data presented shows the reverse effect, PGE_2 has a more pronounced effect on the WT HS mice compared to WT LS mice.

According to well know literature studies, AngII induces enhanced Na^+ transport through its actions on the AT1a receptor[12, 73,74]. Freshly made AngII 10^{-6}M caused a slight depolarization of ~2mV, a puzzling result.

I believe the electrophysiological setup in our lab is not sensitive enough to record the minute changes in J_{Na+}. Without going into details, a couple techniques could be used to improve the electrophysiological experiments. An agarose bridge could be employed to connect the electrode probe and the CCD tubule[64,75,76]. Radioactive $^{22}Na^+$ could be used as a tracer[33,77,32], with the experiment performed in a similar manner as the ^{3}H-inulin water flux experiments. Patch clamp electrophysiology on an isolated principal cell in the CCD[68,69,75]could be performed.

The *ex vivo* experiments conclusively prove that EP1, not EP3, is the prostanoid receptor subtype responsible for inhibiting water reabsorption in the collecting duct. This begs the question, how did the literature believe EP3 was involved? Hébert *et al.* showed that PGE_2 inhibited AVP induced water reabsorption, an effect attenuated with the addition of pertussis toxin[32,34]. This proves there is a Gi induced effect. However, this does not rule out the possibility that EP1 activates PKC, in turn activating Gi in the collecting duct as previously reported[78,79].

Tamma *et al.* argue[40] that EP3 is the inhibitory receptor based on their use of the EP1 antagonist SC19220. SC19220 is an EP1 antagonists with a Ki of 6.7μM[80]. By using SC19220 at 10 μM, only a 60% blockade of EP1 receptor is achieved based on the dose response curve[80]. In

the water perfusion experiments, there was a statistical difference between the EP1-/- and WT SC19220 10 μM treated tubules, consistent with a partial but not complete blockade of the EP1 receptor. The authors believed that by using SC19220, they were inhibiting the majority of the EP1 receptors when in reality they were only inhibiting a little over half of the EP1 receptors.

Before trying to understanding the physiological alterations occurring in the EP1-/- and Ren mice, the physiological changes of WT mice on the LS and HS diet were examined. When WT mice are subjected to a LS diet couple key actions take place. First, the macula densa senses a low urine osmolarity and juxtamedullary cells release PGE_2 into the afferent arteriole[1]. PGE_2 binds the EP4 receptor in the granular cells of the afferent arteriole eliciting the release of renin[81]. Renin activates the RAAS system with one of the key actions being the upregulation of aldosterone. Aldosterone's main tool to increase sodium reabsorption is the upregulation of αENaC production[17]. At the same time, ENaC channel activity (open probability) is boosted through inactivation of intracellular signaling of PKC[82].

The results confirm these actions. αENaC stains much stronger in WT LS CCD tubules compared to WT HS CCD tubules mice. This confirms elevated αENaC levels in WT LS mice. αENaC is more membrane localized in the WT LS group over the WT HS group, suggesting more active ENaC. COX-2 are levels are down in WT LS mice compared to WT HS mice, confirming PGE_2 production is not desired in a LS environment in the collecting duct. As a result of these actions, plasma homeostasis and the BP do not change on a LS diet.

In the WT HS scenario, the immediate consequence of the HS diet is an increase in plasma tonicity. This triggers the thirst centres in the brain to become activated by the hypothalamus. The hypothalamus also responds by increasing AVP production and release from the hypothalamus to the posterior pituitary[1]. AVP makes its way to the V2R receptor through the

bloodstream and enhances water reabsoprtion through AQP2 activation. In response to the increased tonicity and shear stress from the urinary flow rate, COX-2 is upregulated in the collecting duct[39]. This stimulates production of PGE_2 which contributes to natriuresis[36].

The results confirm these physiological actions. AVP levels are boosted ~2 fold in the HS WT mice compared to the NS WT mice. AQP2 is more preferentially located in the apical membrane of the medulla in the WT HS mice compared to the WT NS mice. COX-2 is detected in the WT HS mice group whereas it was not detected on the NS diet. αENaC is not present in the CCD of the WT HS group whereas it is found on the NS diet. BP doesn't change and plasma homeostasis is restored. This is consistent with literature findings [83,84,85] that rodent models of hypertension require an additional challenge on top of a HS diet to induce hypertension (e.g DOCA pellet implantation, uninephrectomy, AngII minipump).

EP1-/- mice react to the salt diets similar to WT mice, with some slight alterations. In the NS scenario: BP, urinary parameters and ACR are unchanged between the groups. The same holds true in the LS scenario, no parameters are different between the WT and EP1-/- group. On the HS diet, urinary AVP levels are ~2.5 fold lower in EP1-/- group compared the WT group. Urine volume, water intake, urine osmolarity are statistically the same between WT and EP1-/- mice groups. This indicates that the impaired AVP release in the hypothalamus is being cancelled out by the enhanced ability of AVP to concentrate urine in the collecting duct. This supports the running hypothesis that the EP1 receptor positively enhances AVP release in the hypothalamus but antagonizes AVP action in the collecting duct.

Ren mice have a chronically activated RAAS, causing a pronounced increase in blood pressure. Compared to WT mice, Ren mice have the same urinary output and water intake yet their osmolarity is lower on a NS diet. This suggests increased Na^+ reabsorption is contributing

to the increased BP. On a LS diet, the BP differential between the WT and Ren mice was cut in half. This proves that approximately half of the Ren mice's hypertension can be attributed to Na^+ with the other half due to other AngII effects (e.g ↑ Vasoconstriction, ↑ sympathetic tone, ↑ plasma epinephrine).

Compare to WT mice on a HS diet, Ren mice experience a statistical increase in BP. Unlike WT mice, Ren mice cannot turn off the RAAS under HS conditions. As evidence by the IF staining, αENaC is still present in Ren mice even in a HS situation. The BP rises as a result of enhanced Na^+ reabsorption. Despite the beneficial actions of AVP on water reabsorption in a HS scenario, it would be extremely detrimental to have AVP levels rise due to AVP's role in enhancing Na^+ reabsorption. The data supports this hypothesis as AVP levels in Ren mice do not rise as they do in the WT mice group on a HS diet. Without an increased AVP release, the only mechanism by which plasma tonicity can be maintained is through an augmented fluid intake. Hence the polyuria and polydipsia observed in the Ren mice on the HS diet.

The Ren EP1-/- mice behave paradoxically in some scenarios. Fixating on the collecting duct alone, the Ren EP1-/- mice are expected to have enhanced urinary concentrating ability. The enhanced Na^+ sodium reabsorption caused by the Ren gene coupled with the removal of the EP1 brakes should result in the Ren EP1-/- group having the highest blood pressure with the most concentrated urine. This does not happen, the Ren EP1-/- mice have a urinary concentrating defect and their BP is the same as Ren mice on a NS diet. With the lowest amount of AVP release due to the combined EP1-/- and Ren factors, the Ren EP1-/- mice can only resort to fluid intake as a means to water down their plasma. This justifies why the Ren EP1-/- mice have the highest water intake and urine volume of all the groups. Indeed, the Ren EP1-/- mice are successful in maintaining normal plasma tonicity as their blood hematocrit is not abnormal.

The LS scenario has two interesting features that provide insight into the EP1's role in the collecting duct. First, AVP levels are unchanged amongst all groups, eliminating the confounding factor of EP1's influence in the hypothalamus. Secondly, Na^+ transporter effects are exaggerated due to the severe salt restriction. From the IF images, αENaC levels are much higher and more membrane bound in the Ren EP1-/- CCD tubules compared to Ren mice. Versus WT mice, urine osmolarity is statically down in the Ren EP1-/- but not Ren mice. Taken together, this suggests slightly more sodium reabsorption is occurring in the Ren EP1-/- mice. Being able to save just that little extra Na^+ could justify why the blood pressure does not drop in the Ren EP1-/- mice on a LS diet.

On a HS diet, the Ren EP1-/- do not experience an increase in BP whereas the Ren mice do. I argue that the increased GFR observed in Ren EP1-/- mice is acting analogous to a diuretic, increasing the amount of water and sodium excreted. The inflated fluid excretion due to the GFR is being counteracted acted by the upsurge in fluid reabsorption occurring in the collecting duct. This offers an explanation as to why the BP does not rise in the Ren EP1-/- mice on a HS diet.

GFR is elevated only under the triple whammy scenario: a HS diet with over expressed renin and the absence of the EP1 receptor. Each of the three factors contributes to an increase in GFR in a different way. EP1 is a vasoconstrictor in the vasculature smooth muscle and PGE_2 regulates GFR in the afferent arteriole. The absence of the EP1 receptor in the afferent arteriole will cause afferent arteriole dilation. AngII is a vasoconstrictor in the efferent arteriole. The enhanced production of AngII in Ren mice will cause a further increase in efferent arteriole constriction. HS diet increases the osmolarity of the plasma, placing more osmotic strain on the glomerulus. The fact that the GFR remains constant in all other scenarios proves how tightly the GFR is regulated[86].

Based on the elevated ACR and GFR levels in Ren and Ren EP1-/- mice as well as the tubular dilation, it is safe to say that the Ren and Ren EP1-/- mice are hyperfiltrating on a HS diet. No kidney damage was observed after being on the HS diet for two weeks. If this study were to have lasted longer (1-2 months), I believe kidney damage could have occurred.

One of the overarching goals of this study was to get a better understating of the physiological consequences NSAIDs have on fluid homeostasis. This study accomplishes its goal of providing further knowledge into the renal dysfunction caused by NSAIDs. The data corroborates clinical findings of how NSAIDs can alter BP regulation of those with pre-existing hypertension, congestive heart failure or edema[87]. This study also provides a mechanism for understanding the increased thirst side effect associated with NSAIDs. For physicians, the benefits of inhibiting the COX-2 inflammation pathway should take into consideration the consequences of inhibiting the COX-2/mPGES1/EP1 pathway in the kidney.

Another goal of this study was to determine whether or not the collecting duct plays a role in the development of AngII-salt sensitive hypertension. This study confirms that the collecting duct does indeed play a role. However, this study establishes that the collecting duct is just one of the many important pieces of the puzzle in the understanding of salt sensitive hypertension.

In conclusion, Ren mice were sensitive to salt, accompanied with a normally urinary concentrating mechanism on a NS diet. In contrast, the Ren EP1-/- mice showed no sensitivity to salt but an impaired urinary concentrating ability on a NS diet. The actions in the collecting duct play an important role in explaining the lack of salt sensitivity and the urinary concentrating defect of Ren EP1-/- mice. The findings confirm that other physiological systems such as the hypothalamus, glomerulus and the vasculature have a complex interaction with the collecting

duct in playing a role in AngII induced salt sensitivity. These results represent compelling evidence supporting the collecting duct role of the EP1 receptor in regulating blood pressure and fluid homeostasis.

5.1 Major Limitation

Urinary and plasma Na^+,Cl^-,K^+ and urea levels were not evaluated. The central argument being made is that Na^+ and H_2O reabsorption in the collecting duct is vital to the ability of regulating blood pressure and fluid balance. This study is relying on spot urine osmolarity as a fill in for electrolyte values. This doesn't give a full picture as to what is truly occurring.

5.2 Minor Limitations

Plasma aldosterone levels were not measured. Aldosterone plays a vital role in the RAAS system, with its main action being increasing αENaC production. It is crucial to know whether or not the EP1-/- receptor's effect on the collecting duct is aldosterone dependent or independent.

Urinary PGE_2 metabolites were not assessed. COX-2 levels were assessed in the medulla, but the antibody was messy and western blots only yield semi-quantitative values. COX-1 levels were assessed, but only in the NS mice. You cannot simply add the COX-1 and

COX-2 signal together to infer medullary PGE_2 levels. PGE_2 is a short lived compound[88], thus PGE_2 metabolites are commonly measured from spot urine as an indicator of PGE_2 levels.

6 Summary and Future Studies

The data presented in the thesis advances the knowledge of EP1 receptor's role in salt sensitivity, AngII hypertension and the collecting duct (Figure 39).

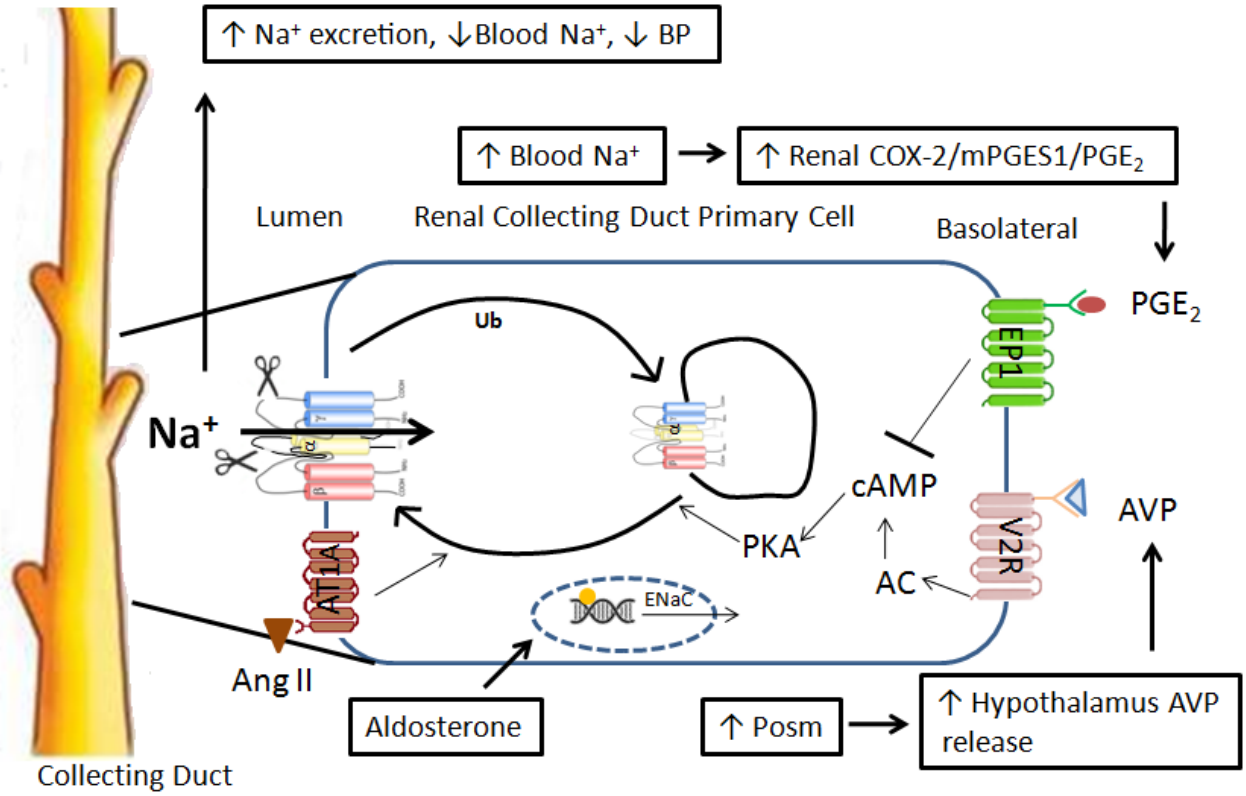

Figure 39. Schematic representation of PGE_2 inhibition of RAAS regulated sodium transport in the renal collecting duct through its actions on the EP1 receptor.

New questions have emerged as a result of this work. Now that this study has proven IMCD PGE_2 signaling is exclusively through the EP1 receptor, what is the exact signaling mechanism? It is perplexing how the AT1a receptor, a Gq coupled GPCR[89], has a completely opposite effect of the EP1 receptor, another Gq GPCR. Perhaps this has to do with cell polarity[90]; the AT1a receptor is located on the luminal membrane side while the EP1 receptor is on the basolateral membrane. Another question is how does EP1 inhibit cAMP production if it is not directly Gi linked? One possibility is PKC can stimulate Gi[78,79], another possibility is elevated Ca^{2+} levels inactivates adenylyl cyclase[91] or activates phosphodiesterases[92].

This study was done entirely on male mice. It begs the questions as to whether these findings would hold true in female mice. Females were excluded from this study because of the sexual dimorphism in baseline urinary parameters[93], RAAS[94] and salt responses[95]. It is well established that female rodents have a larger baseline water intake and urine volume[93]. Multiple rodent studies have confirmed that females have higher renin levels but lower angiotensinogen levels compared to males[94,96,97]. Models of hypertension are known to be much stronger in males than females[95,98,99]. All these factors would have compounded an already complex story if females were used.

Finally, a collecting duct or kidney specific knockout of the EP1 receptor would be beneficial in conclusively determining EP1's role in the collecting duct. This could be achieved by floxing the EP1 gene and crossing it with an AQP2Cre mouse. Another option would be to perform a kidney transplant between EP1-/- mice and WT mice.

7 References

1. Berne RM. *Physiology*. 5th ed. St. Louis, MO: Mosby; 2004.

2. Bertram JF, Douglas-Denton RN, Diouf B, Hughson MD, Hoy WE. Human nephron number: implications for health and disease. *Pediatr Nephrol*. 2011;26(9):1529-1533. doi:10.1007/s00467-011-1843-8.

3. David B. Mount MRP. *Molecular and Genetic Basis of Renal Disease*. Philadelphia, PA: Elsevier; 2007.

4. Klussmann E, Maric K, Rosenthal W. The mechanisms of aquaporin control in the renal collecting duct. *Rev Physiol Biochem Pharmacol*. 2000;141:33-95. http://www.ncbi.nlm.nih.gov/pubmed/10916423. Accessed February 8, 2017.

5. Nielsen S, Frøkiær J, Marples D, Kwon T-H, Agre P, Knepper MA. Aquaporins in the Kidney: From Molecules to Medicine. *Physiol Rev*. 2002;82(1).

6. Birnbaumer M, Seibold A, Gilbert S, et al. Molecular cloning of the receptor for human antidiuretic hormone. *Nature*. 1992;357(6376):333-335. doi:10.1038/357333a0.

7. Klussmann E, Tamma G, Lorenz D, et al. An inhibitory role of Rho in the vasopressin-mediated translocation of aquaporin-2 into cell membranes of renal principal cells. *J Biol Chem*. 2001;276(23):20451-20457. doi:10.1074/jbc.M010270200.

8. Christensen BM, Zelenina M, Aperia A, Nielsen S. Localization and regulation of PKA-phosphorylated AQP2 in response to V2-receptor agonist/antagonist treatment. *Am J Physiol - Ren Physiol*. 2000;278(1).

9. Umenishi F, Narikiyo T, Vandewalle A, Schrier RW. cAMP regulates vasopressin-induced AQP2 expression via protein kinase A-independent pathway. *Biochim Biophys Acta - Biomembr*. 2006;1758(8):1100-1105. doi:10.1016/j.bbamem.2006.06.001.

10. Boron WF. *Medical Physiology: A Cellular And Molecular Approaoch*. Philadelphia, PA: Elsevier/Saunders; 2005.

11. Stegbauer J, Gurley SB, Sparks MA, et al. AT1 receptors in the collecting duct directly modulate the concentration of urine. *J Am Soc Nephrol*. 2011;22(12):2237-2246. doi:10.1681/ASN.2010101095.

12. Chen D, Stegbauer J, Sparks MA, et al. Impact of Angiotensin Type 1A Receptors in Principal Cells of the Collecting Duct on Blood Pressure and HypertensionNovelty and Significance. *Hypertension*. 2016;67(6).

13. Mamenko M, Zaika O, Prieto MC, et al. Chronic Angiotensin II Infusion Drives Extensive Aldosterone-Independent Epithelial Na+ Channel ActivationNovelty and Significance. *Hypertension*. 2013;62(6).

14. Beutler KT, Masilamani S, Turban S, et al. Long-Term Regulation of ENaC Expression in Kidney by Angiotensin II. *Hypertension*. 2003;41(5).

15. D Craig Brater M. Mechanism of action of diuretics. http://www.uptodate.com/contents/mechanism-of-action-of-diuretics?source=search_result&search=amiloride&selectedTitle=3~55. Published 2015. Accessed February 8, 2017.

16. Bankir L, Bichet DG, Bouby N. Vasopressin V2 receptors, ENaC, and sodium

reabsorption: a risk factor for hypertension? *Am J Physiol - Ren Physiol*. 2010;299(5).

17. Masilamani S, Kim GH, Mitchell C, Wade JB, Knepper MA. Aldosterone-mediated regulation of ENaC alpha, beta, and gamma subunit proteins in rat kidney. *J Clin Invest*. 1999;104(7):R19-23. doi:10.1172/JCI7840.

18. Czogalla J, Vohra T, Penton D, Kirschmann M, Craigie E, Loffing J. The mineralocorticoid receptor (MR) regulates ENaC but not NCC in mice with random MR deletion. *Pflügers Arch - Eur J Physiol*. 2016;468(5):849-858. doi:10.1007/s00424-016-1798-5.

19. Morrell ED, Kellum JA, Hallows KR, Pastor-Soler NM. Epithelial transport during septic acute kidney injury. *Nephrol Dial Transplant*. 2014;29(7):1312-1319. doi:10.1093/ndt/gft503.

20. Nguyen MTX, Yang LE, Fletcher NK, et al. Effects of K+-deficient diets with and without NaCl supplementation on Na+, K+, and H2O transporters' abundance along the nephron. *Am J Physiol - Ren Physiol*. 2012;303(1).

21. Ergonul Z, Frindt G, Palmer LG. Regulation of maturation and processing of ENaC subunits in the rat kidney. *Am J Physiol - Ren Physiol*. 2006;291(3).

22. Eaton DC, Malik B, Bao H-F, Yu L, Jain L. Regulation of epithelial sodium channel trafficking by ubiquitination. *Proc Am Thorac Soc*. 2010;7(1):54-64. doi:10.1513/pats.200909-096JS.

23. Carattino MD, Mueller GM, Palmer LG, et al. Prostasin interacts with the epithelial Na+ channel and facilitates cleavage of the γ-subunit by a second protease. *Am J Physiol Renal*

Physiol. 2014;307(9):F1080-7. doi:10.1152/ajprenal.00157.2014.

24. Breyer MD, Zhang Y, Guan YF, Hao CM, Hebert RL, Breyer RM. Regulation of renal function by prostaglandin E receptors. *Kidney Int Suppl*. 1998;67:S88-94. http://www.ncbi.nlm.nih.gov/pubmed/9736261. Accessed February 8, 2017.

25. Harris RC. Physiologic and pathophysiologic roles of cyclooxygenase-2 in the kidney. *Trans Am Clin Climatol Assoc*. 2013;124:139-151. http://www.ncbi.nlm.nih.gov/pubmed/23874018. Accessed February 8, 2017.

26. Breyer MD, Breyer RM. Prostaglandin E receptors and the kidney. *Am J Physiol - Ren Physiol*. 2000;279(1).

27. Olesen ETB, Fenton RA. Is there a role for PGE2 in urinary concentration? *J Am Soc Nephrol*. 2013;24(2):169-178. doi:10.1681/ASN.2012020217.

28. Poschke A, Kern N, Maruyama T, et al. The PGE2-EP4 receptor is necessary for stimulation of the renin-angiotensin-aldosterone system in response to low dietary salt intake in vivo. *AJP Ren Physiol*. 2012;303(10):F1435-F1442. doi:10.1152/ajprenal.00512.2011.

29. Hébert RL. Cellular signalling of PGE2 and its selective receptor analogue sulprostone in rabbit cortical collecting duct. *Prostaglandins Leukot Essent Fatty Acids*. 1994;51(3):147-155. http://www.ncbi.nlm.nih.gov/pubmed/7824528. Accessed February 9, 2017.

30. Natarajan C, Hata AN, Hamm HE, Zent R, Breyer RM. Extracellular loop II modulates GTP sensitivity of the prostaglandin EP3 receptor. *Mol Pharmacol*. 2013;83(1):206-216. doi:10.1124/mol.112.080473.

31. Chun K-S, Lao H-C, Langenbach R. The prostaglandin E2 receptor, EP2, stimulates keratinocyte proliferation in mouse skin by G protein-dependent and {beta}-arrestin1-dependent signaling pathways. *J Biol Chem*. 2010;285(51):39672-39681. doi:10.1074/jbc.M110.117689.

32. Hébert RL, Jacobson HR, Fredin D, Breyer MD. Evidence that separate PGE2 receptors modulate water and sodium transport in rabbit cortical collecting duct. *Am J Physiol*. 1993;265(5 Pt 2):F643-50. http://www.ncbi.nlm.nih.gov/pubmed/8238544. Accessed February 9, 2017.

33. Guan Y, Zhang Y, Breyer RM, et al. Prostaglandin E2 inhibits renal collecting duct Na+ absorption by activating the EP1 receptor. *J Clin Invest*. 1998;102(1):194-201. doi:10.1172/JCI2872.

34. Noland TD, Carter CE, Jacobson HR, Breyer MD. PGE2 regulates cAMP production in cultured rabbit CCD cells: evidence for dual inhibitory mechanisms. *Am J Physiol - Cell Physiol*. 1992;263(6).

35. Michell AR, Moss P. Responses to reduced water intake, including dehydration natriuresis, in sheep excreting sodium predominantly in urine or in faeces. *Exp Physiol*. 1995;80(2):265-274. http://www.ncbi.nlm.nih.gov/pubmed/7786517. Accessed February 10, 2017.

36. Jia Z, Liu G, Sun Y, et al. mPGES-1-derived PGE2 mediates dehydration natriuresis. *Am J Physiol Renal Physiol*. 2013;304(2):F214-21. doi:10.1152/ajprenal.00588.2011.

37. Yang T, Schnermann JB, Briggs JP. Regulation of cyclooxygenase-2 expression in renal medulla by tonicity in vivo and in vitro. *Am J Physiol - Ren Physiol*. 1999;277(1).

38. Zhang M-Z, Lopez PS, McKanna JA, Harris RC. Regulation of Cyclooxygenase Expression by Vasopressin in Rat Renal Medulla. *Endocrinology*. 2004;145(3):1402-1409. doi:10.1210/en.2003-0903.

39. Jensen BL, Kurtz A. Differential regulation of renal cyclooxygenase mRNA by dietary salt intake. *Kidney Int*. 1997;52(5):1242-1249. http://www.ncbi.nlm.nih.gov/pubmed/9350647. Accessed February 9, 2017.

40. Tamma G, Wiesner B, Furkert J, et al. The prostaglandin E2 analogue sulprostone antagonizes vasopressin-induced antidiuresis through activation of Rho. *J Cell Sci*. 2003;116(16).

41. González AA, Céspedes C, Villanueva S, Michea L, Vio CP. *E Prostanoid-1 Receptor Regulates Renal Medullary αENaC in Rats Infused with Angiotensin II*. Vol 389.; 2009. doi:10.1016/j.bbrc.2009.08.157.

42. Guan Y, Zhang Y, Wu J, et al. Antihypertensive effects of selective prostaglandin E2 receptor subtype 1 targeting. *J Clin Invest*. 2007;117(9):2496-2505. doi:10.1172/JCI29838.

43. Kennedy CRJ, Xiong H, Rahal S, et al. Urine concentrating defect in prostaglandin EP1-deficient mice. *Am J Physiol - Ren Physiol*. 2007;292(2).

44. Cao X, Peterson JR, Wang G, et al. Angiotensin II-Dependent Hypertension Requires Cyclooxygenase 1-Derived Prostaglandin E2 and EP1 Receptor Signaling in the Subfornical Organ of the Brain. *Hypertension*. 2012;59(4):869-876. doi:10.1161/HYPERTENSIONAHA.111.182071.

45. Norman M Kaplan M, Raymond R Townsend M. NSAIDs and acetaminophen: Effects on blood pressure and hypertension. http://www.uptodate.com/contents/nsaids-and-acetaminophen-effects-on-blood-pressure-and-hypertension. Accessed February 9, 2017.

46. Hörl WH. Nonsteroidal Anti-Inflammatory Drugs and the Kidney. *Pharmaceuticals (Basel)*. 2010;3(7):2291-2321. doi:10.3390/ph3072291.

47. Loboz KK, Shenfield GM. Drug combinations and impaired renal function -- the "triple whammy". *Br J Clin Pharmacol*. 2005;59(2):239-243. doi:10.1111/j.0306-5251.2004.2188.x.

48. SODIUM REDUCTION STRATEGY FOR CANADA. 2010. http://www.hc-sc.gc.ca/fn-an/alt_formats/pdf/nutrition/sodium/strateg/reduct-strat-eng.pdf. Accessed March 18, 2017.

49. Khan JM, Beevers DG. Management of hypertension in ethnic minorities. *Heart*. 2005;91(8):1105-1109. doi:10.1136/hrt.2004.044560.

50. Yu H, Yang T, Gao P, et al. Caffeine intake antagonizes salt sensitive hypertension through improvement of renal sodium handling. *Sci Rep*. 2016;6:25746. doi:10.1038/srep25746.

51. Coffman TM, Coffman TM. The inextricable role of the kidney in hypertension. *J Clin Invest*. 2014;124(6):2341-2347. doi:10.1172/JCI72274.

52. Sanada H, Jones JE, Jose PA. Genetics of salt-sensitive hypertension. *Curr Hypertens Rep*. 2011;13(1):55-66. doi:10.1007/s11906-010-0167-6.

53. Kusche-Vihrog K, Oberleithner H. An emerging concept of vascular salt sensitivity.

F1000 Biol Rep. 2012;4:20. doi:10.3410/B4-20.

54. Choi HY, Park HC, Ha SK. Salt Sensitivity and Hypertension: A Paradigm Shift from Kidney Malfunction to Vascular Endothelial Dysfunction. *Electrolyte Blood Press*. 2015;13(1):7-16. doi:10.5049/EBP.2015.13.1.7.

55. Kurtz TW, DiCarlo SE, Pravenec M, Schmidlin O, Tanaka M, Morris RC. An alternative hypothesis to the widely held view that renal excretion of sodium accounts for resistance to salt-induced hypertension. *Kidney Int*. 2016;90(5):965-973. doi:10.1016/j.kint.2016.05.032.

56. Prescott G, Silversides DW, Mei S, Chiu L, Reudelhuber TL. Contribution of circulating renin to local synthesis of angiotensin peptides in the heart.

57. Nadler SP, Zimpelmann JA, Hébert RL. Endothelin inhibits vasopressin-stimulated water permeability in rat terminal inner medullary collecting duct. *J Clin Invest*. 1992;90(4):1458-1466. doi:10.1172/JCI116013.

58. Bartlett CS, Boyd KL, Harris RC, Zent R, Breyer RM. EP1 disruption attenuates end-organ damage in a mouse model of hypertension. *Hypertens (Dallas, Tex 1979)*. 2012;60(5):1184-1191. doi:10.1161/HYPERTENSIONAHA.112.199026.

59. Jacob F, Ariza P, Osborn JW. Renal denervation chronically lowers arterial pressure independent of dietary sodium intake in normal rats. *Am J Physiol - Hear Circ Physiol*. 2003;284(6):H2302-H2310. doi:10.1152/ajpheart.01029.2002.

60. Mangrum AJ, Gomez RA, Norwood VF. Effects of AT_{1A} receptor deletion on blood pressure and sodium excretion during altered dietary salt intake. *Am J Physiol - Ren*

Physiol. 2002;283(3):F447-F453. doi:10.1152/ajprenal.00259.2001.

61. Ayalew Tefferi M. Diagnostic approach to the patient with polycythemia. http://www.uptodate.com/contents/diagnostic-approach-to-the-patient-with-polycythemia. Accessed February 9, 2017.

62. Jeffrey S Berns M. Treatment of anemia in hemodialysis patients. http://www.uptodate.com/contents/treatment-of-anemia-in-hemodialysis-patients. Accessed February 9, 2017.

63. Brosius FC, Alpers CE, Bottinger EP, et al. Mouse models of diabetic nephropathy. *J Am Soc Nephrol*. 2009;20(12):2503-2512. doi:10.1681/ASN.2009070721.

64. Ando Y, Asano Y. Luminal prostaglandin E2 modulates sodium and water transport in rabbit cortical collecting ducts. *Am J Physiol - Ren Physiol*. 1995;268(6).

65. Mironova E, Chen Y, Pao AC, et al. Activation of ENaC by AVP contributes to the urinary concentrating mechanism and dilution of plasma. *Am J Physiol Renal Physiol*. 2015;308(3):F237-43. doi:10.1152/ajprenal.00246.2014.

66. Aoyagi T, Koshimizu T, Tanoue A. Vasopressin regulation of blood pressure and volume: findings from V1a receptor–deficient mice. *Kidney Int*. 2009;76(10):1035-1039. doi:10.1038/ki.2009.319.

67. Schrier RW. Body water homeostasis: clinical disorders of urinary dilution and concentration. *J Am Soc Nephrol*. 2006;17(7):1820-1832. doi:10.1681/ASN.2006030240.

68. Mironova E, Bugay V, Pochynyuk O, Staruschenko A, Stockand JD. Recording ion channels in isolated, split-opened tubules. *Methods Mol Biol*. 2013;998:341-353.

doi:10.1007/978-1-62703-351-0_27.

69. Bugaj V, Mironova E, Kohan DE, Stockand JD. Collecting duct-specific endothelin B receptor knockout increases ENaC activity. *Am J Physiol Cell Physiol*. 2012;302(1):C188-94. doi:10.1152/ajpcell.00301.2011.

70. Mironova E, Peti-Peterdi J, Bugaj V, Stockand JD. Diminished paracrine regulation of the epithelial Na+ channel by purinergic signaling in mice lacking connexin 30. *J Biol Chem*. 2011;286(2):1054-1060. doi:10.1074/jbc.M110.176552.

71. Staruschenko A, Pochynyuk O, Vandewalle A, Bugaj V, Stockand JD. Acute regulation of the epithelial Na+ channel by phosphatidylinositide 3-OH kinase signaling in native collecting duct principal cells. *J Am Soc Nephrol*. 2007;18(6):1652-1661. doi:10.1681/ASN.2007010020.

72. Sun P, Lin D-H, Wang T, et al. Low Na intake suppresses expression of CYP2C23 and arachidonic acid-induced inhibition of ENaC. *Am J Physiol - Ren Physiol*. 2006;291(6).

73. Oliverio MI, Best CF, Smithies O, Coffman TM. Regulation of Sodium Balance and Blood Pressure by the AT1A Receptor for Angiotensin II. *Hypertension*. 2000;35(2).

74. Peti-Peterdi J, Warnock DG, Bell PD. Angiotensin II directly stimulates ENaC activity in the cortical collecting duct via AT(1) receptors. *J Am Soc Nephrol*. 2002;13(5):1131-1135. doi:10.1097/01.ASN.0000013292.78621.FD.

75. Pech V, Pham TD, Hong S, et al. Pendrin modulates ENaC function by changing luminal HCO3-. *J Am Soc Nephrol*. 2010;21(11):1928-1941. doi:10.1681/ASN.2009121257.

76. Pech V, Thumova M, Kim YH, et al. ENaC inhibition stimulates Cl- secretion in the

mouse cortical collecting duct through an NKCC1-dependent mechanism. *Am J Physiol Renal Physiol*. 2012;303(1):F45-55. doi:10.1152/ajprenal.00030.2012.

77. Hébert RL, Jacobson HR, Breyer MD. Prostaglandin E2 inhibits sodium transport in rabbit cortical collecting duct by increasing intracellular calcium. *J Clin Invest*. 1991;87(6):1992-1998. doi:10.1172/JCI115227.

78. Kishore BK, Chou CL, Knepper MA. Extracellular nucleotide receptor inhibits AVP-stimulated water permeability in inner medullary collecting duct. *Am J Physiol*. 1995;269(6 Pt 2):F863-9. http://www.ncbi.nlm.nih.gov/pubmed/8594881. Accessed February 10, 2017.

79. Teitelbaum I. Protein kinase C inhibits arginine vasopressin-stimulated cAMP accumulation via a Gi-dependent mechanism. *Am J Physiol - Ren Physiol*. 1993;264(2).

80. Funk$ CD, Furci L, Fitzgeraldo GA, et al. THE JOURNAL OF BIOLOGICAL CHEMISTRY Cloning and Expression of a cDNA for the Human Prostaglandin E Receptor EPI Subtype*. 1993;268(35):26767-26772.

81. Breyer MD, Breyer RM. Prostaglandin receptors: their role in regulating renal function. *Curr Opin Nephrol Hypertens*. 2000;9(1):23-29. http://www.ncbi.nlm.nih.gov/pubmed/10654821. Accessed February 10, 2017.

82. Bao H-F, Thai TL, Yue Q, et al. ENaC activity is increased in isolated, split-open cortical collecting ducts from protein kinase Cα knockout mice. *Am J Physiol Renal Physiol*. 2014;306(3):F309-20. doi:10.1152/ajprenal.00519.2013.

83. Iyer A, Chan V, Brown L. The DOCA-Salt Hypertensive Rat as a Model of

Cardiovascular Oxidative and Inflammatory Stress. *Curr Cardiol Rev*. 2010;6(4):291-297. doi:10.2174/157340310793566109.

84. Johns C, Gavras I, Handy DE, Salomao A, Gavras H. Models of Experimental Hypertension in Mice. *Hypertension*. 1996;28(6).

85. Yemane H, Busauskas M, Burris SK, Knuepfer MM. Neurohumoral mechanisms in deoxycorticosterone acetate (DOCA)-salt hypertension in rats. *Exp Physiol*. 2010;95(1):51-55. doi:10.1113/expphysiol.2008.046334.

86. Chade AR. Renal vascular structure and rarefaction. *Compr Physiol*. 2013;3(2):817-831. doi:10.1002/cphy.c120012.

87. White WB. Cardiovascular Effects of the Cyclooxygenase Inhibitors. *Hypertension*. 2007;49(3).

88. Kozak KR, Crews BC, Ray JL, Tai H-H, Morrow JD, Marnett LJ. Metabolism of Prostaglandin Glycerol Esters and Prostaglandin Ethanolamides in Vitro and in Vivo*. 2001. doi:10.1074/jbc.M105854200.

89. Coffman TM. Under pressure: the search for the essential mechanisms of hypertension. *Nat Med*. 2011;17(11):1402-1409. doi:10.1038/nm.2541.

90. Thai TL, Yu L, Galarza-Paez L, et al. The Polarized Effect of Intracellular Calcium on the Renal Epithelial Sodium Channel Occurs as a Result of Subcellular Calcium Signaling Domains Maintained by Mitochondria. *J Biol Chem*. 2015;290(48):28805-28811. doi:10.1074/jbc.M115.668293.

91. Chou CL, Yip KP, Michea L, et al. Regulation of aquaporin-2 trafficking by vasopressin

in the renal collecting duct. Roles of ryanodine-sensitive Ca2+ stores and calmodulin. *J Biol Chem*. 2000;275(47):36839-36846. doi:10.1074/jbc.M005552200.

92. Yamaki M, McIntyre S, Rassier ME, Schwartz JH, Dousa TP. Cyclic 3',5'-nucleotide diesterases in dynamics of cAMP and cGMP in rat collecting duct cells. *Am J Physiol*. 1992;262(6 Pt 2):F957-64. http://www.ncbi.nlm.nih.gov/pubmed/1320333. Accessed May 30, 2017.

93. Stechman MJ, Ahmad BN, Loh NY, et al. Establishing normal plasma and 24-hour urinary biochemistry ranges in C3H, BALB/c and C57BL/6J mice following acclimatization in metabolic cages. *Lab Anim*. 2010;44(3):218-225. doi:10.1258/la.2010.009128.

94. Cuffe JSM, Burgess DJ, O'Sullivan L, Singh RR, Moritz KM. Maternal corticosterone exposure in the mouse programs sex-specific renal adaptations in the renin–angiotensin–aldosterone system in 6-month offspring. *Physiol Rep*. 2016;4(8).

95. Calhoun DA, Zhu S-T, Chen Y-F, Oparil S. Gender and Dietary NaCl in Spontaneously Hypertensive and Wistar-Kyoto Rats. *Hypertension*. 1995;26(2).

96. Stock JL, Shinjo K, Burkhardt J, et al. The prostaglandin E2 EP1 receptor mediates pain perception and regulates blood pressure. *J Clin Invest*. 2001;107(3):325-331. doi:10.1172/JCI6749.

97. Yanes LL, Romero DG, Iles JW, Iliescu R, Gomez-Sanchez C, Reckelhoff JF. Sexual dimorphism in the renin-angiotensin system in aging spontaneously hypertensive rats. *Am J Physiol - Regul Integr Comp Physiol*. 2006;291(2).

98. Elmarakby AA, Bhatia K, Crislip R, Sullivan JC. Hemodynamic responses to acute angiotensin II infusion are exacerbated in male versus female spontaneously hypertensive rats. *Physiol Rep*. 2016;4(1).

99. Karatas A, Hegner B, De Windt LJ, et al. Deoxycorticosterone Acetate-Salt Mice Exhibit Blood Pressure–Independent Sexual Dimorphism. doi:10.1161/HYPERTENSIONAHA.107.107938.